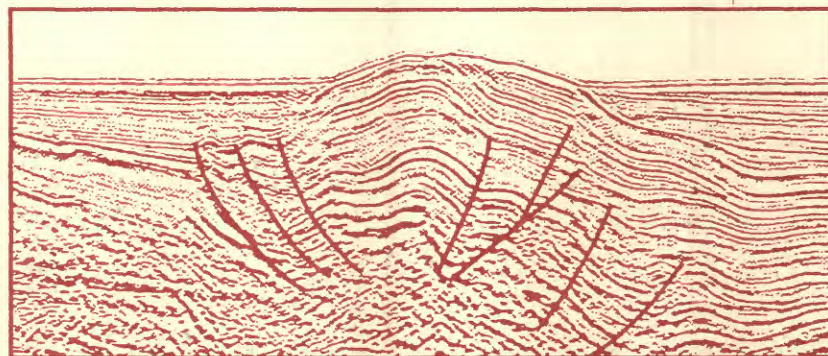
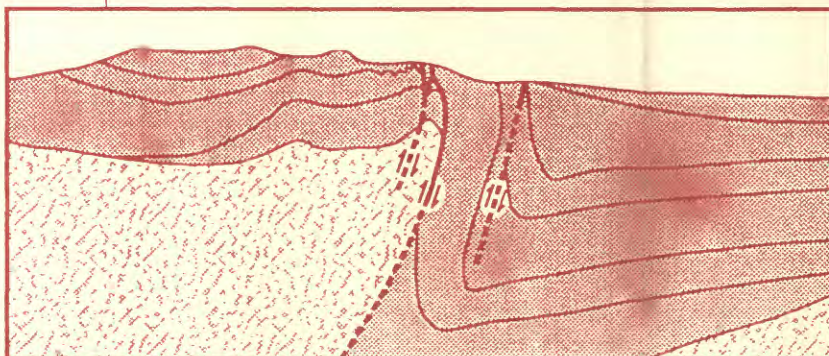


Strontium Isotope Evidence for the Age of the Vaqueros Formation and Latest Oligocene Marine Transgression in the Northern Santa Maria Province, Central California

Stratigraphic Sections and Gamma-Ray Spectrometry from Five Outcrops of the Monterey Formation in Southwestern California: Naples Beach, Point Pedernales, Lion's Head, Shell Beach, and Point Buchon



Geophysical section offshore Santa Maria basin



Geologic section onshore Santa Maria basin

AVAILABILITY OF BOOKS AND MAPS OF THE U.S. GEOLOGICAL SURVEY

Instructions on ordering publications of the U.S. Geological Survey, along with prices of the last offerings, are given in the current-year issues of the monthly catalog "New Publications of the U.S. Geological Survey." Prices of available U.S. Geological Survey publications released prior to the current year are listed in the most recent annual "Price and Availability List." Publications that are listed in various U.S. Geological Survey catalogs (see **back inside cover**) but not listed in the most recent annual "Price and Availability List" are no longer available.

Reports released through the NTIS may be obtained by writing to the National Technical Information Service, U.S. Department of Commerce, Springfield, VA 22161; please include NTIS report number with inquiry.

Order U.S. Geological Survey publications **by mail** or **over the counter** from the offices given below.

BY MAIL

Books

Professional Papers, Bulletins, Water-Supply Papers, Techniques of Water-Resources Investigations, Circulars, publications of general interest (such as leaflets, pamphlets, booklets), single copies of Earthquakes & Volcanoes, Preliminary Determination of Epicenters, and some miscellaneous reports, including some of the foregoing series that have gone out of print at the Superintendent of Documents, are obtainable by mail from

**U.S. Geological Survey, Information Services
Box 25286, Federal Center
Denver, CO 80225**

Subscriptions to periodicals (Earthquakes & Volcanoes and Preliminary Determination of Epicenters) can be obtained **ONLY** from the

**Superintendent of Documents
Government Printing Office
Washington, DC 20402**

(Check or money order must be payable to Superintendent of Documents.)

Maps

For maps, address mail orders to

**U.S. Geological Survey, Map Distribution
Box 25286, Bldg. 810, Federal Center
Denver, CO 80225**

Residents of Alaska may order maps from

**U.S. Geological Survey, Earth Science Information Center
101 Twelfth Ave., Box 12
Fairbanks, AK 99701**

OVER THE COUNTER

Books and Maps

Books and maps of the U.S. Geological Survey are available over the counter at the following U.S. Geological Survey offices, all of which are authorized agents of the Superintendent of Documents.

- **ANCHORAGE, Alaska**—4230 University Dr., Rm. 101
- **LAKEWOOD, Colorado**—Federal Center, Bldg. 810
- **MENLO PARK, California**—Bldg. 3, Rm. 3128, 345 Middlefield Rd.
- **RESTON, Virginia**—National Center, Rm. 1C402, 12201 Sunrise Valley Dr.
- **SALT LAKE CITY, Utah**—Federal Bldg., Rm. 8105, 125 South State St.
- **SPOKANE, Washington**—U.S. Post Office Bldg., Rm. 135, W. 904 Riverside Ave.
- **WASHINGTON, D.C.**—Main Interior Bldg., Rm. 2650, 18th and C Sts., NW.

Maps Only

Maps may be purchased over the counter at the U.S. Geological Survey offices:

- **FAIRBANKS, Alaska**—New Federal Building, 101 Twelfth Ave.
- **ROLLA, Missouri**—1400 Independence Rd.
- **STENNIS SPACE CENTER, Mississippi**—Bldg. 3101

Strontium Isotope Evidence for the Age of the Vaqueros Formation and Latest Oligocene Marine Transgression in the Northern Santa Maria Province, Central California

By MARGARET A. KELLER, MARILYN E. TENNYSON, and RODGER E. DENISON

Stratigraphic Sections and Gamma-Ray Spectrometry from Five Outcrops of the Monterey Formation in Southwestern California: Naples Beach, Point Pedernales, Lion's Head, Shell Beach, and Point Buchon

By JON R. SCHWALBACH AND KEVIN M. BOHACS

Chapters P and Q are issued as a single volume and are not available separately

U.S. GEOLOGICAL SURVEY BULLETIN 1995

EVOLUTION OF SEDIMENTARY BASINS/ONSHORE OIL AND GAS INVESTIGATIONS—
SANTA MARIA PROVINCE

Edited by Margaret A. Keller

U.S. DEPARTMENT OF THE INTERIOR

BRUCE BABBITT, Secretary



U.S. GEOLOGICAL SURVEY

Gordon P. Eaton, Director

Any use of trade, product, or firm names
in this publication is for descriptive purposes only
and does not imply endorsement by the U.S. Government

UNITED STATES GOVERNMENT PRINTING OFFICE, WASHINGTON : 1996

For sale by
U.S. Geological Survey
Information Services
Box 25286, Federal Center
Denver, CO 80225

Chapter P

Strontium Isotope Evidence for the Age of the Vaqueros Formation and Latest Oligocene Marine Transgression in the Northern Santa Maria Province, Central California

By MARGARET A. KELLER, MARILYN E. TENNYSON, and RODGER E. DENISON

U.S. GEOLOGICAL SURVEY BULLETIN 1995

EVOLUTION OF SEDIMENTARY BASINS/ONSHORE OIL AND GAS INVESTIGATIONS—
SANTA MARIA PROVINCE

Edited by Margaret A. Keller

CONTENTS

Abstract	P1
Introduction	P1
Stratigraphy and depositional environment	P4
Sample collection	P4
Methodology and results	P5
Strontium isotope measurements	P5
Trace element chemistry	P6
Summary and conclusions	P7
Acknowledgments	P7
References cited	P7

FIGURES

1. Index map of the northern Santa Maria province, showing field identification numbers and location of mollusk samples **P2**
2. Schematic lithologic columns for the Vaqueros Formation and bounding rock formations in the Green Valley and Villa Creek areas and in the Pismo syncline **P3**
3. Plot of ΔSW values from table 1 **P6**

TABLES

1. Sample data table and $^{87}\text{Sr}/^{86}\text{Sr}$ analyses for shell fragments from the Vaqueros Formation **P6**
2. Chemical analyses of selected samples of shell fragments from the Vaqueros Formation **P7**

Strontium Isotope Evidence for the Age of the Vaqueros Formation and Latest Oligocene Marine Transgression in the Northern Santa Maria Province, Central California

By Margaret A. Keller, Marilyn E. Tennyson, and Rodger E. Denison¹

ABSTRACT

In the northern Santa Maria province of central California, shallow-marine sandstone and conglomerate of the upper Oligocene and lower Miocene(?) Vaqueros Formation locally overlies unfossiliferous conglomerate, interpreted to be nonmarine, which in turn overlies the Cambria Felsite; the Vaqueros also onlaps the Cambria Felsite and Mesozoic basement rocks of the Franciscan Complex. The Vaqueros Formation is in turn overlain by a Miocene and Pliocene marine sequence of mostly bathyal mudrocks that locally includes middle Miocene extrusive volcanics. Previous workers in this area placed the Vaqueros within the Oligocene, not younger than foraminifers assigned to the late Zemorrian (now questioned) in overlying mudrocks, and not older than the Oligocene Cambria Felsite (thought to be consanguineous with the Morro Rock–Islay Hill complex (Ernst and Hall, 1974), which has K/Ar dates of between 27.2 ± 0.8 Ma and 22.7 ± 0.9 Ma).

In this study, strontium isotopes were measured on eight mollusk samples from Vaqueros Formation outcrops in five widely separated areas—two east of Cambria in Green Valley and near Villa Creek almost due south of Black Mountain, and three sites near San Luis Obispo along the northern limb of the Pismo syncline. Samples from two additional areas on the southern limb of the Pismo syncline proved to be unsuitable because of diagenetic replacement of shell material. Trace elements were analyzed on four of the eight samples as an additional criterion to determine whether diagenesis had altered the original shell chemistry of these mollusks. The high Sr concentration, small amounts of insoluble residue, and low Mn and Fe concentrations on three of these samples indicate that their strontium isotope ratios were probably not reset by

diagenesis. Thus, the measured $^{87}\text{Sr}/^{86}\text{Sr}$ ratio for these samples is probably close to the seawater ratio approximately 25 Ma. Because this age is in close agreement with the other five samples (24.4 ± 1 – 26.3 ± 1 Ma), even one which has anomalously high Mn, we believe that the age of the basal part of the Vaqueros and the timing of the marine transgression that it represents fall within this range of late Oligocene to within error of the Oligocene-Miocene boundary. Support for this age for Vaqueros deposition comes from new $^{40}\text{Ar}/^{39}\text{Ar}$ data for the underlying Cambria Felsite (27 ± 1 Ma) and earliest Miocene calcareous nannofossils (zone CN1) in the overlying mudrocks.

INTRODUCTION

Many studies have been done in parts of central and southern California on the shallow-marine transgressive sandstone and conglomerate of the late Oligocene and early Miocene Vaqueros Formation (Loel and Corey, 1932; Edwards, 1971; Prior, 1974; Rigsby, 1989, 1994, 1996; Miles and Rigsby, 1990; Rigsby and Schwartz, 1990; see also references within these papers). The present strontium isotope study of samples from six sections of the Vaqueros located between Pismo Beach and Cambria in central California (fig. 1) was done in conjunction with two other studies of the Santa Maria province for this volume: a reevaluation of the sedimentation and tectonics of the Cenozoic section of the northern Santa Maria province between approximately Santa Maria and Point Piedras Blancas (M.E. Tennyson, M.A. Keller, and others, unpublished data, 1996), and an integrated biostratigraphic study—mainly of Miocene marine mudrocks—throughout the Santa Maria province by the UNOCAL paleontology and stratigraphy group (M.L. Cotton and others, unpublished data, 1996). The latter study utilized foraminifers, diatoms, calcareous nannofossils, and palynomorphs. Detailed descriptions of the lithostratigraphy and biostratigraphy of the sections where the

¹ Denison's affiliation: University of Texas at Dallas, Box 830688, Richardson TX 75083-0688

Vaqueros was sampled for the present report are contained in these two studies; preliminary results are given in abstracts (Tennyson, Keller, and others, 1990, 1991).

The Vaqueros Formation in this region of central California (fig. 1) had been thoroughly described (Prior, 1974) and mapped (Hall, 1973a, b, 1974; Hall and Prior, 1975; Prior, 1974) before the detailed studies of this project (M.L. Cotton

and others, unpublished data, 1996; Tennyson, Keller, and others, 1990, 1991, unpublished data—1996). However, even though the Vaqueros commonly has fossiliferous beds with a shallow-marine fauna including pectens, oysters, barnacles, and echinoid parts (Prior, 1974), its age is problematic. Furthermore, in some locations such as where the Vaqueros overlies much older Mesozoic basement or where the top is eroded,

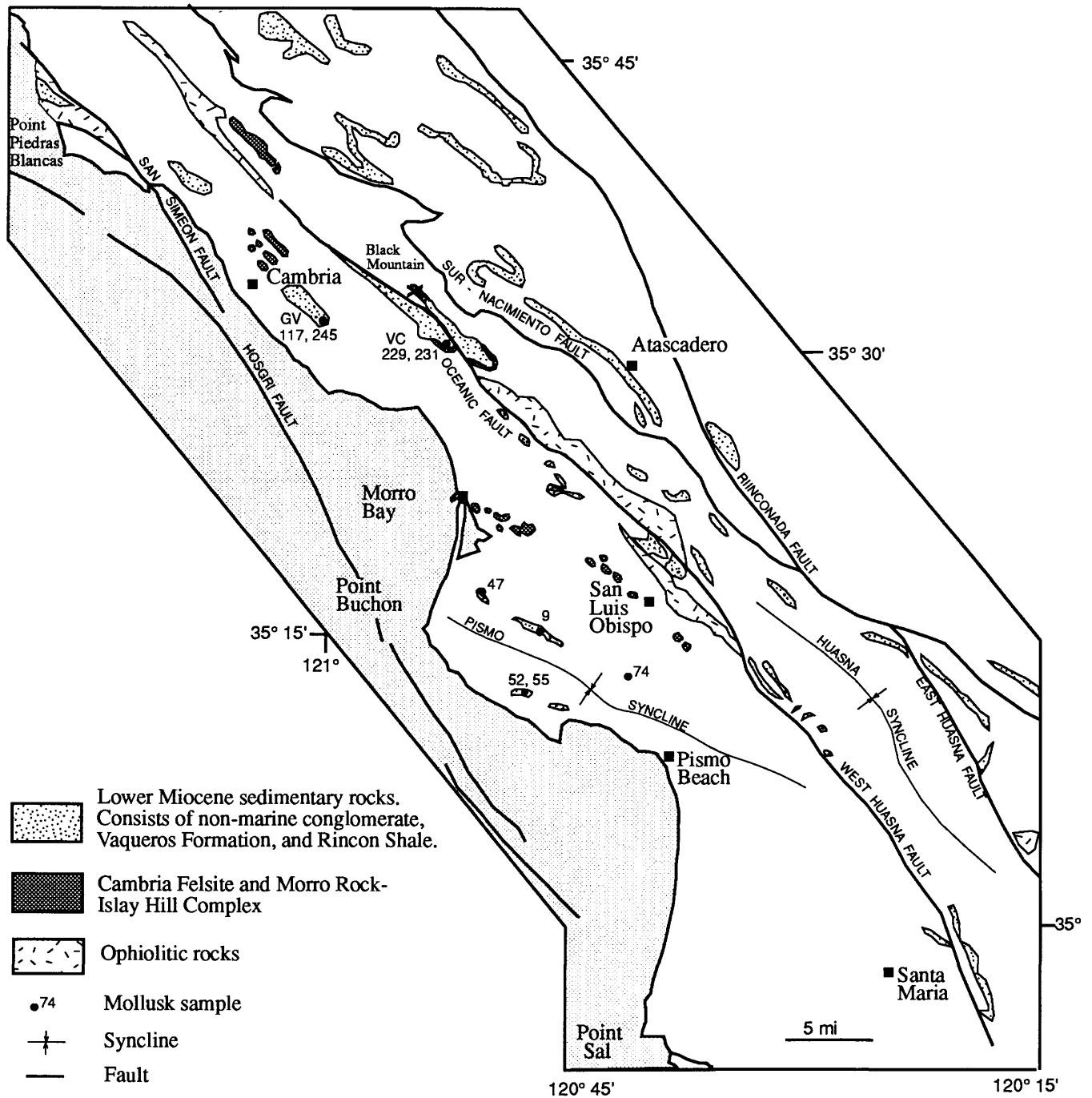


Figure 1. Index map of the northern part of the Santa Maria province in central California, showing field identification numbers and location of mollusk samples. Abbreviations: GV, Green Valley; VC, Villa Creek.

its age cannot be narrowly constrained by bounding formations (fig. 2). Also, many studies have hypothesized or concluded that the Vaqueros is not the same age everywhere—a reasonable hypothesis for a transgressive deposit (Prior, 1974; Rigsby, 1996; T. H. McCulloh, oral commun., 1989).

Prior to the studies described in this volume, only a few K-Ar radiometric ages had been determined on the volcanic units in the region, and none had been done on the Cambria Felsite, which could serve as an older limit for the Vaqueros Formation. Ernst and Hall (1974) inferred the age of the Cambria Felsite to be the same age as the Morro Rock–Islay Hill complex, or between 27.2 ± 0.8 Ma and 22.7 ± 0.9 Ma (ages corrected from Turner (1968) and Turner and others (1970) by P. Weigand, written commun. (1986)). In addition, the science of biostratigraphy had not advanced to the point of using the much higher age resolution possible with calcareous nannofossils as compared with benthic foraminifers. Thus, the younger limit for the age of the Vaqueros could only be constrained by the benthic foraminiferal stage of the mudrocks overlying the Vaqueros. Prior (1974, p. 33) speculated that the Vaqueros might be of slightly different ages in different parts of his study area based on the stage found in the basal sections of these mudrocks (in most places Zemorrian, but in a few Saucesian). He noted (p. 32) the presence of the Zemorrian Stage in the Cambria and Cypress Mountain areas, which constrained the upper part of the Vaqueros in his study to no younger than late Zemorrian (now considered Saucesian by

M.L. Cotton and others, unpublished data, 1996). Thus, Prior's (1974) study bracketed the age of the Vaqueros between the time of deposition of nonmarine conglomerate, which in some places overlies the Cambria Felsite, and deposition of overlying bathyal mudrocks of the Sandholdt Member of the Monterey Formation (Rincon Shale of this study, and as used by Hall and others, 1979). Prior's (1974) study placed all these units in the Oligocene, except for a few places where he found Saucesian foraminifers in the basal mudrocks.

The major focus of this study is to directly determine the age of the Vaqueros Formation and the timing of the marine transgression that it represents in this area of California. Because the lower part of the Vaqueros commonly contains a variety of bivalve mollusks, we have dated the lower Vaqueros by comparing strontium isotope values from shell material to seawater strontium isotope ratios determined from Deep Sea Drilling Program (DSDP) and Ocean Drilling Program (ODP) cores from the open ocean. Because the upper part of the Vaqueros in this area does not contain macroinvertebrates, we have only addressed the age of the lower part of the Vaqueros with this methodology. This has largely been possible because of advances during the past decade in $^{87}\text{Sr}/^{86}\text{Sr}$ stratigraphy owing mainly to its integration with DSDP/ODP magnetostratigraphy (Miller and others, 1988; Hess and others, 1989; Oslick and others, 1994), but also to advances in identifying and dealing with diagenetically altered shell material. Our results and conclusions are contained in this report.

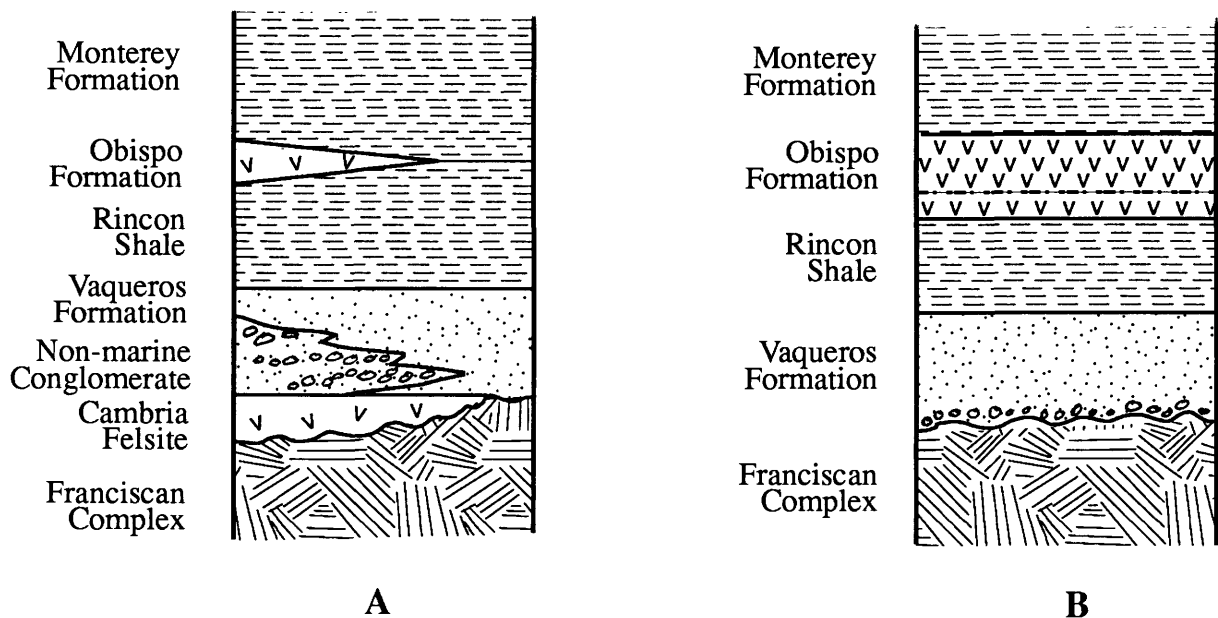


Figure 2. Schematic lithologic columns for the Vaqueros Formation and bounding rock formations in the Green Valley and Villa Creek areas (A) and the Pismo syncline (B). Rock units not to scale.

STRATIGRAPHY AND DEPOSITIONAL ENVIRONMENT

In central and southern California, shallow-marine sandstone and coarser clastic rocks of the late Oligocene and early Miocene Vaqueros Formation commonly overlie a range of older rocks: nonmarine, and in places marine, conglomerate and coarse clastics, and onlapped older formations and basement rocks (Prior, 1974; Fisher, 1977; Rigsby, 1996). In the northern Santa Maria province of central California, the Vaqueros Formation typically overlies nonmarine conglomerate or onlaps 27 ± 1 Ma Cambria Felsite (Tennyson, Keller, and others, 1991) or basement rocks of the Franciscan Complex (fig. 2). The Vaqueros Formation is in turn overlain by a bathyal marine mudrock sequence of Miocene and Pliocene age consisting of the Rincon Shale (lower Miocene), the Monterey Formation (Miocene), and the basal part of the Pismo Formation (upper Miocene). This bathyal sequence is capped by shallow-marine and nonmarine coarse clastics of Pliocene and Pleistocene age consisting of the upper part of the Pismo Formation (upper Pliocene), the Careaga Sandstone (Pliocene), and the Paso Robles Formation (Pleistocene) (Hall and others, 1979). The Obispo Formation, a major volcanic unit in the area, was extruded during and after deposition of the lower Miocene Rincon Shale (Fisher, 1977; Schneider and Fisher, 1996).

Deformation and uplift caused erosion of much of the late Paleogene and Neogene section, leaving only discontinuous remnants of the basin-filling sequence that are generally not well exposed (fig. 1). However, common elements in the sections (fig. 2) can be observed from place to place, all of which suggest that the sedimentary sequence represents deposition in a variety of shallow-marine (as also noted by Prior, 1974) and nonmarine environments along a variable coastline during and after a major marine transgression. Subsequent to this transgression, the shallow-marine rocks, as well as all older rocks and basement, were onlapped by very deep marine mudrocks, deposited as these basins subsided abruptly and precipitously sometime during the earliest Miocene (Tennyson, Keller, and others, 1991).

Prior to deposition of the early Miocene bathyal mudrocks, some evidence for gradual transition from very shallow shoreline settings to deeper marine, probably shelf environments exists in some Vaqueros Formation sections. At a location east of Villa Creek (where fossiliferous Vaqueros conglomerate and sandstone onlap the Franciscan; see figs. 1 and 2), the section consists of Cambria Felsite overlain by fluvial or deltaic sandstone and conglomerate, which is overlain by massive fine-grained sandstone approximately 1–2 m thick, underlying bathyal mudrocks. This fine-grained, angular to subangular, glauconitic sandstone is well cemented at its base, forming a very sharp contact with underlying pebble conglomerate; it grades upward from very fine grained, uncemented sandstone to poorly exposed mudrock. The sandstone, a lithologic, stratigraphic, and age equivalent of the Va-

queros, contains abundant glauconite as well as fish bones and other fish parts, suggesting deposition in an offshore marine, probably shelf environment. The fish parts add additional support for this interpretation. Based on the presence of teleost vertebrae and indeterminate scale fragments, a ctenoid fish scale, the tooth of an odontaspid shark—possibly *Carcharis* sp, and a tooth crown from an indeterminate squaloid shark; the environment of deposition for the sandstone could be outer shelf or deeper (B.J. Welton, written commun., 1993). Hall and others (1979) and M.E. Tennyson, M.A. Keller, and others (unpublished data, 1996) also note glauconitic sandstone, stratigraphically equivalent to the Vaqueros, present in other sections in this region, as well as in some places overlying the shallow-marine fossiliferous Vaqueros strata, recording the transition from nearshore deposition to deposition of bathyal mudrocks.

SAMPLE COLLECTION

In conjunction with a study by M.E. Tennyson, M.A. Keller, and others (unpublished data, 1996), the sedimentary section of late Paleogene and early Neogene age at many of Prior's (1974) sites and other locations was studied throughout the northern Santa Maria province between Santa Maria and Point Piedras Blancas (fig. 1). From these outcrops, 10 mollusk samples, both pectens and oysters, were collected from the Vaqueros Formation located in seven widely spaced areas—in Green Valley, near Villa Creek, and from five areas of the Pismo syncline, three on the north limb and two on the south limb (fig. 1).

Macrofossil-bearing beds occur in many places in the lower part or at the base of the Vaqueros Formation sections in this region. Typically, the sections have one fossiliferous bed or lens that contains shell material suitable for strontium isotope analyses. However, some sections have several fossiliferous units, and these sections could be more carefully or extensively studied to determine the duration of time for a part of Vaqueros deposition. This was not possible within the scope of our study. Thus, we analyzed shells from two different beds at only one location near Villa Creek (fig. 1). For our three samples from the Villa Creek site, one is from the basal part of the Vaqueros (#231) and the other two (at #229) are different shells from the bed directly overlying #231.

Our two northernmost samples (#117, 245) are from Green Valley, the only sections we sampled for strontium where the Vaqueros Formation overlies nonmarine conglomerate. Sample #117 is from a roadcut along Highway 46, and #245 is from the Bassi Ranch section southeast of Highway 46. At all of our other sites along the Pismo syncline and at Villa Creek, the Vaqueros rests unconformably on Franciscan Complex basement. Of our five samples from the Pismo syncline, the two (#52, 55) from the south limb were judged to be too altered for analysis. On the north limb of the syncline we sampled the Vaqueros at three places: (1) on a ridge adjacent

to Islay Creek in Montaña de Oro State Park (#47), (2) west of San Luis Obispo near the crest of See Canyon Road (#9), and (3) south of San Luis Obispo and east of Highway 101 on private property (#74) (fig. 1).

METHODOLOGY AND RESULTS

Strontium Isotope Measurements

All samples were analyzed at Mobil Research Labs in Dallas. Samples were prepared in the following manner. A thin section was made and the shell material examined for visual evidence of alteration or replacement as well as for its original characteristics. For example, oysters were examined to identify foliated layers. Fibrous structure layers tend to exchange with foreign strontium more easily. For samples passing these visual tests, the shell material was crushed into <5-mm pieces, from which the best pieces were picked using a binocular microscope. The translucent foliated pieces were selected from the oyster samples. Magnetic separation was then utilized to remove pieces with high Fe. For four of our samples from Villa Creek and Green Valley, trace element chemistry was also done before strontium isotope analysis as an additional means to determine the likelihood of alteration affecting the strontium isotope composition of the shell during diagenesis.

The strontium separation and measurement techniques have been given elsewhere (Denison and others, 1994). All sample measurements are based on an assumed $^{87}\text{Sr}/^{86}\text{Sr}$ value of 0.71014 for NBS 987. We also report the results as a difference from modern seawater as

$$\Delta\text{SW} = \left(\frac{^{87}\text{Sr}}{^{86}\text{Sr}}_{\text{unknown}} - \frac{^{87}\text{Sr}}{^{86}\text{Sr}}_{\text{modern seawater}} \right) \times 10^5.$$

The measured value for modern seawater is 0.709073 ± 3 . The calculated ΔSW for NBS 987 is $+106.7$.

$^{87}\text{Sr}/^{86}\text{Sr}$ values for the eight samples of this study are reported in table 1 along with an analytical error for individual measurements, which is our estimate of reproducibility for mass spectrometer runs at the 95 percent confidence level. The apparently equivalent age reported in table 1 was derived from the Oligocene seawater curve of Oslick and others (1994), which is based on the geomagnetic polarity time scale of Cande and Kent (1992). The error of ± 1 million years given for all the age values is our estimated range for the total analytical error possible in these determinations. We also calculated apparently equivalent age values for our data using other seawater $^{87}\text{Sr}/^{86}\text{Sr}$ curves (Miller and others, 1988; Hess and others, 1989). In all cases using these other seawater curves, our data yield ages that are slightly older, but not by more than 1 million years, and within the late Oligocene.

Our ΔSW values range from -104.1 to -93.8 and equate to apparently equivalent ages of 26.4 to 24.4 ± 1 Ma (table 1).

The ΔSW data cluster around two values at approximately -95.5 and -103 (fig. 3). One possible interpretation of the two clusters is that the basal part of the Vaqueros Formation is not the same age in all our sections. However, because our results are indistinguishable within the analytical uncertainty of our measurements, and because of other geologic considerations, we favor the interpretation that our Vaqueros samples are very close to the same age but have yielded different $^{87}\text{Sr}/^{86}\text{Sr}$ values.

The Vaqueros Formation is approximately 24.7 ± 1 Ma in four of our sections (average of apparent ages) and slightly older, 26.3 ± 1 Ma, at a fifth section (#74) in the Pismo syncline. At a sixth section near Villa Creek, where we measured $^{87}\text{Sr}/^{86}\text{Sr}$ in two beds, the isotope data indicate that the basal Vaqueros bed is apparently younger than the overlying bed. No data from this outcrop indicate that this older (26.3 ± 1 Ma) over younger (24.9 ± 1 Ma) relationship is geologically reasonable. Therefore, although our data do not clearly show that the basal Vaqueros beds are the same age in all our sections, we believe that this is the most plausible interpretation of our results because the difference between the two apparent ages at Villa Creek and their inverted relationship, as well as the apparent age differences between our other five sections, could be a result of either the precision of our measurements or slight diagenetic alteration of the original seawater strontium ratio.

The range in our strontium isotope ratios can be accounted for within the precision of our measurements. However, we cannot rule out minor diagenetic effects, although we carefully screened for them and eliminated some shell material from strontium analysis because of obvious alteration, based on both visual examination and chemical analyses. In most areas the trend of isotope alteration is toward higher ratios, but in areas of rapid Cenozoic sedimentation it is not unusual to find pore waters containing strontium with a lower ratio (Denison and others, 1993). Another recently documented potential influence on the strontium isotope ratios of mollusks in marginal marine settings is freshwater flux (Bryant and others, 1995). However, because of the consistency of our data set over a broad geographic region, and also based on independent geologic data, we consider the effects of diagenesis and freshwater flux, if present in our samples, to be minor. We have no evidence to indicate which of our isotope values is closest to the original seawater ratio.

Most of the geologic data indicate that this late Oligocene transgression happened rapidly and at essentially the same time throughout the region, as well as in adjacent areas to the south and southeast (Lagoe, 1988; Rigsby, 1989, 1996; Howard, 1995). We thus conclude from the isotope data that the basal part of the Vaqueros Formation of this region was deposited during the latest Oligocene or near the Oligocene-Miocene boundary (26.4 ± 1 to 24.4 ± 1 Ma). This conclusion is supported by independent evidence for the age of regional bounding strata. At the sections (1) in Green Valley, (2) about 5 mi southeast of our Villa Creek section, and (3) about 3 mi north of San Luis Obispo, mudrocks overlying the Vaqueros contain

Table 1. Sample data and $^{87}\text{Sr}/^{86}\text{Sr}$ analyses for shell fragments from the Vaqueros Formation

Laboratory sample ID	Field ID and location	Percent insoluble	¹ $^{87}\text{Sr}/^{86}\text{Sr}$	² ΔSW	³ Apparently equiv. (Ma) age	Remarks
8942	# 9 Pismo syncline	0.9	0.708127±24	-94.6	24.6±1	Pecten fragments
8943	#47 Pismo syncline	1.0	.708135±23	-93.8	24.4±1	Oyster fragments
8945	#74 Pismo syncline	0.3	.708041±32	-103.2	26.3±1	Oyster fragments
8990	#117 Green Valley	0.5	.708100±19	-97.3	25.1±1	Mollusk
12224 HP2	#229 Villa Creek	<0.1	.708032±26	-104.1	26.4±1	Pecten fragments
12224 HP3	#229 Villa Creek	<0.1	.708043±13	-102.7	26.2±1	Pecten fragments
12225 HP	#231 Villa Creek	<0.1	.708109±19	-96.4	24.9±1	Pecten fragments
12226 HP	#245 Green Valley	<0.1	.708117±33	-95.6	24.8±1	Fibrous oyster fragments

¹ $^{87}\text{Sr}/^{86}\text{Sr}$ normalized to NBS 987 = 0.71014. Quoted precision is 95 percent confidence level for mass spectrometer runs.

² $\Delta\text{SW} = ({}^{87}\text{Sr}/^{86}\text{Sr} \text{ unknown} - {}^{87}\text{Sr}/^{86}\text{Sr} \text{ modern seawater}) \times 10^5$. Modern seawater = 0.709073.

³ Apparently equivalent age is from the seawater curve of Oslick and others (1994) based on the geomagnetic polarity time scale of Cande and Kent (1992).

earliest Miocene (zone CN1) calcareous nannofossils. New $^{40}\text{Ar}/^{39}\text{Ar}$ data for the underlying Cambria Felsite give its age as 27 ± 1 Ma (M.E. Tennyson, M.A. Keller, and others, 1991, unpublished data—1996). Further strontium isotopic age resolution will require carefully chosen and screened shell samples, more analyses from the same bed, and also $^{87}\text{Sr}/^{86}\text{Sr}$ dating of foraminifers in the overlying mudrock.

TRACE ELEMENT CHEMISTRY

Quantitative trace element analysis is a valuable technique for determining which carbonate samples are likely to have retained the original seawater $^{87}\text{Sr}/^{86}\text{Sr}$ ratio. Denison and others (1994) determined that the concentrations of Sr, Mn, and Fe varied most systematically with diagenetic alteration. They found that shelf limestones high in Sr and low in Fe and Mn are most likely to have retained the original seawater $^{87}\text{Sr}/^{86}\text{Sr}$ ratio. If the Mn content is larger than 300 ppm and the Sr/Mn ratio is less than 2.0, the original $^{87}\text{Sr}/^{86}\text{Sr}$ value is likely to be

altered. Jones and others (1994) found that increases in Fe and, to a lesser extent, Mn signaled a potentially changed $^{87}\text{Sr}/^{86}\text{Sr}$ value in Jurassic belemnites and oysters; shells with less than 150 ppm Fe and less than 25 ppm Mn were found to be most reliable.

Major and trace elements were determined on five samples using ICP (Induction Coupled Plasma) spectrometry at Mobil Research Labs in Dallas, Texas. In table 2 we report five such analyses, but only four were analyzed for strontium isotopes. The first three analyses are from different shells taken from the same bed (#229). The first sample listed (#12224 HP1) was eliminated owing to elevated Fe, Ba, and Mn contents before isotope analysis. The second and third shells from this same bed yielded very similar strontium isotope results and appear to have run well, yet they are from the Villa Creek section, which has an apparent inverted age relationship. The basal Vaqueros Formation (#12225 HP) in this same section has the highest Sr/Mn value and yielded a younger equivalent age. Our final sample from Green Valley (#12226 HP) has a very high Mn content, yet it yields an age similar to most of

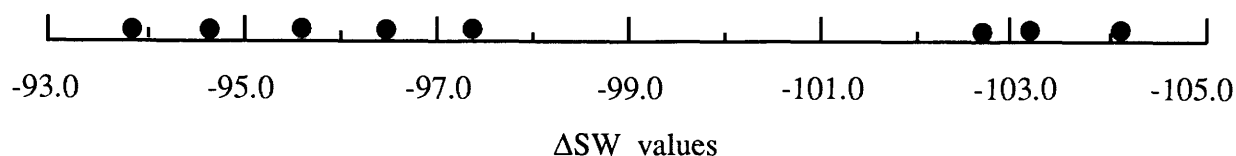


Figure 3. Plot of ΔSW values from table 1. Note that all points represent single data values for basal Vaqueros Formation sections except for three values from the Villa Creek section (-96.4 from the basal bed and -102.7 and -104.1 from the overlying bed).

Table 2. Chemical analyses of selected shell fragments from the Vaqueros Formation

Laboratory sample ID	CaO	MgO weight percent	Na ₂ O weight percent	K ₂ O weight percent	Fe (ppm)	Ba (ppm)	Sr (ppm)	Mn (ppm)	Zn (ppm)	P (ppm)	Ti (ppm)	Rb (ppm)
	THEO weight percent											
12224 HP1	55.257	0.090	0.247	0.222	570	334	558	587	<137	91	<69	<344
12224 HP2	55.260	.097	.182	.309	242	313	807	350	<137	87	<68	<342
12224 HP3	55.386	.094	.189	.216	154	110	803	295	<143	72	<72	<358
12225 HP	55.426	.102	.192	.162	259	97	859	179	<135	85	<67	<337
12226 HP	55.040	.229	.199	.310	68	<33	347	2000	<133	93	<67	<334

¹CaO THEO = theoretical CaO in CaCO₃.

the other samples from the basal part of the Vaqueros sections in our study.

SUMMARY AND CONCLUSIONS

In this study we measured strontium isotopes on eight mollusk samples from six Vaqueros Formation sections in five different areas of the northern Santa Maria province—in Green Valley, near Villa Creek almost due south of Black Mountain, and at three sites along the northern limb of the Pismo syncline. Samples from two additional areas on the southern limb of the Pismo syncline proved to be unsuitable due to diagenesis. Trace elements were analyzed on four of the eight samples as an additional criterion to determine whether diagenesis had altered the original shell chemistry of these mollusks. The high Sr content, small amount of insoluble residue, and low Mn and Fe contents for three of these samples indicate that their strontium isotope ratios are likely to have retained the original seawater ⁸⁷Sr/⁸⁶Sr value, yielding apparent ages of 26.4±1 to 24.9±1 Ma. Because this range is very similar to the age range determined for the other five samples (26.3±1 to 24.4±1 Ma), even one which has an anomalously high Mn content, we believe that the age of the basal part of the Vaqueros and the timing of the marine transgression that it represents fall within this range of late Oligocene to within error of the Oligocene-Miocene boundary.

These results suggest a relatively short time period, previously not recognized, for the initiation of Vaqueros Formation deposition throughout this area. The duration of deposition cannot be determined in this region using strontium isotopes because most Vaqueros sections contain megafossils only near the basal section. In one section, where mollusks from two beds were analyzed, the apparent ages may be reversed, although the results are not distinguishable beyond analytical uncertainty. Nonetheless, there is surprising consistency in the determined ages, and consistency is one of the most powerful criteria for retention of the original isotope ratio. We interpret

these ages to be close to the time of deposition of the Vaqueros Formation. Independent confirmation of this interpretation comes from earliest Miocene nannofossils in overlying mudrocks and from ⁴⁰Ar/³⁹Ar data indicating an age of 27±1 Ma for the underlying Cambria Felsite (M.E. Tennyson, M.A. Keller, and others, 1991, unpublished data—1996). We conclude that the sequence of events beginning with eruption of the Cambria Felsite, followed by deposition of nonmarine conglomerate and subsequent deposition of shallow-marine conglomerate and sandstone of the Vaqueros happened rapidly over a short period of time during the latest Oligocene.

ACKNOWLEDGMENTS

We thank the Fitzhughs, Nicholsons, and Bassis for access to their land. We also thank the Pacific Gas and Electric Corporation for access to the Diablo Canyon area and Sally Krenn for assistance with logistics and collecting samples. We are grateful to Mobil Research and Development Corporation for providing isotope and ICP data. T.H. McCulloh helped get the project going at Mobil, Argell Fletcher did the isotope analyses, and W.K. Blank made the strontium separations. We also thank B. J. Welton for identifying fish teeth from one of our Vaqueros sites and interpreting their probable environment of deposition. P.J. Quintero, Hugh McLean, and J.G. Vedder provided helpful discussions. J.G. Arth, C.A. Rigsby, and T.H. McCulloh provided very helpful reviews.

REFERENCES CITED

- Bryant, J.D., Jones, D.S., and Mueller, P.A., 1995, Influence of freshwater flux on ⁸⁷Sr/⁸⁶Sr chronostratigraphy in marginal marine environments and dating of vertebrate and invertebrate faunas: *Journal of Paleontology*, v. 69, no. 1, p. 1-6.
- Cande, S.C., and Kent, D.V., 1992, A new geomagnetic polarity time scale for the Late Cretaceous and Cenozoic: *Journal of*

- Geophysical Research, v. 97, no. B10, p. 13,917-13,951.
- Denison, R.E., Koepnick, R.B., Fletcher, A., Dahl D.A., and Baker, M.C., 1993, Reevaluation of early Oligocene, Eocene, and Paleocene seawater strontium isotope ratios using outcrop samples from the U.S. Gulf Coast: *Paleoceanography*, v. 8, p. 101-126.
- Denison, R.E., Koepnick, R.B., Fletcher, A., Howell, M.W., and Callaway, W.S., 1994, Criteria for the retention of original seawater $^{87}\text{Sr}/^{86}\text{Sr}$ in ancient shelf limestones: *Chemical Geology (Isotope Geosciences Section)*, v. 112, p. 131-143.
- Edwards, L.N., 1971, *Geology of the Vaqueros and Rincon Formations, Santa Barbara Embayment, California*: Santa Barbara, Calif., University of California, Ph.D. thesis, 240 p.
- Ernst, W.G., and Hall, C. A., 1974, *Geology and petrology of the Cambria Felsite, a new Oligocene formation, west-central California Coast Ranges*: *Geological Society of America Bulletin*, v. 85, p. 523-532.
- Fisher, R.V., 1977, *Geologic guide to subaqueous volcanic rocks in the Nipomo, Pismo Beach, and Avila Beach areas*: The Geological Society of America Penrose Conference on the Geology of Subaqueous Volcanic Rocks, November 30, 1977, 29 p.
- Hall, C. A., Jr., 1973a, *Geology of the Arroyo Grande 15' quadrangle, San Luis Obispo County, California*: California Division of Mines and Geology, Map Sheet 24, scale 1:48,000.
- 1973b, *Geologic map of the Morro Bay South and Port San Luis quadrangles, San Luis Obispo County, California*: U.S. Geological Survey Miscellaneous Field Studies Map MF-511, scale 1:24,000.
- 1974, *Geologic map of the Cambria region San Luis Obispo County, California*: U.S. Geological Survey Miscellaneous Field Studies Map MF-599, scale 1:24,000.
- Hall, C.A., Jr., Ernst, W.G., Prior, S.W., and Wiese, J.W., 1979, *Geologic map of the San Luis Obispo - San Simeon region, California*: U.S. Geological Survey Miscellaneous Investigations Series Map I-1097, scale 1:48,000.
- Hall, C. A., Jr., and Prior, S.W., 1975, *Geologic map of the Cayucos-San Luis Obispo region, San Luis Obispo County, California*: U.S. Geological Survey Miscellaneous Field Studies Map MF-686, scale 1:24,000.
- Hess, J., Stott, L.D., Bender, M.L., Kennett, J.P., and Schilling, J.G., 1989, The Oligocene marine microfossil record: age assignments using strontium isotopes: *Paleoceanography*, v. 4, p. 655-679.
- Howard, J.L., 1995, *Conglomerates of the upper middle Eocene to lower Miocene Sespe Formation along the Santa Ynez Fault—Implications for the geologic history of the eastern Santa Maria basin*, in Keller, M.A., ed., *Evolution of sedimentary basins/onshore oil and gas investigations—Santa Maria province*: U.S. Geological Survey Bulletin 1995-H, 37 p.
- Jones, C.E., Jenkyns, H.C., and Hesselbo, S.P., 1994, *Strontium isotopes in Early Jurassic seawater*: *Geochimica et Cosmochimica Acta*: v. 58, p. 1285-1301.
- Lagoe, M.B., 1988, *An outline of foraminiferal biofacies in the Soda Lake Shale member, Vaqueros Formation, Cuyama basin*, in Bazeley, W.J.M., ed., *Tertiary tectonics and sedimentation in the Cuyama basin, San Luis Obispo, Santa Barbara, and Ventura Counties, California*: Pacific Section, Society for Sedimentary Geology, v. 59, p. 21-27.
- Loel, W., and Corey, W.H., 1932, *The Vaqueros Formation, lower Miocene of California*; I. Paleontology: University of California Publications, v. 22, p. 31-410.
- Miles, G.A., and Rigsby, C.A., 1990, *Lithostratigraphy and depositional environments of the Vaqueros and upper Sespe/Alegria Formations, Hondo Field, Santa Barbara Channel, California*, in Keller, M.A. and McGowen, M.K., eds., *Miocene and Oligocene petroleum reservoirs of the Santa Maria and Santa Barbara-Ventura basins, California*: Society for Sedimentary Geology, Core Workshop No. 14, p. 39-87.
- Miller, K.G., Feigenson, M.D., Kent D.V., and Olsson, R.K., 1988, *Upper Eocene to Oligocene isotope ($^{87}\text{Sr}/^{86}\text{Sr}$, ^{18}O , ^{13}C) standard section, Deep Sea Drilling Project site 522*: *Paleoceanography*, v. 3, p. 223-233.
- Oslick, J.S., Miller, K.G., and Feigenson, M.D., 1994, *Oligocene-Miocene strontium isotopes: stratigraphic revisions and correlations to an inferred glacioeustatic record*: *Paleoceanography*, v. 9, no. 3, p. 427-443.
- Prior, S.W., 1974, *Geology and Tertiary biostratigraphy of a portion of western San Luis Obispo County, California*: Los Angeles, Calif., University of California, M.S. thesis, 195 p.
- Rigsby, C.A., 1989, *Depositional environments, paleogeography, and tectonics and eustatic implications of the Oligocene-early Miocene Vaqueros Formation in the Western Transverse Ranges, California*: Santa Cruz, Calif., University of California, Ph.D. thesis, 144 p.
- 1994, *Deepening upward sequences in Oligocene fan-delta deposits, western Santa Ynez Mountains, California*: *Journal of Sedimentary Research*, B64, p. 380-391.
- 1996, *Paleogeography of the Western Transverse Ranges province, California: new evidence from the late Oligocene-early Miocene Vaqueros Formation*, in Keller, M.A., ed., *Evolution of sedimentary basins/onshore oil and gas investigations—Santa Maria Province*: U.S. Geological Survey Bulletin 1995 (in press).
- Rigsby, C.A., and Schwartz, D.A., 1990, *Lithostratigraphy and depositional environments of the Vaqueros Formation, Capitan Field, California*, in Keller, M.A. and McGowen, M.K., eds., *Miocene and Oligocene petroleum reservoirs of the Santa Maria and Santa Barbara-Ventura basins, California*: Society for Sedimentary Geology, Core Workshop No. 14, p. 88-136.
- Schneider, J.-L., and Fisher, R.V., 1996, *Obispo Formation, California: remobilized pyroclastic material*, in Keller, M.A., ed., *Evolution of sedimentary basins/onshore oil and gas investigations—Santa Maria province*: U.S. Geological Survey Bulletin 1995 (in press).
- Tennyson, M.E., Keller, M.A., Filewicz, M.V., Thornton, M.L., and Vork, D.R., 1990, *Early Miocene sedimentation and tectonics in western San Luis Obispo County, central California [abs]*: *American Association of Petroleum Geologists Bulletin*, v. 74, no. 5, p. 777.
- Tennyson, M.E., Keller, M.A., Filewicz, M.V., and Cotton Thornton, M.L., 1991, *Contrasts in early Miocene subsidence history across Oceanic-West Huasna fault system, northern Santa Maria province, California [abs]*: *American Association of Petroleum Geologists Bulletin*, v. 75, no. 2, p. 383.
- Turner, D.L., 1968, *Potassium-argon dates concerning the Tertiary foraminiferal time scale and San Andreas displacement*: Berkeley, Calif., University of California, Ph.D. thesis, 99 p.
- Turner, D.L., Surdam, R.C., and Hall, C.A., Jr., 1970, *The Obispo Formation and associated volcanic rocks in the central California Coast Ranges—K-Ar ages and biochronologic significance [abs]*: *Geological Society of America Abstracts with Programs (Cordilleran Section)*, v. 2, no. 2, p. 155.

Chapter Q

Stratigraphic Sections and Gamma-Ray
Spectrometry from Five Outcrops of the
Monterey Formation in Southwestern California:
Naples Beach, Point Pedernales, Lion's Head,
Shell Beach and Point Buchon

By JON R. SCHWALBACH and KEVIN M. BOHACS

U.S. GEOLOGICAL SURVEY BULLETIN 1995–Q

EVOLUTION OF SEDIMENTARY BASINS/ONSHORE OIL AND GAS INVESTIGATIONS—
SANTA MARIA PROVINCE

Edited by Margaret A. Keller

CONTENTS

Abstract	Q1
Introduction	Q1
Acknowledgments	Q2
Data collection	Q2
Lithofacies	Q2
Gamma-ray spectrometry	Q3
Data resolution	Q4
Rock composition, elemental concentrations, and gamma-ray spectra	Q4
Prediction of total organic carbon from uranium	Q8
Prediction of detritus from potassium	Q11
Estimation of source-rock quality	Q11
Stratigraphic sections of the Monterey Formation	Q11
Naples Beach outcrop	Q11
Lithostratigraphy and gamma-ray spectra	Q14
Point Pedernales outcrop	Q17
Lithostratigraphy and gamma-ray spectra	Q17
Lion's Head outcrop	Q20
Lithostratigraphy and gamma-ray spectra	Q20
Shell Beach outcrop	Q22
Lithostratigraphy and gamma-ray spectra	Q22
Point Buchon outcrop	Q29
Lithostratigraphy and gamma-ray spectra	Q30
Discussion and conclusions	Q33
References cited	Q35

FIGURES

1. Base map of study area, illustrating the location of the five outcrop sections and the offshore wells referenced in this study **Q2**
2. Ternary diagram illustrating approximate composition of lithofacies of the Monterey Formation **Q3**
3. Schematic diagram of data-collection techniques using the gamma-ray spectrometer at the outcrop **Q5**
4. Elemental data from outcrop samples compared with gamma-ray spectrometer survey for Shell Beach **Q6**
5. Elemental data from outcrop samples compared with gamma-ray spectrometer survey for Point Buchon **Q7**
6. Potassium (percent) vs. aluminum (percent) cross-plot **Q8**
7. Thorium (ppm) vs. aluminum (percent) cross-plot **Q9**
8. Uranium (ppm) vs. TOC (percent) for Naples Beach outcrop samples **Q9**
9. Predicted TOC from spectrometer data compared with laboratory-measured values for Naples Beach **Q10**
10. Measured and predicted TOC for offshore 408-1 well **Q10**
11. Comparison of trends for potassium/uranium and aluminum/TOC ratios and TOC content for the Naples Beach outcrop section **Q12**
12. Microfossil zonations and spectral gamma-ray data from Naples Beach outcrop **Q13**

13. Stratigraphic section from Naples Beach outcrop with accompanying gamma-ray survey **Q14**
- 14–15. Photographs showing:
 14. Naples Beach outcrop at 438 ft **Q16**
 15. Naples Beach outcrop at 732 ft illustrating phosphatic-rich strata in condensed interval **Q16**
16. Stratigraphic section from Point Pedernales outcrop with accompanying gamma-ray survey **Q18**
- 17A, B. Photographs of slump-folded strata at Point Pedernales, 1,080 and 1,325 ft above the base of the section **Q19**
18. Stratigraphic section from Lion's Head outcrop with accompanying gamma-ray survey **Q21**
19. Magnetostratigraphy correlated to the spectral gamma-ray profile of Shell Beach **Q23**
20. Shell Beach outcrop location map **Q24**
21. Stratigraphic section from Shell Beach outcrop with accompanying gamma-ray survey **Q25**
- 22–27. Photographs showing:
 22. Shell Beach outcrop illustrating disrupted, slump-folded beds between 170 and 180 ft **Q26**
 23. Shell Beach outcrop at 233 ft **Q26**
 24. Shell Beach outcrop at 286 ft **Q27**
 25. Shell Beach outcrop at 370 ft **Q27**
 26. Shell Beach outcrop at 1082 ft **Q28**
 27. Burrowed sandstone of the Pismo Formation **Q29**
 28. Location map of Point Buchon measured section **Q30**
 29. Stratigraphic section from Point Buchon outcrop with accompanying gamma-ray survey **Q31**
- 30–32. Photographs showing:
 30. Point Buchon outcrop from 184 ft **Q32**
 31. Point Buchon outcrop from 600 to 640 ft **Q32**
 32. Point Buchon outcrop from 1,356 ft **Q33**
 33. Stratigraphic cross sections of (A) Naples Beach to Point Pedernales to Lion's Head and (B) Lion's Head to Shell Beach to Point Buchon **Q34**
 34. Correlation of single sequence between Point Pedernales and Naples Beach **Q36**
 35. Stratigraphic cross section of lower part of the Monterey Formation between the Shell Beach outcrop and the 427-1 well from the offshore Santa Maria Basin **Q37**

TABLE

1. Field characterization of lithotypes of the Monterey Formation **Q4**

Stratigraphic Sections and Gamma-Ray Spectrometry from Five Outcrops of the Monterey Formation in Southwestern California: Naples Beach, Point Pedernales, Lion's Head, Shell Beach, and Point Buchon

By Jon R. Schwabach¹ and Kevin M. Bohacs²

Abstract

The combination of detailed outcrop descriptions and natural gamma-ray spectrometry is a powerful method for the interpretation of fine-grained strata. The gamma-ray spectra of outcrop sections of the Monterey Formation reveal many compositional and stratigraphic aspects: lithologic variation, organic matter content, hydrocarbon source quality, and stratal stacking. These data, when regionally distributed and combined with chronostratigraphic data, enable the identification of significant stratigraphic surfaces, the development of sequence stratigraphic frameworks, and the assessment of depositional processes and controls.

Based on the evaluation of five outcrop sections of the Monterey Formation, potassium (K) and thorium (Th) are indicators of detritus content ($r^2 = 0.75$ vs. Al_2O_3); high levels of thorium occur coincident with volcanic ash beds; uranium (U) correlates with total organic carbon content (TOC; $r^2 = 0.80$); and K/U correlates with hydrocarbon source quality measured by alumina/TOC.

Utilizing the strong dependence of gamma-ray spectra on lithologic composition, the variable but generally good quality of age control for some of the outcrops, and the broad geographic distribution of the outcrops, we have clearly shown that the lithofacies comprising the Monterey Formation are time transgressive. Thus, the data are particularly valuable for constraining depositional models within a stratigraphic framework. The outcrop gamma-ray data are also essentially equivalent to the gamma-ray data collected from borehole logging tools, and therefore they provide a critical link between outcrop observations and subsurface prediction.

INTRODUCTION

This paper presents data for five measured sections of the Monterey Formation located in southwestern California. These five measured sections are from well exposed coastal outcrops at Point Buchon, Shell Beach, Lion's Head, Point Pedernales, and Naples Beach (fig. 1). The outcrops occur over a broad geographic area and exhibit significant lateral and vertical stratal variability.

Studies of fine-grained rocks are often hindered by our inability to quantify compositional variation during outcrop description. Particularly in the Monterey Formation, the fine-grained nature of the strata, the overprint of silica diagenesis, and the subtle textural variation limit our field descriptions to a qualitative assessment of rock composition (Isaacs, 1981a). We collected spectral gamma-ray surveys of the outcrops in conjunction with sedimentologic and stratigraphic descriptions as a method of quantifying key components of rock composition. The detailed lithostratigraphy, in conjunction with the gamma-ray data, is a critical element for our interpretation. The links between the composition and the physical stratigraphy, reflected by lamina, bed, and bedset geometry and by the stratal stacking of the lithofacies, are emphasized. Identifying major stratal surfaces and deciphering indicators of bottom energy levels add important dimensions to the interpretive scheme (Bohacs and Schwabach, 1992).

Natural gamma-ray spectrometry measures the distribution of three elements in sedimentary rocks: uranium (U), potassium (K), and thorium (Th). The distribution of these elements reflects the composition of the lithofacies comprising the Monterey Formation. Potassium and thorium are reliable indicators of detritus ($r^2=0.75$ vs. Al_2O_3), although high levels of thorium are also associated with volcanic ash beds. Total organic carbon content (TOC) is accurately predicted from uranium ($r^2=0.80$). The ratios of these elements (such as K/U) have been used to predict source-rock quality (Bohacs, 1993; Bohacs and Schwabach, 1994).

¹Exxon Company, USA, P.O. Box 5025, Thousand Oaks, CA, 91359.

²Exxon Production Research Company, P.O. Box 2189, Houston, TX, 77252.

Thus, the gamma-ray spectra provide compositional data that help to reveal lithologic variation, stratal stacking patterns, and significant stratigraphic surfaces. These data have been interpreted in terms of mudrock depositional environments (Zelt, 1985; Myers and Wignall, 1987; Bohacs and Schwalbach, 1992). Spectral gamma-ray profiles of outcrop sections are useful for regional correlations and provide a crudely quantitative comparison of different outcrop sections. Since the outcrop data are essentially equivalent to data collected by the Natural Gamma-Ray Tool (NGT) from boreholes, outcrops can also be correlated to subsurface well bores (Schwalbach and Bohacs, 1992b).

ACKNOWLEDGMENTS

We thank many people whose efforts contributed to this paper. Numerous workers at Exxon participated in regional studies of the Monterey Formation during the middle 1980's. We benefited from technical discussions with Caroline Isaacs and Margaret Keller of the U.S. Geological Survey, along with many others associated with the Survey's Santa Maria Province Project. Keller, Mark Richardson (Exxon), Ken Bird (U.S. Geological Survey), and Mitch Lyle (Boise State University) reviewed the manuscript and suggested numerous improvements. Schwalbach also thanks Donn Gorsline (University of

Southern California) for arranging funding for his dissertation research at Shell Beach and Point Buchon. Finally, Exxon Co., U.S.A., and Exxon Production Research Co. approved information releases that enabled us to publish these results.

DATA COLLECTION

Lithofacies

The fine-grained nature of the rocks comprising the Monterey Formation hinders megascopic determination of composition. A number of excellent field guides have been published that deal with the complexities of lithologic description of the Monterey Formation (Bramlette, 1946; Isaacs, 1980, 1981a, b; Dunham and Blake, 1987). These publications provide rock-naming schemes based on outcrop observations and simple physical tests that can be conducted in the field. Isaacs (1981a) has investigated the reliability of these tests to discern mineralogic composition and has reported on some of the limitations.

The most complete descriptions of these fine-grained rocks integrate results from mineral identification by X-ray diffraction, major element composition from X-ray fluorescence, petrography, and analysis of physical properties. The basis for lithofacies designation in this study rests predomi-

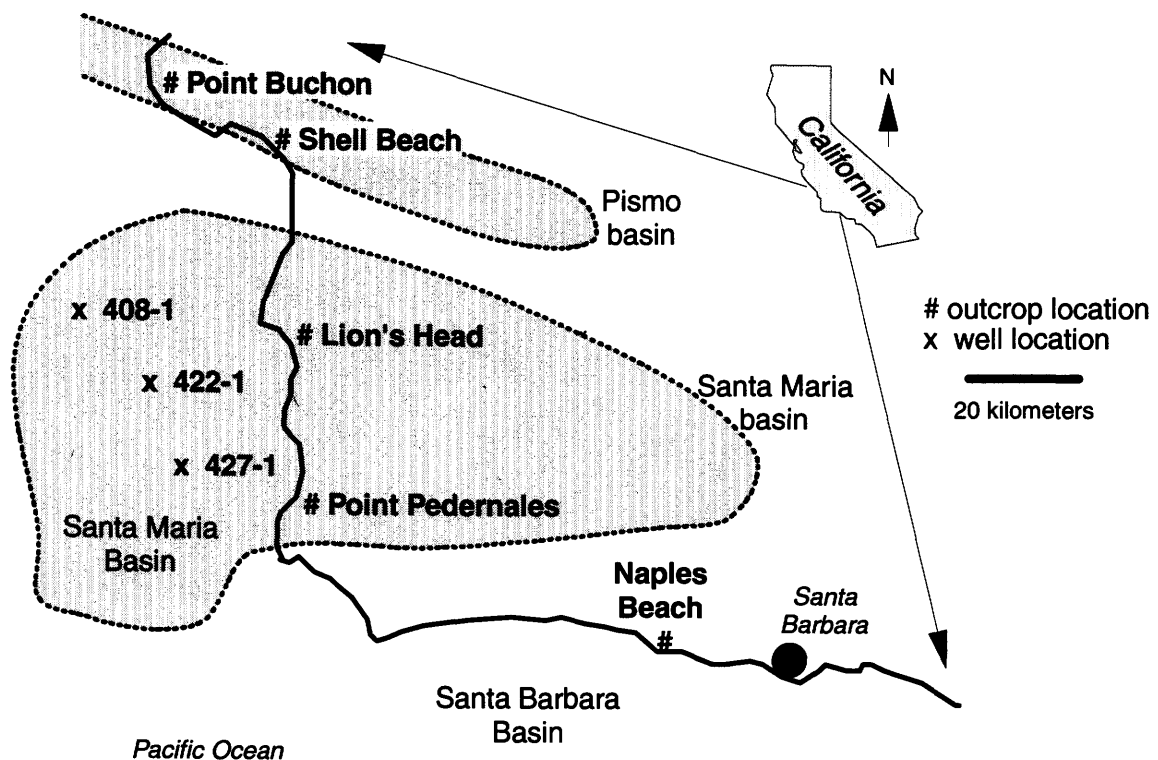


Figure 1. Base map of study area, illustrating the location of the five outcrop sections and the offshore wells referenced in this study.

nantly on the excellent work of Isaacs (1980, 1981a,b), with some slight modifications suggested by Dunham and Blake (1987) and Bohacs (1990). Isaacs' initial work followed descriptions offered by Bramlette (1946), Keene (1975), and Murata and Larson (1975). She showed that compositional variations are partially reflected in the physical properties of the rocks. However, differences in porosity and diagenetic grade also affect physical rock properties and make precise assessment of composition based on physical properties impractical. The large component of biogenic silica and the processes of silica diagenesis cause textural variations that are only partly related to rock composition.

Most lithofacies schemes characterize the rocks of the Monterey Formation within a three-component system, comprising varying amounts of biogenic silica, detritus, and carbonate. Relatively minor components, such as apatite and pyrite, are difficult to fit into these schemes. Their presence and abundance, however, provide valuable insights about depositional environment and diagenesis. A very generalized ternary lithology diagram that identifies compositional fields for most common Monterey rock types is shown in figure 2. Major fine-grained lithofacies described in the outcrop sections include dolomite and (or) limestone, chert, porcelanite, siliceous shale, clay shale, and phosphatic shale. The compositions of these fields are not rigidly defined because the rock-naming schemes are at least in part based on textural and physical properties.

Neatly classifying the lithofacies of the Monterey Formation is also complicated by the presence of additional rock types. Volcanic ash beds, phosphates, siltstones, sandstones, and conglomerates occur in Monterey strata. Isaacs (1981a) notes the high degree of compositional variability that can

occur on the bed (centimeter) to lamina (millimeter) scales. Dunham and Blake (1987) point out the gradational spectrum between porcelanite, siliceous shale, and clay shale, and the subjectivity of assigning lithofacies based solely on physical criteria.

The criteria used during this study (a modification of a scheme offered by Bohacs, 1990) for field classification of Monterey lithofacies are summarized in table 1. Most of these criteria agree fundamentally with characteristics designated for lithofacies by Isaacs (1981a,b) and Dunham and Blake (1987), and the schemes may be used nearly interchangeably. However, the limitations of physical and textural-based schemes remain.

Despite the limitations of lithotype designation in the field, careful analysis and classification of the fine-grained Monterey rocks using physical criteria can be used to assess relative compositional variation. The proportions of clay shale, siliceous shale, and porcelanite (each with progressively less detritus content, respectively) co-vary with the thorium and potassium concentrations (indicators of detritus) as measured by the outcrop gamma-ray spectrometer. Some of our outcrop data illustrate this relation. For example, in carbonate-free rocks, the silica/detritus ratio relates to physical rock properties such as resistance to erosion, brittleness and fracture character, hardness, texture, and sound emitted by hammer tap (Isaacs, 1981a). Petrographic work, elemental analysis by X-ray fluorescence, and sample reaction to HCl indicate that the Point Buchon section is relatively carbonate free. Therefore, physical characteristics and spectral gamma-ray data reflect compositional variation at Point Buchon in a reasonably straightforward manner.

Gamma-Ray Spectrometry

A gamma-ray survey was collected during lithostratigraphic description of the outcrops at Naples Beach, Point Pedernales, Shell Beach, and Point Buchon. At Lion's Head, the measured section published by Dunham and Blake (1987) served as a framework for collecting the gamma-ray survey. We used a hand-held gamma-ray spectrometer (Scintrex GAD-6, with a sodium iodide crystal detector, GSP-3S; see Scintrex, 1979) to measure total gamma radiation and the individual contributions from uranium, thorium, and potassium.

Gamma radiation was measured for each lithostratigraphic package, provided that the thickness of the package was at least 30–50 cm. The maximum spacing between measurements in homogenous intervals was about 1.5 m. Larger gaps between gamma-ray measurements generally indicate outcrop access problems or covered intervals.

The ideal detector to sample geometry is a flat, planar outcrop surface over an area of approximately 1.5 m². The gamma-ray detector, placed in the center of the sample area, is calibrated to measure the elemental concentration of K (percent), U (ppm), and Th (ppm) for the half-sphere of rock

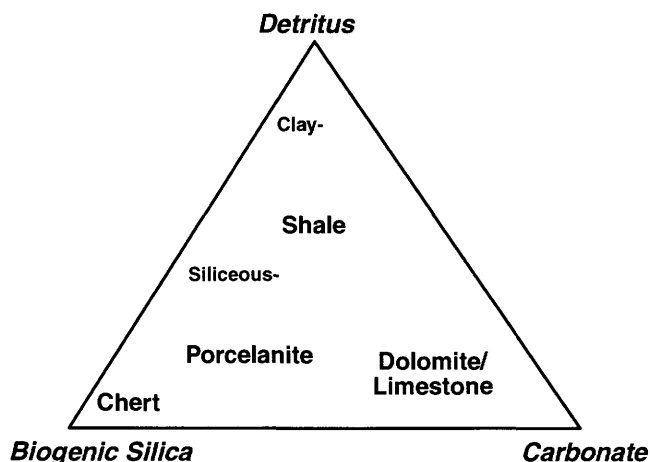


Figure 2. Ternary diagram illustrating approximate composition of lithotypes of the Monterey Formation (from Schwalbach, 1992).

Table 1. Field characterization of lithotypes of the Monterey Formation (modified from Bohacs, 1990).

Attributes	Conglomerate/ Sandstone	Chert	Dolomite	Porcelanite	Siliceous Shale	Clay Shale	Phosphatic Shale
Luster - Fresh surface	Dull, grainy	Glassy, waxy	Dull	Matter	Dull, Matte	Dull, Waxy	Dull
Fracture Character	Grainy	Smooth, Conchoidal	Rough, Splintery	Rough, Splintery	Rough and Rounded	Rough	Rough
Grain size:							
Median	Cgl > 2 mm 0.06 < Ss < 2mm	< 0.002 mm	Clay, Silt	< 0.06 mm	< 0.06 mm	< 0.06 mm	< 0.06 mm
Range	Wide	-----	Wide	-----	----- Silty Mudstone to Clay Shale	-----	-----
Hardness	-----	> Steel (> 5)	≤ Steel (3 to 5)	< Steel (≤ 3)	<< Steel	<< Steel	<< Steel
Luster: Scratch	-----	No scratch	White, dull	White, dull	Dull	Waxy	Waxy
Effervescence in HCl *	None	None	Powder only	None	None	Strong to None (calcareous)	
Nodules:							
Present	As clasts	None	Some	None	Some	Some to none	Abund to some
Color	Dark to light	-----	Dark to light	-----	Dark to light	Dark to light	White, cream
Habit	Rounded	-----	Rounded	-----	--- Rounded to Irregular ---	---	Irregular to rounded
Mineralogy	Apatite, Dolomite, Chert	-----	Chert	-----	-- Dolomite, Chert, Apatite --	---	Apatite

Note: Apatite nodules are soft (< 3) but in general are more resistant to weathering than the surrounding shale; they range in size from < 0.001 to > 5 cm

* Each main siliceous and clay lithology is modified as calcareous or non-calcareous according to effervescence

directly surrounding it. The largest contribution of gamma-ray counts comes from the rocks closest to the detector. Rocks at the outer edge of the sphere contribute to a lesser extent. These geometric constraints as applied to the typical outcrops of the Monterey Formation that we measured are illustrated in figure 3. Our goal during gamma-ray surveying was to match the ideal geometry as much as possible. More specific details of the techniques and a review of some geologic applications can be found in Zelt (1985), Myers and Wignall (1987), and Schwalbach (1992).

Data Resolution

Evaluating the resolution of the elemental data from the spectral gamma-ray data is somewhat subjective. Outcrop samples relate to very specific stratal intervals, typically 1 cm thick. Sample volume is on the order of a cubic centimeter. Outcrop gamma-ray measurements have a much larger sample volume (on the order of cubic meters). Therefore, individual hand samples from outcrop are not strictly compatible with outcrop gamma-ray spectrometer survey points, and the two data sets cannot rigorously be compared using routine statistical techniques.

This situation bears some resemblance to the problem of matching traditional core-plug mineralogic data to various geophysical well logs. One approach has been to use strip samples along the core length to derive volume-averaged min-

eralogy (D. Fitz, Exxon Production Research, Co., written commun., 1986; Isaacs, 1992; Piper and Isaacs, 1995). However, it was not practical nor politically acceptable to conduct such sampling of long stretches of outcrop.

Laboratory-derived data points from hand samples and gamma-ray measurements along the profiles of the Shell Beach and Point Buchon outcrops are compared in figures 4 and 5. In both examples, the values for the hand samples generally bracket the curve generated from the gamma-ray spectrometer survey. The values for the discrete hand samples range higher and lower than the spectrometer values, an expected result given the different sample sizes and the thinly bedded heterogeneous strata.

ROCK COMPOSITION, ELEMENTAL CONCENTRATIONS, AND GAMMA-RAY SPECTRA

First-order controls on the abundance of uranium, potassium, and thorium in sedimentary rocks are depositional environment and diagenesis. The radioactive elements are generally associated with clay minerals, organic matter, heavy minerals such as zircon and rutile, or concentrated in volcanic ash beds. Diagenetic processes can alter these elemental abundances.

The relations among rock composition, elemental concentrations, and spectral gamma-ray data are the basis of this discussion. The link between these parameters provides a

method of facies analysis that integrates megascopic lithotype identification from outcrop and cores, laboratory analysis of these samples, outcrop spectral gamma-ray data, and subsurface spectral gamma-ray data from well logs. Thus, the data from these varied sources can be considered in a compatible format.

Elemental analysis of individual outcrop and core samples by X-ray fluorescence is a proven technique for determining Monterey Formation lithotype and estimating bulk rock constituents (Isaacs, 1981a). In this scheme, aluminum is an excellent indicator of total detritus in the rock. Likewise, phosphorus is used to predict apatite content, and magnesium and calcium concentrations are used to predict dolomite and

calcite contents. Biogenic silica is determined from silicon dioxide after making an allowance for silica content of the detritus material.

Spectral gamma-ray data estimate the potassium, uranium, and thorium content of rocks. None of these elements are part of the scheme used by Isaacs for her rock-component determinations. However, these three elements measured by the spectral gamma-ray data correlate very well with some of the elements used in her calculations.

Potassium correlates with aluminum and is useful for predicting detritus content. A cross-plot of aluminum versus potassium for 323 outcrop and core samples from a variety of localities (Shell Beach, Point Buchon, Point Pedernales, Naples Beach, and offshore well 408-1) is shown in figure 6. The correlation equation ($r^2 = 0.75$) is

$$\text{Al}_2\text{O}_3 \text{ (weight percent)} = 5.38 \times \text{K}_2\text{O (weight percent)} + 0.16.$$

Thorium also correlates with aluminum, except in volcanic ash beds or samples with a high volcanic ash content. A data set of 57 samples is illustrated in figure 7, a cross-plot of aluminum versus thorium from a number of outcrop and core localities. The one outlier in the data set (aluminum = 0.5 percent, thorium = 18 ppm) is a sample with significant volcanic ash content. The coefficient of determination (after eliminating the volcanic-enriched sample) is 0.75. If the zones of volcanic ash are eliminated, then either potassium or thorium, or a combination of the two elements, can be used to predict detritus in rocks of the Monterey Formation. The volcanic ash beds with high thorium content are excellent chronostratigraphic correlation points and provide information about depositional conditions.

The accumulation of both organic matter and uranium in many marine environments is favored by anoxia and low sediment accumulation rates. These relations are reviewed in Langmuir (1978), Zelt (1985), and Schwalbach (1992). These conditions persisted during much of Monterey Formation deposition.

Several factors sometimes obscure this relation in the rock record. Surface outcrops are subjected to a variety of weathering processes that can alter the uranium and TOC content of strata. Leythaeuser (1973) documented a decrease of 25 percent organic matter over the upper 3 m of shallow core holes in the Upper Cretaceous Mancos Shale. Soluble organic matter decreased by 50 percent over the same interval. He attributed much of the reduction to processes such as mechanical disintegration, solution, oxidation, hydrolysis, and microbe attack. Clayton and Swetland (1978) compared organic matter content to weathering profiles in the Pierre Shale and Phosphoria Formation. No decrease in organic matter content was recognized in the Pierre Shale, but TOC in the Phosphoria Formation was up to 60 percent lower in the 2-ft-thick surface-weathering zone. Some of the major factors influencing the preservation of organic matter in near-surface environments

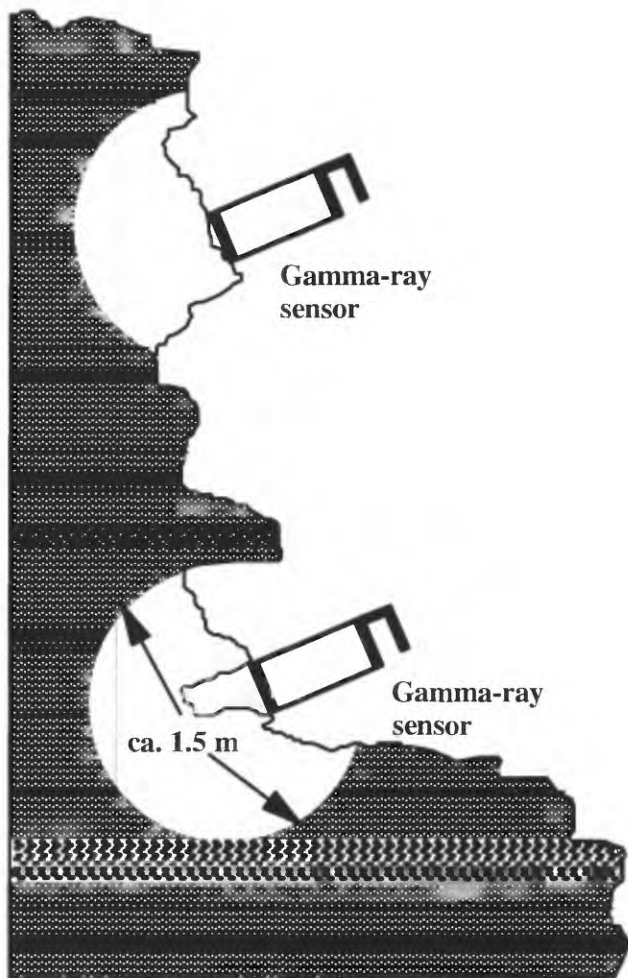


Figure 3. Schematic diagram of data-collection techniques using the gamma-ray spectrometer at the outcrop (from Schwalbach and Bohacs, 1992a). The gamma-ray detector intercepts radiation emitted during the breakdown of potassium (K), uranium (U), and thorium (Th) from the half-sphere of rocks directly surrounding it. The geometry of the outcrop and the placement of the detector influences the volume sampled. We strive to achieve a constant half-sphere sampling in all cases.

include the permeability and porosity of the rocks and the abundance of fractures. The rocks of the Phosphoria Formation have more fractures than those of the Pierre Shale.

Uranium content can also be altered by near-surface diagenetic processes. A critical consideration in uranium's behavior is its high solubility in oxidizing environments. Uranium is very mobile and often leached from zones of near-surface weathering. Zelt (1985) considered this behavior in reference to uranium content of outcrop samples from Upper Cretaceous shales of the U.S. Western Interior. His data reveal a much poorer correlation between sample-measured and spectrometer-measured uranium in weathered outcrops (indicated by alteration of pyrite) than in unweathered outcrops (unaltered pyrite).

Since uranium and TOC content are both affected by surface weathering, it is very important to obtain unaltered samples. This was possible only some of the time during the outcrop sampling.

Composition affects the rock properties in a number of ways. Rocks of the Monterey Formation with high detritus content and low biogenic silica content tend to have lower levels of fracturing in a given structural position (Schwalbach and Lockman, 1988; Schwalbach, 1991). Higher clay content also correlates with lower matrix porosity and permeability in siliceous shales, porcelanites, and dolomites. These factors would tend to minimize the degree of alteration due to surface weathering in detritus-rich strata. Monterey rocks that are composed primarily of biogenic silica tend to have the highest levels of fracturing in a given structural position. These fractures provide excellent pathways for meteoric waters to percolate through the outcrop and increase the potential for surface-related diagenesis.

Samples from the Naples Beach outcrop had the highest detritus and lowest biogenic silica contents of all the outcrop samples that we collected. A cross-plot of TOC versus ura-

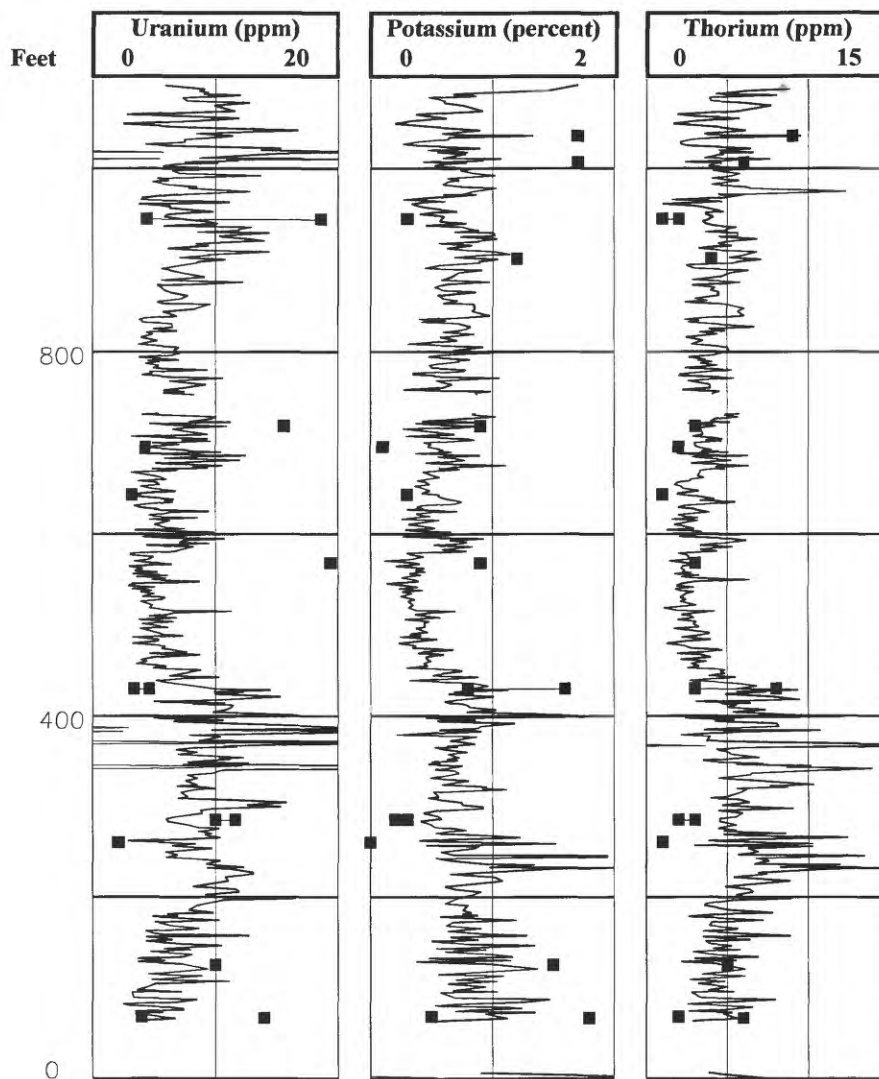


Figure 4. Elemental data from outcrop samples compared with gamma-ray spectrometer survey for Shell Beach. Laboratory-derived values (squares) generally bracket the spectrometer values indicated by the solid line (modified from Schwalbach, 1992).

nium for outcrop samples from Naples Beach ($r^2 = 0.80$) shows excellent correlation (fig. 8). This correlation is interpreted to indicate that the conditions that favored the accumulation and preservation of organic matter in the Monterey Formation also

favored the concentration and preservation of uranium in the sediments, and that the degree of weathering alteration with respect to TOC and uranium has been minimal. These samples were collected specifically as part of a source-rock

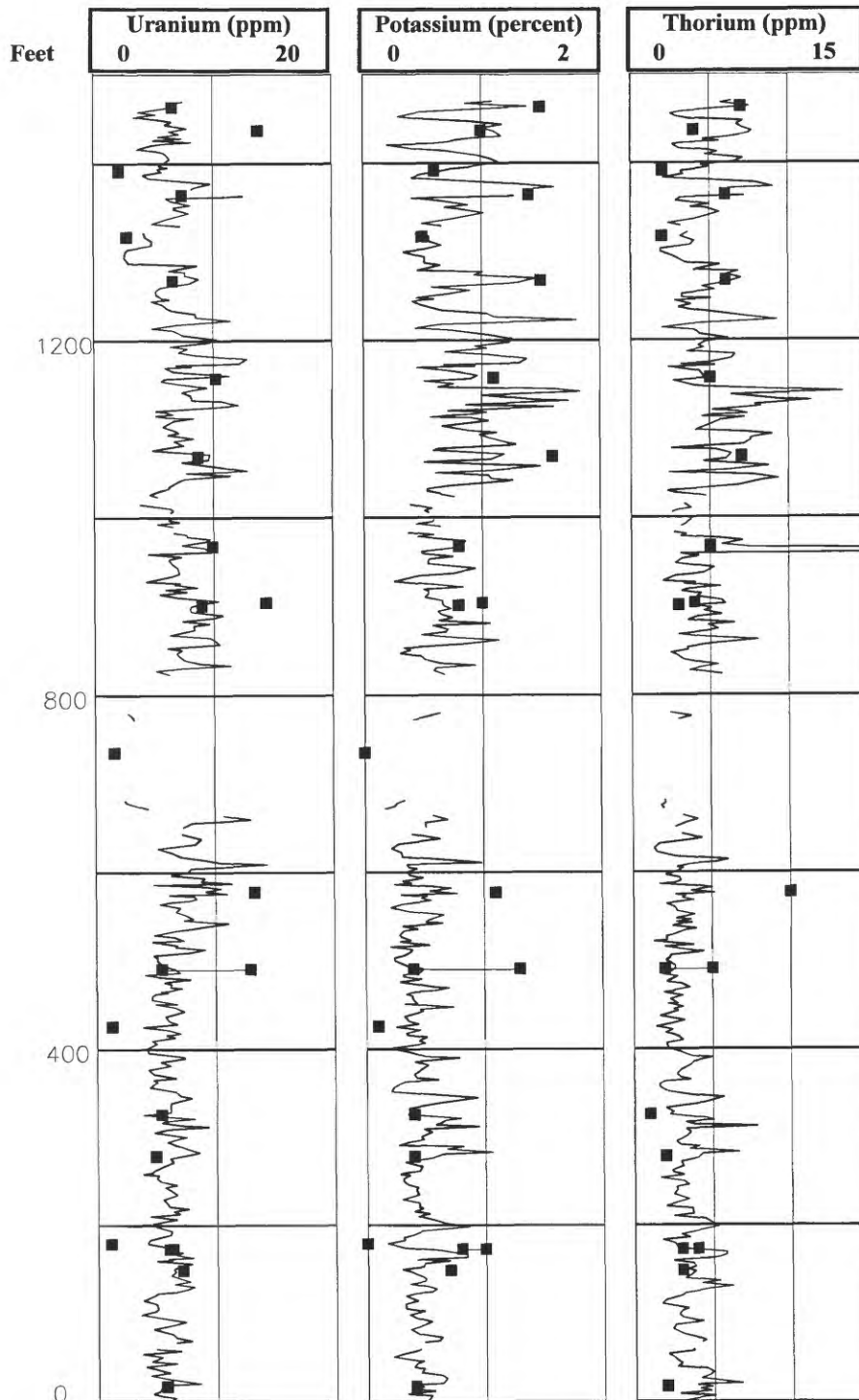


Figure 5. Elemental data from outcrop samples compared with gamma-ray spectrometer survey for Point Buchon. Laboratory-derived values (squares) generally bracket the spectrometer values denoted by the solid line (modified from Schwalbach, 1992).

evaluation, and a major effort was expended to ensure the collection of fresh sample material. As another qualitative measure of degree of alteration, microfossil preservation at Naples Beach is exceptionally good, making this locality a favorite stratigraphic section for micropaleontological studies (see Arends and Blake, 1986; Barron, 1986b).

The sample set collected from the Point Buchon outcrop does not meet these same preservation criteria. An effort was made to collect samples beyond the surface-weathering zone, but the outcrop conditions made it very difficult to match the preservational quality of the Naples Beach samples. The rocks at Point Buchon are very siliceous and much more highly fractured than those at Naples Beach. Meteoric waters (and accompanying diagenetic processes) penetrate deeply into the outcrop. The high silica content also makes it very difficult to dig deeply into the outcrop. Calcareous microfossil preservation is poor, with only microfossil fragments and molds occasionally present (C.E. Pflum, written commun., 1992).

These factors are probably responsible for the very low correlation between uranium and TOC content for Point Buchon ($r^2 = 0.09$). The much greater extent of surface weathering in these outcrop samples obscures any relation between

the two parameters and highlights the need for caution when interpreting organic carbon and uranium contents from outcrop samples. Additionally, the lack of detritus material may limit the pathways available for the uranium to accumulate in the sediments.

Other factors also obscure the relation between uranium and organic carbon. Uranium is sometimes introduced into the sediments with accessory minerals such as zircon and apatite, and it can also be incorporated into the authigenic apatite of phosphatic shales.

Prediction of Total Organic Carbon from Uranium

The equation developed to correlate uranium and TOC for samples from Naples Beach can be used to predict TOC from uranium concentrations measured by the gamma-ray spectrometer. Based on linear regression analysis, the best fit equation is

$$\text{TOC (weight percent)} = 0.75 \times \text{U (ppm)} - 3.63.$$

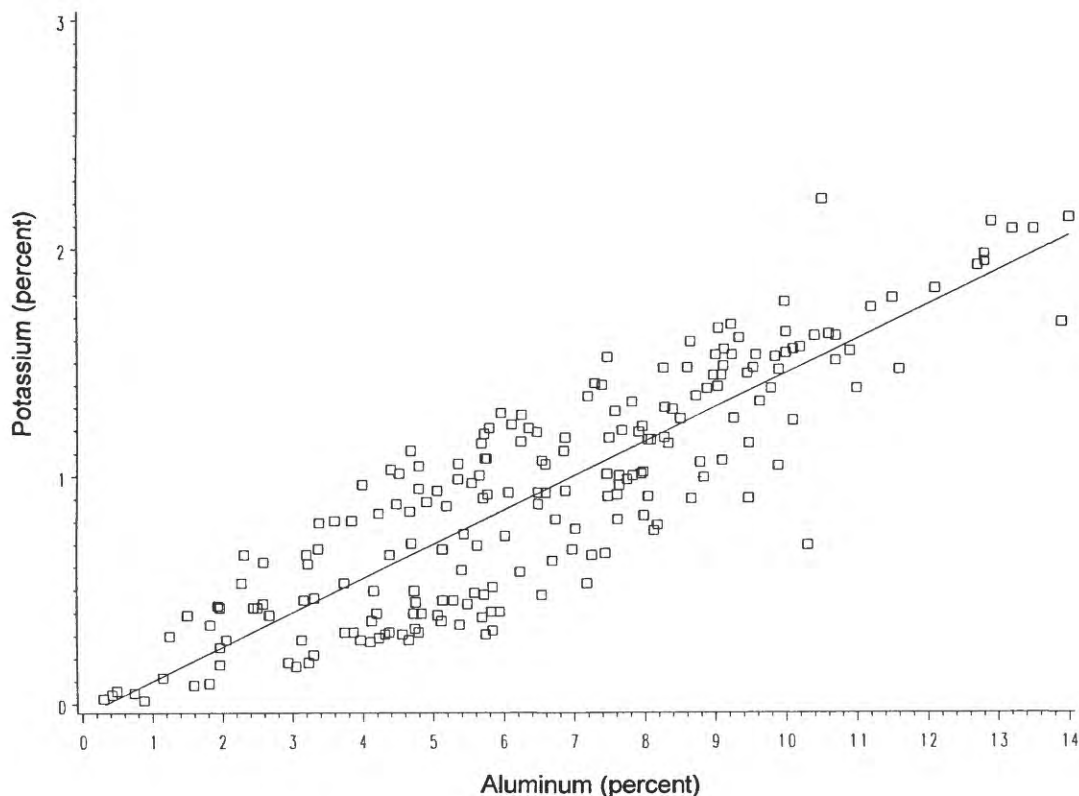


Figure 6. Potassium (percent) vs. aluminum (percent) cross-plot. Element oxides measured by X-ray fluorescence for 323 samples from Shell Beach, Point Buchon, Point Pedernales, Naples Beach, and offshore well 408-1. Coefficient of determination: $r^2 = 0.75$ (from Schwalbach and Bohacs, 1992a).

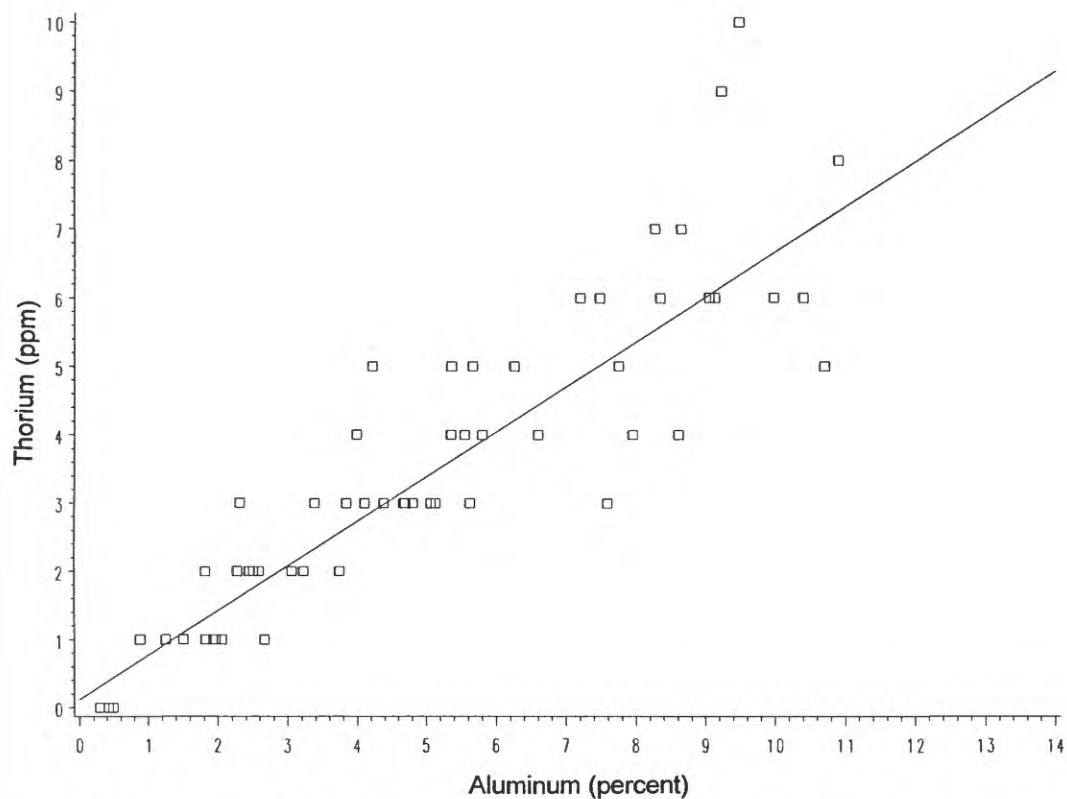


Figure 7. Thorium (ppm) vs. aluminum (percent) cross-plot. Measurements for 57 samples from Point Buchon and Shell Beach outcrops and offshore 408-1 well. Coefficient of determination: $r^2 = 0.75$ (from Schwalbach and Bohacs, 1992a).

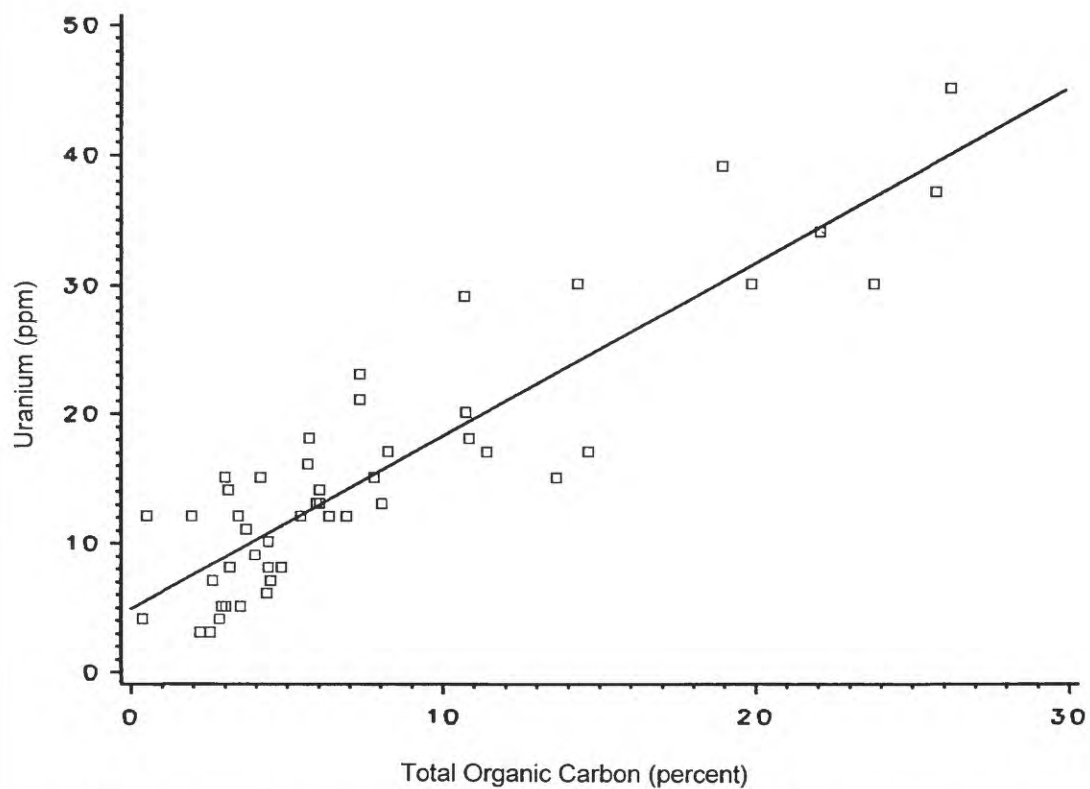


Figure 8. Uranium (ppm) vs. TOC (percent) for Naples Beach outcrop samples. Coefficient of determination: $r^2 = 0.80$ (from Schwalbach and Bohacs, 1992a).

Predicted TOC from the uranium concentration measured by the outcrop gamma-ray spectrometer at Naples Beach is plotted in figure 9 alongside laboratory-derived values from

hand samples. Despite the significant inequality in sample size between the laboratory analysis and gamma-ray spectrometer measurements, and the tendency to sample the most organic-rich rocks during a source-rock evaluation, there is reasonable visual correlation between the two data sources.

A comparison of data from the Phillips 408-1 well also reveals similar data trends. The leftmost column of figure 10 depicts the total gamma-ray profile through a portion of the Monterey Formation. The center column is a profile of the uranium component. This distribution of uranium determined by the well log, and the correlation of U to TOC developed for the Naples Beach outcrop data, are used to predict the TOC content in the stratigraphic section penetrated by the well (dotted line in column 3). Squares on the same track represent TOC values measured from core samples and indicate that the prediction is quite good.

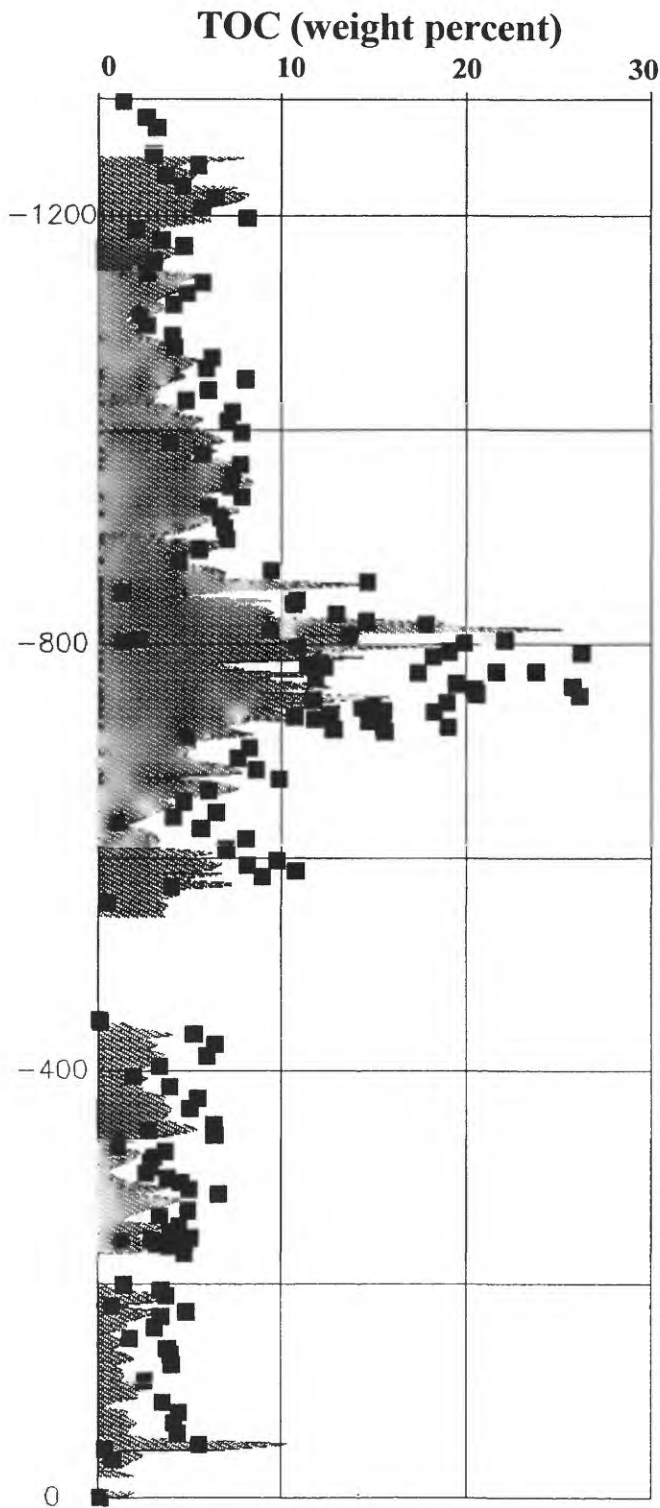


Figure 9. Predicted TOC from spectrometer data (shaded curve) compared with laboratory-measured values (squares) for Naples Beach (from Schwalbach and Bohacs, 1992a).

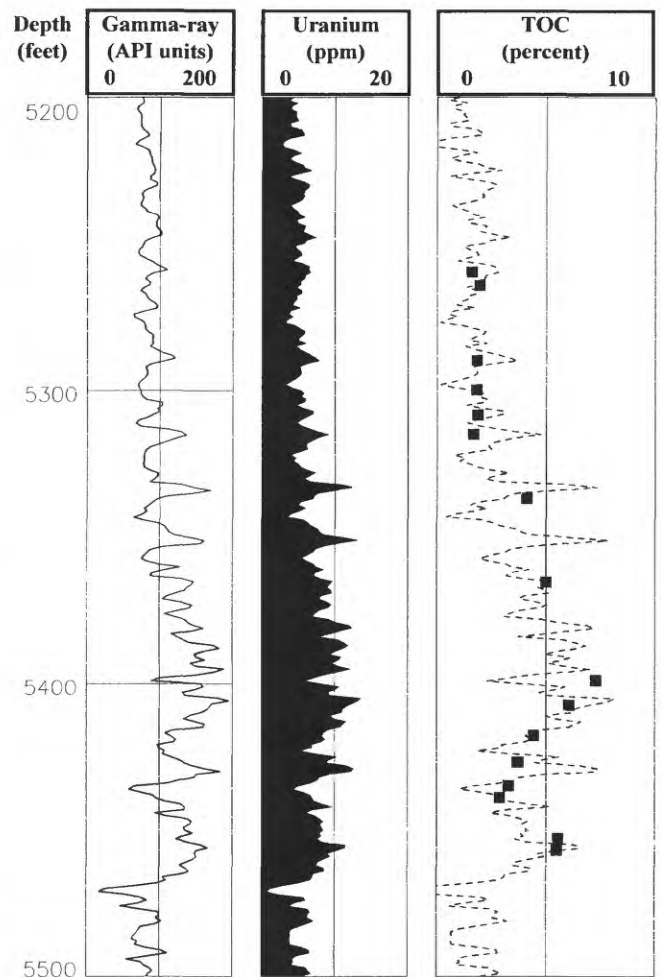


Figure 10. Measured and predicted TOC for offshore 408-1 well (modified from Schwalbach and Bohacs, 1992a). The left track displays total gamma-ray, and the center track displays the uranium component. The dashed line in the right track is the TOC profile predicted from the uranium component of the gamma-ray, using the uranium-to-TOC relation determined for the Naples Beach outcrop samples. Squares show measured values determined from core samples.

Prediction of Detritus from Potassium

In a manner similar to that used for predicting TOC from uranium, we can combine the correlation of potassium to alumina from this study and the relation between alumina and detritus determined by Isaacs (1981a) to predict detritus based on potassium concentration using the equation

$$\text{Detritus (weight percent)} = 36.3 \times K \text{ (weight percent)} + 0.9.$$

Estimation of Source-Rock Quality

Hydrocarbon source-rock quality in the Monterey Formation is a function of the sulfur content of the organic matter (see Bohacs, 1993; Isaksen and Bohacs, 1995). Typical organic matter may contain approximately 1 percent sulfur initially, but these sulfur forms are generally labile and not long-lasting in the basin environments. The anoxic Monterey sediments are enriched in sulfur as sulfur-reducing bacteria consume organic matter. The sulfur combines first with any iron in the sediments and then binds with any remaining organic matter. Iron comes into the sediments with terrigenous detritus. The amount of iron in the system is the key to the source quality because the iron combines with an equivalent amount of sulfur to form pyrite, removing the sulfur from the organic-geochemical system and improving the quality of the kerogen (Raiswell and Berner, 1986; P.J. Mankiewicz, oral commun., 1994).

We demonstrated in an earlier section that potassium is a proxy for alumina and therefore detritus in rocks of the Monterey Formation, and that organic matter can be predicted from the uranium content of the rocks. Therefore, we can use the K/U ratio measured by gamma-ray spectrometry as an estimate of the detritus/TOC ratio and thus a predictor of source-rock quality.

Data from the Naples Beach outcrop illustrates this relation (fig. 11). The maximum TOC values are measured for phosphatic shales from the interval between 700 and 850 ft of the measured section. These rocks have the lowest alumina/TOC and potassium/uranium ratios. These source rocks, among the richest sampled in the Santa Barbara–Santa Maria basins, would be expected to generate a low-gravity, high-sulfur crude oil. Source rocks higher in the stratigraphic section (for example, between 1,000 and 1,200 ft) are not nearly as rich. Because of their higher detritus content, however, these rocks would be expected to generate higher gravity crude oil.

STRATIGRAPHIC SECTIONS OF THE MONTEREY FORMATION

The measured sections presented in this report were compiled as parts of various field studies completed during the late 1980's and during 1990. The Naples Beach and Point

Pedernales outcrops were described as part of a regional source-rock study by Exxon in 1987. Thus, the data collected and presented for these outcrops lean more heavily toward source-rock characterization. Outcrop gamma-ray spectrometer surveys were collected along with a large number of hand samples in conjunction with construction of detailed measured sections. Much of this information was published by Bohacs (1990), and more details of the Naples Beach section were subsequently presented in Bohacs and Schwalbach (1994). The Shell Beach and Point Buchon outcrop sections were described and reported on in detail as part of dissertation research by Schwalbach (1992). However, this work focused on general stratigraphic and sedimentologic analyses and, therefore, had less emphasis on source-rock characteristics. A summary of these data was published in Schwalbach and Bohacs (1992b). The data bases from Shell Beach, Point Buchon, Naples Beach, and Point Pedernales are generally very compatible.

Lithologic and stratigraphic data from the Lion's Head outcrop are based on the description of Dunham and Blake (1987). Their measured section was used as the template for our gamma-ray spectrometer survey. The similarities in lithofacies classification between the Lion's Head data and the other outcrops were discussed in a previous section, and the same gamma-ray techniques and equipment were used for all the outcrops.

The following section contains stratigraphic information for each of the five outcrop locations. Chronostratigraphic data varies significantly for the outcrops; ages are relatively well known for some intervals and poorly constrained for others. We present a lithostratigraphic column and profile of gamma-ray spectra for each outcrop. The far-left column portrays the proportions of lithotypes identified for each interval. The remaining columns contain total gamma radiation (API units), uranium (ppm), potassium (percent), and thorium (ppm) as measured by the gamma-ray spectrometer.

Naples Beach Outcrop

The Naples Beach outcrop section is located at the northern margin of Santa Barbara Basin, in the area of Dos Pueblos Creek. We interpret that these strata were deposited on proximal upper to lower slopes that were consistently anoxic. Slump and debris-flow deposits are common throughout the stratigraphic interval. Micropaleontologic analyses indicate a displaced fauna consistent with slope environments. Compared with other outcrops of the Monterey Formation, there are relatively low proportions of siliceous lithotypes, few signs of benthic infauna, and an abundance of calcareous and phosphatic mudrocks. The microfossil groups from this outcrop are the most extensively studied of the Neogene sections of California (Barron, 1986b; Arends and Blake, 1986). Thus, this section is valuable for establishing a gross stratigraphic framework and for evaluating the expression of significant stratigraphic surfaces.

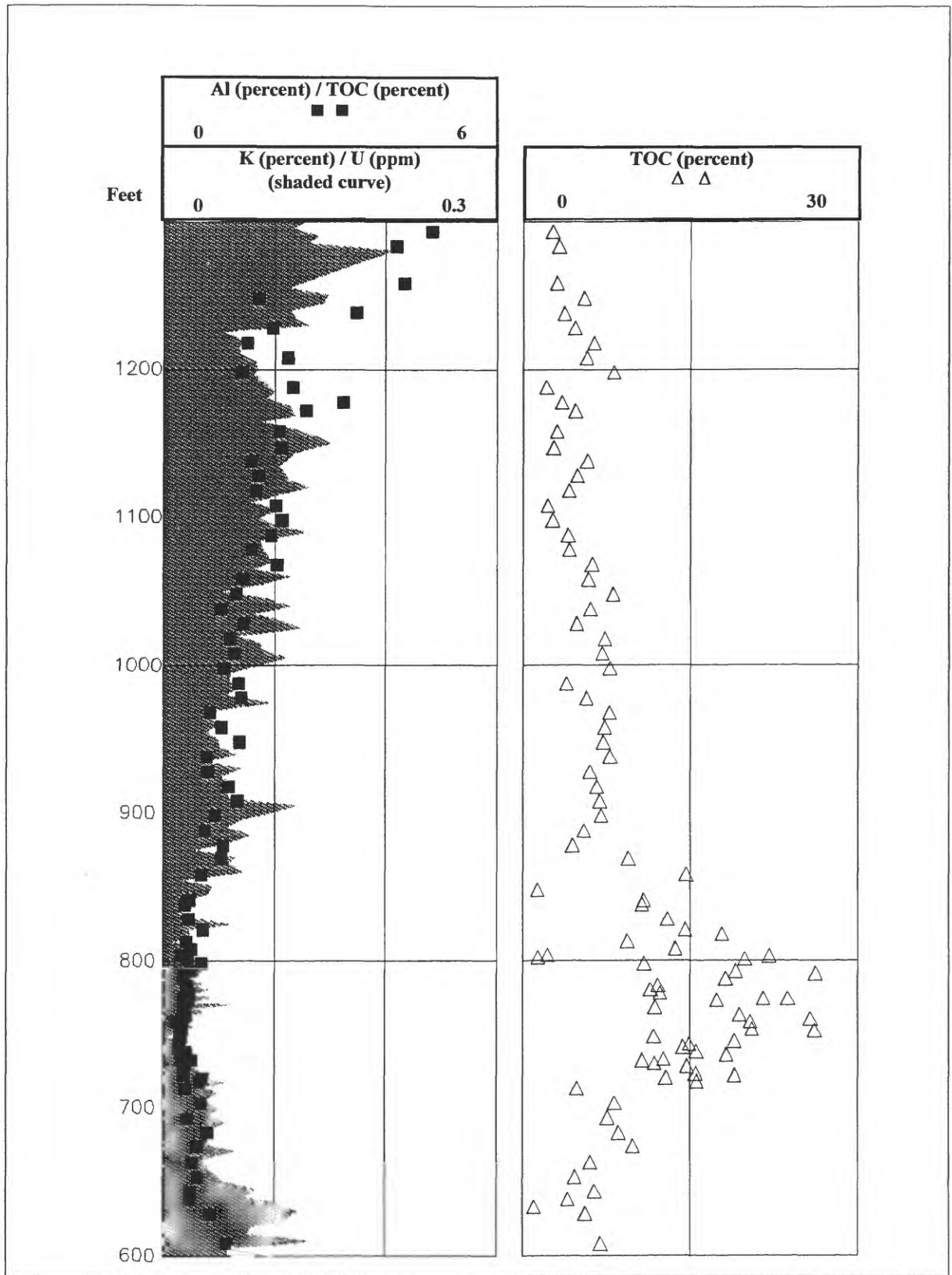


Figure 11. Comparison of trends for potassium/uranium and aluminum/TOC ratios and TOC content for the Naples Beach outcrop section. The potassium/uranium ratio is a proxy for aluminum/TOC, and therefore it is a valuable parameter for assessing source-rock quality.

The chronostratigraphic data for the Naples Beach outcrop are related to the gamma-ray stratigraphy in figure 12. The microfossil data are derived from Arends and Blake (1986), Barron (1986b), and G.H. Blake (oral commun., 1990). Bohacs and Schwabach (1994) provide three strontium isotope dates that constrain the upper, middle, and lower parts of the measured section. Additional age control, in general agreement with data presented but not shown on the figure, includes

magnetostratigraphy for the part of the section south of Dos Pueblos Creek (Hornafius, 1985) and a high-density strontium isotope study by DePaolo and Finger (1991). These chronostratigraphic data have been tied to the gamma-ray stratigraphy within a stratigraphic range of ± 10 –15 ft.

There is some uncertainty over the duration of a hiatus in the middle part of the Naples Beach section. DePaolo and Finger (1991) argue that the 5-m.y.-long hiatus of Arends and

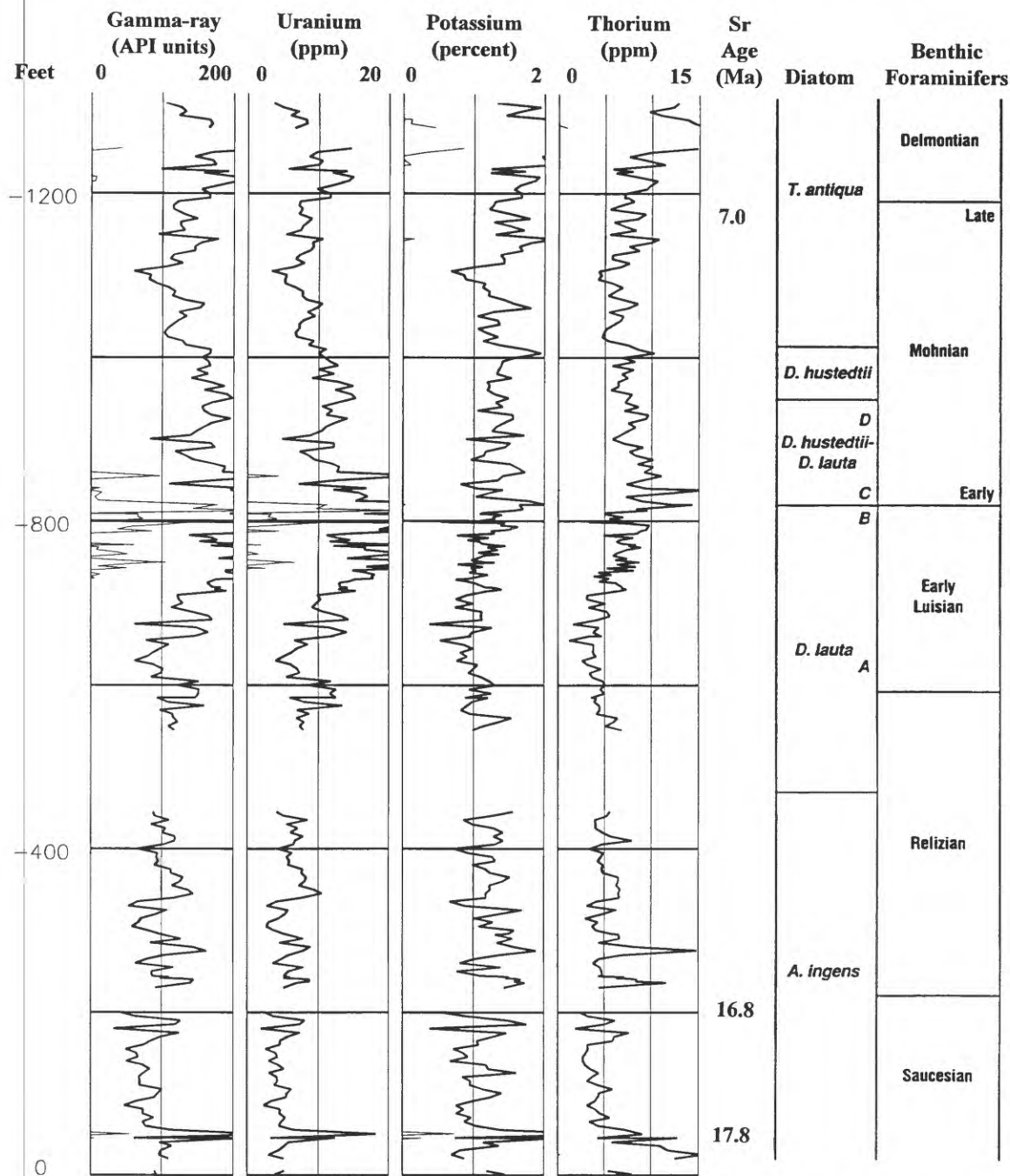


Figure 12. Microfossil zonation and spectral gamma-ray data from Naples Beach outcrop (after Schwabach, 1992). Microfossil data from Arends and Blake (1986) and Barron (1986b). Strontium isotopes from Schwabach and Bohacs (1991). The proposed 5 m.y. hiatus of Arends and Blake (1986) occurs at approximately 810 ft of our measured section.

Blake (1986) is actually no longer than 1.1 m.y. in duration. However, the hiatus correlates to a very flat portion of the strontium isotope calibration curve, increasing the uncertainty of ages assigned for this part of the Miocene.

Lithostratigraphy and Gamma-Ray Spectra

The measured lithostratigraphic section and accompanying gamma-ray spectra for the Naples Beach outcrop are portrayed in figure 13:

0 to 340 ft

The basal part consists of cyclic packages of dolomitic mudstone, clay shale, and phosphatic shale in bedsets 0.75 to 3 m thick. Bedsets of porcelanite and sandstone are thinner and rarer. Two intervals with slumps occur between 100 to 125 ft and 207 to 225 ft.

- Total gamma-ray (GR), U, and Th activities are relatively constant, fluctuating about stable means of 100 API, 7 ppm, and 5 ppm, respectively. This reflects a total organic carbon content (TOC) average of about 4 percent (ranges from less than 1 to approximately 6 percent) and alumina/TOC ratios that vary from 5 to 21, with a stable average ≈ 10 .
- Th spikes (local maxima) at 30 and 50 ft are associated with bentonitic mudstones, possibly altered volcanic ash. Th spikes at 240 and 274 ft are associated with fining-upward bedsets of pebbly sandstones and sandstones with scoured bases. They probably represent turbidity-current deposits bringing in detrital heavy minerals or reworked volcanic rock fragments with elevated Th content.

340 to 450 ft

This interval contains two major packages: a lower slump zone of clay shale and dolomite with blocks up to 5 m long (340–401 ft), and an upper zone of matrix-supported intraformational conglomerate probably deposited as a debris flow (401–450 ft; see fig. 14).

- Total GR, K, and Th are relatively constant, with subdued amplitudes. U has reduced amplitudes and decreases slightly from 11 to 5 ppm. The subdued amplitudes are probably due to the apparent thickening of the bedsets seen by the gamma-ray survey that are associated with the slumping and folding. This relation is seen in some well logs through base-of-slope deposits.
- Within the slump zones throughout the Naples Beach section, K and Th are typically low and only increase just above the slumps, indicating that these zones are the result of increased productivity and energy level in the lowstand, not necessarily increased hemipelagic input. If the terrigenous clastic fraction of the slump materials were greater than the adjacent strata, we would expect

higher K and Th measurements (see discussion in Bohacs and Schwalbach, 1992).

450 to 540 ft, Dos Pueblos Creek

We estimate 90 ft of stratigraphic section eroded by Dos Pueblos Creek.

540 to 710 ft

Thinly bedded porcelanite and phosphatic shale in bedsets 1 to 3 m thick thin upward through this interval. This stratal stacking trend coincides with an increase in organic richness.

- TOC has a distinct shift at 600 ft to a higher average of 8 percent (range of 4 to 10 percent). U is relatively constant, shifted to a higher average of 10 ppm, reflecting increased TOC content.
- Alumina/TOC shifts to a lower average (4) and lower range (1.5–6). K and Th show distinct overall decreases through the section due to decreased terrigenous detrital content.

710 to 810 ft

Thinly bedded phosphatic shale and kerogenous marls with common to abundant phosphatic concretions record very low sediment accumulation rates (fig. 15). The base of Isaacs's (1981b) organic shale member is at approximately 710 ft. She later revised her stratigraphic nomenclature and designated these rocks the carbonaceous marl member (Isaacs, 1983).

- TOC rapidly increases to a maximum of 27 percent through widely varying bedsets of relatively thin phosphatic mudrocks and rich marls. Alumina/TOC is low throughout, ranging from 1 to 2. The lowest alumina/TOC values in the entire section occur in the thickest TOC bedsets around 755 ft, reflecting the minimum input of terrigenous detritus. The maxima of total GR and U are about 45 ft above the thickest TOC bedsets (≈ 755 ft), resulting from the high concentration of radioactive minerals in the phosphatic rocks above the most organically enriched bedsets (see discussion of such occurrences in Bohacs and Schwalbach, 1991).

Lithofacies of the Monterey Formation

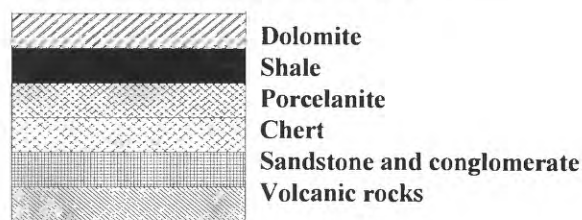


Figure 13. Stratigraphic section from Naples Beach outcrop with accompanying gamma-ray survey. The lithofacies symbols used in this figure are the same for all the stratigraphic sections used in this report.

- K decreases to its overall lowest concentration in the entire section (0.1 percent), reflecting the minimum input of terrigenous detritus.

810 to 1,100 ft

This section contains heterolithic interbedding of phosphatic shale and grainstone, clay shale, porcelanite, and cal-

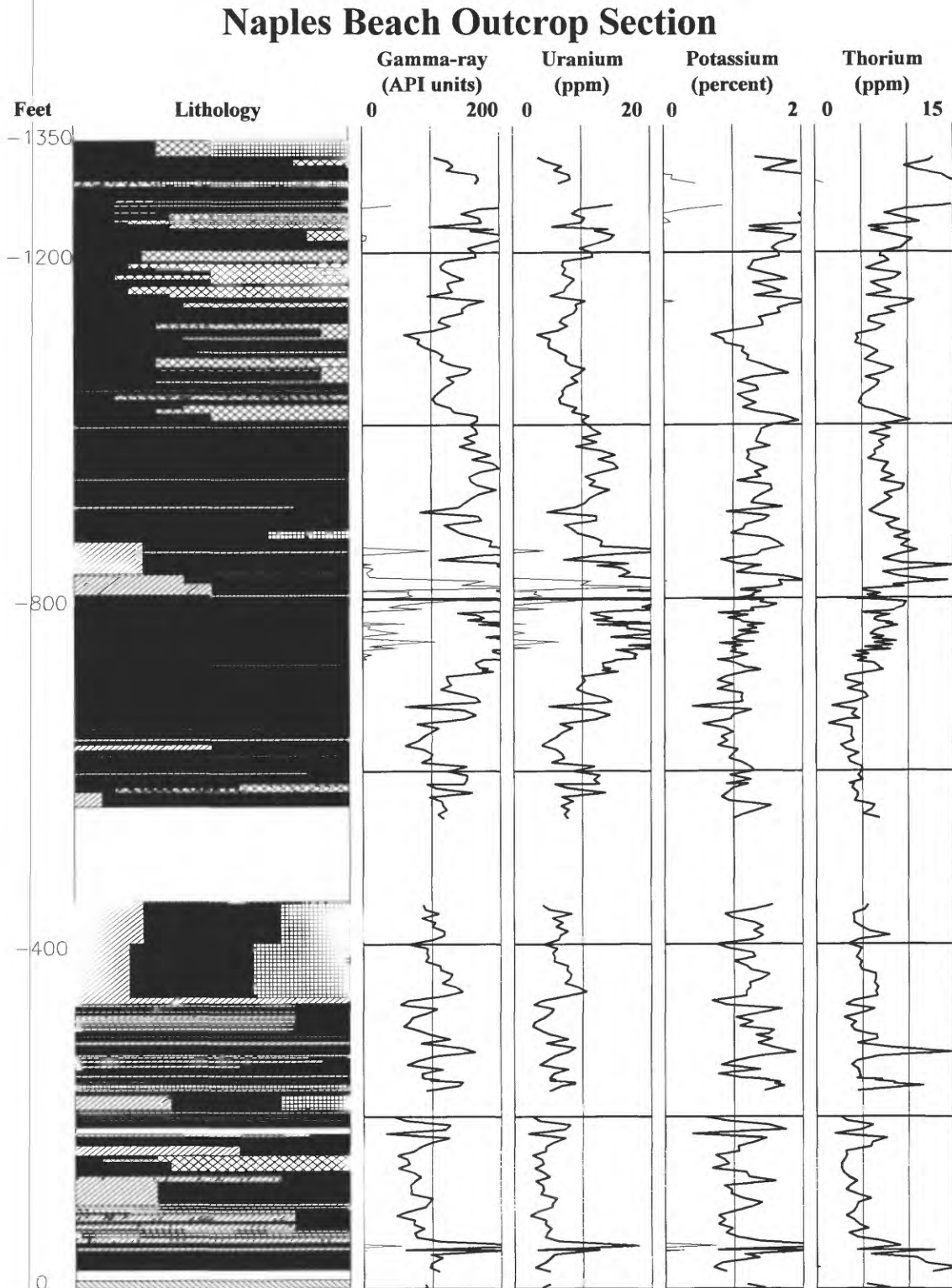


Figure 13. Continued.

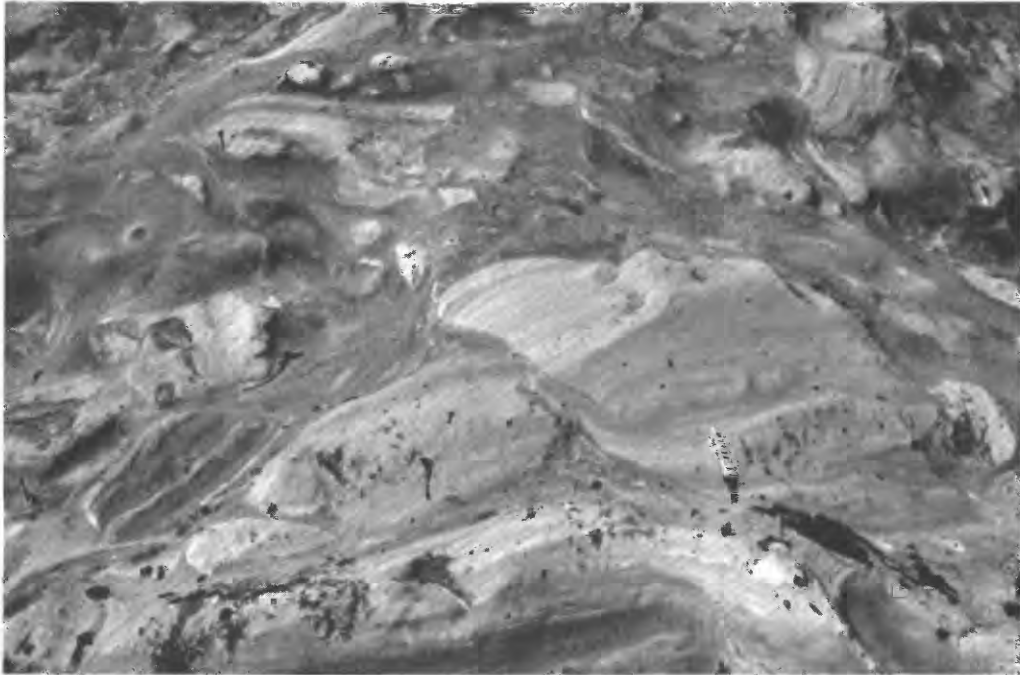


Figure 14. Naples Beach outcrop at 438 ft. This matrix-supported intraformational conglomerate was probably deposited as a debris flow. Small chisel for scale is 14 cm long.



Figure 15. Naples Beach outcrop at 732 ft illustrating phosphatic-rich strata in condensed interval. Small chisel for scale is 14 cm long.

careous grainstone. A slump zone occurs between 832 and 855 ft.

- TOC decreases in two distinct steps, to 11 percent between 810 and 890 ft, and to ≈ 6 percent between 890 and 1,100 ft. Isaacs (1981b) placed the top of the organic shale member at ≈ 975 ft. Alumina/TOC increases constantly from ≈ 2 to ≈ 9 , ranging from 1.5 to 11.
- Total GR and U rapidly decrease from 810 to 840 ft, then gradually decrease throughout to ≈ 90 API and 6 ppm, respectively, reflecting mainly the decrease in TOC content. All spectra demonstrate thicker bedsets due to increased sediment accumulation rates.

1,100 to 1,310 ft

This interval contains interbedded porcelanite, phosphatic shale, and clay shale, with siliceous shale content increasing upward to a dominance of porcelanite and siliceous shale above 1,237 ft in the Sisquoc Formation. The interval covers parts of Isaacs's upper calcareous shale and transition members (975–1,130 ft) and her siliceous member (1,130–1,237 ft).

- TOC decreases throughout to an average of <3 percent. Alumina/TOC continues its overall increase, increasing and varying more rapidly above 1,237 ft in the Sisquoc Formation. U activity drops off abruptly in the top 60 ft of the section to 3 ppm. This decrease reflects the overall decreasing concentration of organic matter probably due to increased dilution by terrigenous detritus.
- K and Th increase steadily to the top of the section to their highest averages of 1.1 percent and 12 ppm, respectively, recording the increased content of terrigenous detritus.

Point Pedernales Outcrop

The Point Pedernales outcrop section is located in the Santa Maria basin on Vandenberg Air Force Base. Grivetti (1982) provides a detailed location map for the outcrop. The strata at Point Pedernales were deposited in distal lower slope and basin floor settings based on the high proportion of siliceous lithotypes and the physical expression of the rocks. The measured section and spectral gamma-ray data (adapted from Bohacs, 1990) are shown in figure 16.

Only limited chronostratigraphic data are available from Point Pedernales. Most of the age interpretation is based on the physical stratigraphy, published with gamma-ray profiles, from Bohacs (1990). The paucity of biostratigraphic control in the outcrop is primarily due to the highly siliceous nature of the strata, the significant amount of silica diagenesis (most of the silica is diagenetic quartz), and the poor preservation of calcareous forms. For these reasons, attempts at establishing rigorous chronostratigraphy for the outcrop have been mostly unsuccessful.

Bohacs (1990) relied on palynologic work by William Gregory (Exxon Co., U.S.A., written commun., 1989) to help interpret the strata in a sequence stratigraphic framework. A review of Gregory's original report documents the existence of a number of palynological zonation. A missing factor is the link to an absolute time scale of either regional or global significance. Based on a gross composite zonation utilizing palynology, the interval from the base of the measured section up to 805 ft is designated as early Miocene in age, the middle part of the section from 864 to 1,499 ft as middle Miocene, and the upper part of the stratigraphic section from 1,519 to 2,215 ft as late Miocene.

Lithostratigraphy and Gamma-Ray Spectra

0 to 941 ft

The Monterey Formation rests unconformably on the rhyolitic welded tuffs of the Tranquillon Formation; the contact is well exposed just north of Point Pedernales (Grivetti, 1982; Dunham and Blake, 1987). The basal part of the section contains a broad variety of lithologies: porcelanite, dolomite, sandstone, mudstone, clay shale, phosphatic shale, and debris-flow conglomerates. These bedsets have a wide range of thicknesses (0.5–20 ft) and are disrupted by a number of high-angle faults.

- Some syndimentary slumps occur, mostly in the basal interval below 744 ft. A sandstone and conglomerate bedset with a scoured base occurs at 510 ft. Just above this bed is a 30-ft-thick slump-folded unit of dolomite, conglomerate, porcelanite, and clay and phosphatic shale. This association of strata is indicative of higher levels of bottom energy and increased biogenic silica deposition. A similar association of lithofacies occurs at 760 ft.
- The total gamma-ray activity throughout the entire Point Pedernales section is strongly influenced by the uranium content, so both total gamma-ray and uranium activities display very similar patterns. In the basal part of the section, the curves are highly variable but are slightly lower in intervals with the most biogenic silica (for example, 440–560 ft).
- Total organic carbon content is also highly variable, ranging from 0.7 to 8.6 weight percent (with an average of 3.7 percent).

941 to 1,280 ft

This interval contains mostly thin porcelanite and phosphatic shale bedsets. Dolomite bedsets occur throughout but are more common at the base, becoming thinner and sparser upward—the upper bedsets are more obviously formed by replacement of clay shale. The dominant stratal geometry is planar parallel. Significant chert bedsets occur above 1,055 ft, concurrent with indicators of higher bottom-energy levels. Intervals of folded strata occur above 1,080, 1,410, and 1,650

ft (fig. 17). These are interpreted as representing slump and debris flows that are consistent with a lower slope depositional environment.

- The total gamma-ray and uranium activities are more uniform and less variable in this interval. There is a slight decrease in uranium content upward, which grossly

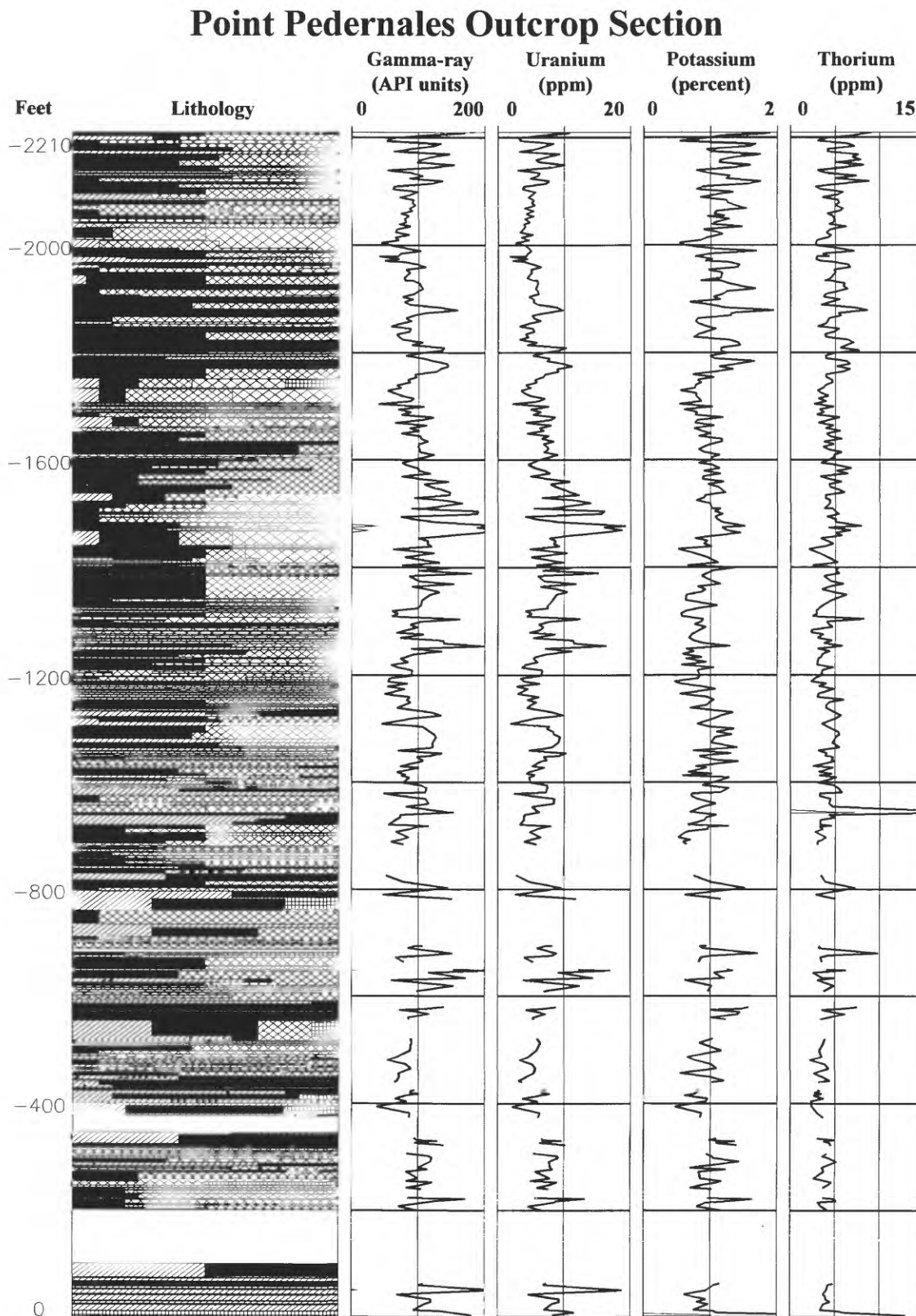


Figure 16. Stratigraphic section from Point Pedernales outcrop with accompanying gamma-ray survey.

trends with TOC content that averages 4.8 percent. The largest thorium values (>20 ppm) occur around 942 ft in an interval with phosphatic shales, abundant phosphatic nodules, and phosphatic grainstones 2 to 7 mm

thick. Similar rock and gamma-ray associations have been interpreted as representing deposition during sediment-starved conditions (see Bohacs and Schwalbach, 1991).



Figure 17A, B. Examples of slump-folded strata at Point Pedernales, 1,080 and 1,325 ft above the base of the section. White bands on the staff mark 1-ft increments.



Figure 17A, B. Continued.

1,280 to 1,624 ft

This interval is dominated by siliceous lithofacies, with abundant bedsets of porcelanite and chert interbedded with phosphatic shale. Stratal geometries are mostly planar parallel. However, the association of slumps and biosiliceous sediments noted in the previous interval continues (1,280–1,425 ft and 1,540–1,624 ft). Additional indicators of higher bottom energy in these zones includes occasional to common current scours, graded beds, and T_{ab} turbidites ranging up to 3 cm thick.

- The highest uranium values are associated with thinly bedded phosphatic shales with the highest TOC in the section (ranging up to 20 percent, with an interval average of 10.1 percent). The high-TOC phosphatic shales are often associated with thicker beds of chert, indicators of high biogenic productivity but containing very little organic matter. The association of these bedsets creates highly variable TOC and U profiles.

1,625 to 1,782 ft

This interval is composed primarily of phosphatic and organic-rich shale bedsets, interbedded with thin bedsets of siliceous shales and porcelanites. Some slumps are present, current scours up to 10 cm deep are common, and graded beds containing chert clasts, phosphatic clasts, and turbidites are common to abundant.

- Total gamma-ray and element components are relatively stable over this interval. Uranium decreases upwards in concordance with lower TOC values.

1,782 to 2,215 ft

This interval contains a much higher proportion of siliceous rocks than the interval below. Chert, porcelanite, and siliceous shales are the dominant rock types, while dolomites and mudstones are subordinate. Syndimentary slumping of siliceous bedsets is common. Vein structures indicative of slope deposition are scattered throughout. Bohacs (1990) notes that there are approximately 500 ft of additional strata of the Monterey Formation above the 2,210-ft level, but during the field investigation this interval was inaccessible because of tides and surf conditions.

- Total gamma-ray activity is similar to the intervals below, but the relative contributions of the individual elements is quite different. Uranium, generally the dominant component of the total gamma-ray signal, generally shows a baseline decrease. Potassium and thorium, however, exhibit a baseline increase throughout the interval. The gamma-ray signature likely reflects an increased hemipelagic detritus component in this stratigraphic package.

Lion's Head Outcrop

The Lion's Head outcrop is also located in the Santa Maria basin, at the north end of Vandenberg Air Force Base. The

Lion's Head measured section uses the published data by Dunham and Blake (1987; additional information provided by G.H. Blake, oral commun., 1990) as a base for a relatively coarse-scale outcrop gamma-ray survey (fig. 18). In most instances, the match between the published section and the outcrop was readily accomplished. The error between the measured section and the plotted gamma-ray values is generally less than 5 ft and should not be greater than 15 ft at any point on the section.

The measured section of Dunham and Blake (1987) can roughly be divided into two lithostratigraphic units, a lower calcareous and phosphatic facies and an upper siliceous facies. A lithofacies identification scheme similar to that employed for the other outcrops was used for the Lion's Head outcrop (described in Dunham and Blake, 1987). However, Dunham and Blake record only the dominant lithology per foot of measured strata, although certain combination lithologies are recorded. This methodology is not strictly compatible with the procedures employed at the other outcrops in which the proportions of all strata present in an interval were recorded, but it does capture the general character of the outcrop quite well.

Chronostratigraphic data for the Lion's Head outcrop section are derived from microfossil studies and provide only limited constraints on stratigraphic correlations. Dunham and Blake (1987) and Dunham and Cotton-Thornton (1990) note a possible Luisian designation at 870 ft and a definite Luisian call at 650 ft (all depths referenced to the measured section of Dunham and Blake, 1987; 0 ft is the base of the Monterey Formation). A Relizian fauna was recovered from a sample at 42 ft.

White (1989) measured the upper 75 m of strata at Lion's Head, corresponding to the siliceous facies of Dunham and Blake (865–980 ft). She sampled dolomites and recovered sufficient diatoms to constrain the maximum age at the base of that interval at 11.4 Ma. The age at the top of the exposed section is estimated at between 9.3 to 10.3 Ma. White also reports a strontium isotope date by Clark (1989) of 12.7 ± 0.3 Ma from samples taken from the stratigraphic interval between 535 and 685 ft of the section published by Dunham and Blake (1987). This date fits the general chronostratigraphic range determined by the other data sources.

Lithostratigraphy and Gamma-Ray Spectra

0 to 685 ft

The Monterey Formation at Lion's Head is in fault contact with ultramafic rocks of the Point Sal ophiolite of Jurassic age. Based on stratigraphic similarities to other sections in the region, Dunham and Blake (1987) postulate that this section is close to the actual base of the Monterey Formation. This interval is composed primarily of phosphatic shales and dolomites.

- Sediment gravity-flow deposits occur in the lower part of the section. Dunham and Blake (1987) note the presence of thinly bedded turbidite sandstones above 225 ft and debris-flow conglomerates at 245 and 270 ft.
- Two siliceous intervals occur in the lower phosphate-rich zone. One occurs between 375 and 435 ft and the other between 570 and 640 ft (Dunham and Blake, 1987).

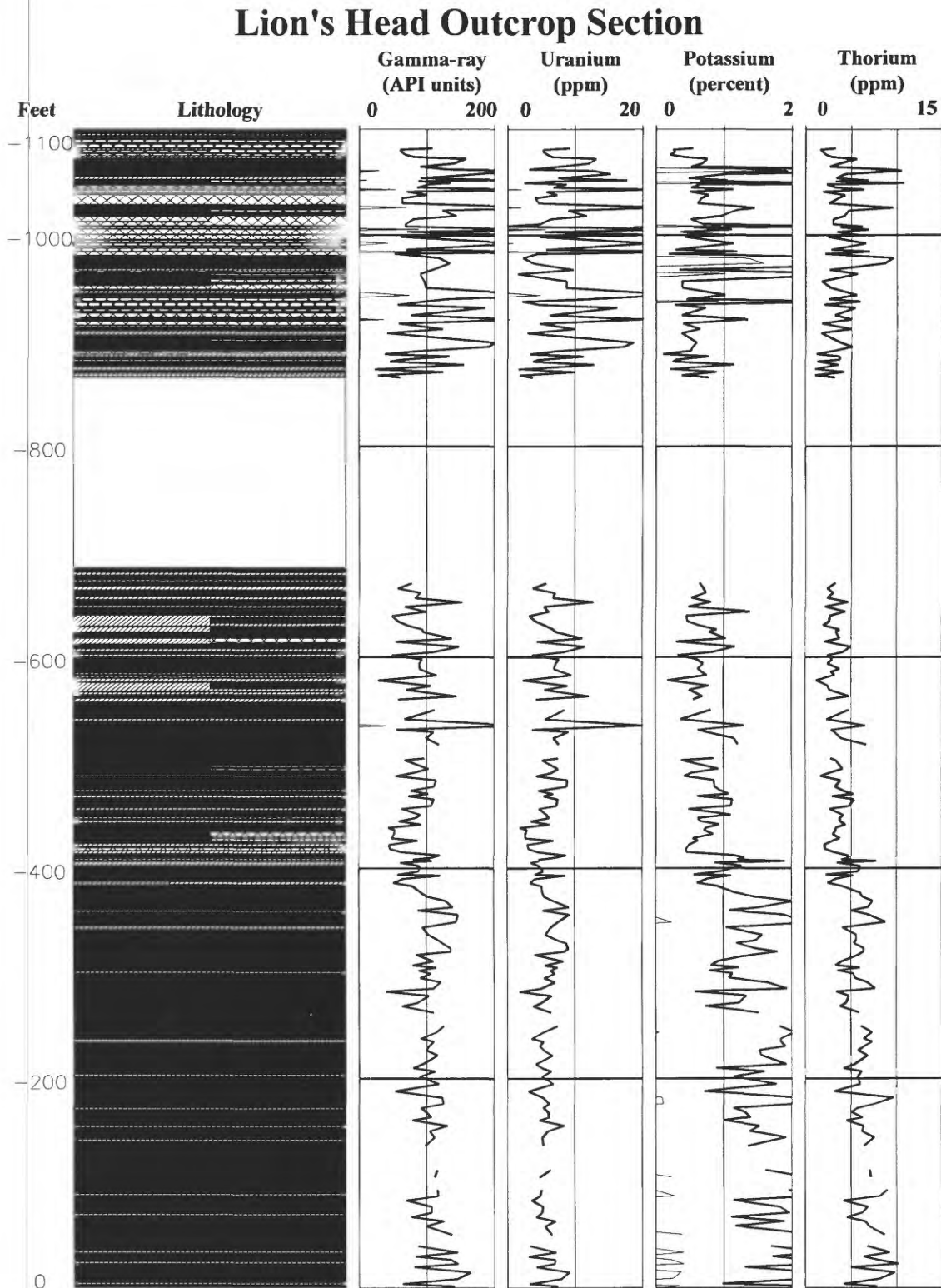


Figure 18. Stratigraphic section from Lion's Head outcrop with accompanying gamma-ray survey.

685 to 865 ft

Dunham and Blake (1987) estimate 180 ft of covered section.

865 to 980 ft

The strata above the covered section contain a much higher proportion of siliceous rocks (mostly cherts, porcelanites, and siliceous shales) than the interval below. Dolomites and phosphatic shales also are present.

- Many of the chert beds are tightly folded. Dunham and Blake (1987) argue for a tectonic origin of these folds, but their characteristics are similar to those that we describe at Point Buchon and attribute to slump folding.
- There is extreme variation in the gamma-ray measurements of the strata in this interval. Some of the thin phosphatic shale beds have very high K and U contents. We did not collect samples from this outcrop section, but we suspect these high values relate to high TOC content and perhaps high concentrations of fine-grained detritus and apatite.

Shell Beach Outcrop

The Shell Beach outcrop is a sometimes structurally complex but excellently exposed partial stratigraphic section of the Monterey Formation, located in the Pismo basin. We interpret these strata to have been deposited in a lower slope to basinal environment based on lithofacies associations, stratal stacking patterns, and the lamina to bedset geometries that are readily observed on the outcrop. Chronostratigraphic control at Shell Beach is one of the most complete for California Neogene sections due to the magnetostratigraphy of Khan and others (1989). They calibrated polarity reversals of a densely sampled, detailed measured section to diatom and calcareous nannofossil zonations. Their zonations are also in agreement with chronostratigraphy based on benthic foraminifers (M.L. Cotton-Thornton, oral commun., 1990). The ages of significant stratigraphic surfaces are well constrained by magnetostratigraphy and micropaleontology. The magnetostratigraphy has been correlated to the measured section of this study (fig. 19).

The Monterey Formation rests on volcanic rocks of the Obispo Formation that have been dated at 16.5–15.5 Ma (Turner, 1970). The top of the section is marked by an erosional surface. A conglomerate with rounded Monterey clasts and bituminous sandstone rests unconformably on the Monterey Formation. Khan and others (1989) recorded about 290 m of Monterey strata in their measured section. A total of 1,082 ft (about 328 m) of Monterey stratigraphic section were measured during this study. Much of the difference is accounted for in the lower part of the section, where Khan and others (1989) report about 86 m of calcareous-phosphatic rocks. About 125 m of phosphatic shale and dolomite were mea-

sured for the lower unit in this study. Numerous areas of tectonic disruption and synsedimentary slumping complicate stratigraphic interpretation in the interval, so the thickness differences are not too surprising.

Above the calcareous-phosphatic facies rocks are 203 m of dominantly siliceous rocks (porcelanites and cherts). Lesser amounts of phosphatic and siliceous shale and dolomites are interbedded with the porcelanites and cherts. A map illustrating the location of the Shell Beach measured section and the compiled stratigraphic section from this outcrop are shown in figures 20 and 21, respectively.

Lithostratigraphy and Gamma-Ray Spectra

0 to 262 ft

The basal part of the Monterey Formation overlies a thick (>3 m) homogeneous bed of siliceous volcanic rocks, approximately opposite the intersection of Wawona Avenue and Ocean Boulevard in Shell Beach. Tectonic disruption (low-angle faults and folding) complicate the stratal geometry of this interval. However, lithofacies associations and bedset geometry indicate that deposition occurred in slope environments.

- Planar, parallel-bedded dolomites and phosphatic shales dominate the stratigraphic section up to about 75 ft. Siliceous shales and some minor amounts of porcelanite are present in the interval up to about 90 ft. There is evidence of bottom-water current activity in the phosphatic shales around 78 ft with broad, shallow scours and low-angle onlap.
- Examples of mass-flow deposits occur at 93, 170, 210, and 230 ft (fig. 22). They span a spectrum from slumps with significant rotational movement of competent strata to matrix-supported debris flows to turbidites. The units at 210 and 230 ft have significant relief on their basal surfaces, contain a large amount of coarse clastic material along with boulder-sized chunks of phosphatic shales, and are composite deposits representing numerous events. They may be the expression of a significant erosional event on a basin margin.
- Total gamma-ray values generally increase toward the top of this interval, tracking the increasing proportions of phosphatic and clay shales, as well as organic matter. However, within the major debris-flow unit at 230 ft, total gamma-ray and uranium values drop off significantly. The thorium component increases in the debris-flow unit, reflecting the increase in coarser grained clastic materials (fig. 23).

262 to 453 ft

A 2-ft-thick dolomite bed at 262–264 ft caps the slump-folded and debris-flow units. Compared with the strata at the base of the section, this interval comprises relatively planar,

parallel strata, with minimal tectonic disruption. The main lithotypes are phosphatic and clay shales, with interbedded dolomites and volcanic ash beds.

- Lamina geometry in the phosphatic shales provides clues about the depositional environments. Small faults and vein structures, interpreted as indicators of slope deposition, occur at 285–287 ft (fig. 24). These structures are best viewed in the freshly eroded intertidal exposures.

Other bedsets in this interval contain discontinuous phosphatic lamina, possibly the result of short episodes of bioturbation.

- Phosphatic nodules, formed at times of slow sediment accumulation and related to bottom-current reworking, occur in conjunction with volcanic ash beds at 346 and 370–388 ft (fig. 25). A unique spectral gamma-ray signature characterizes these intervals of low sediment ac-

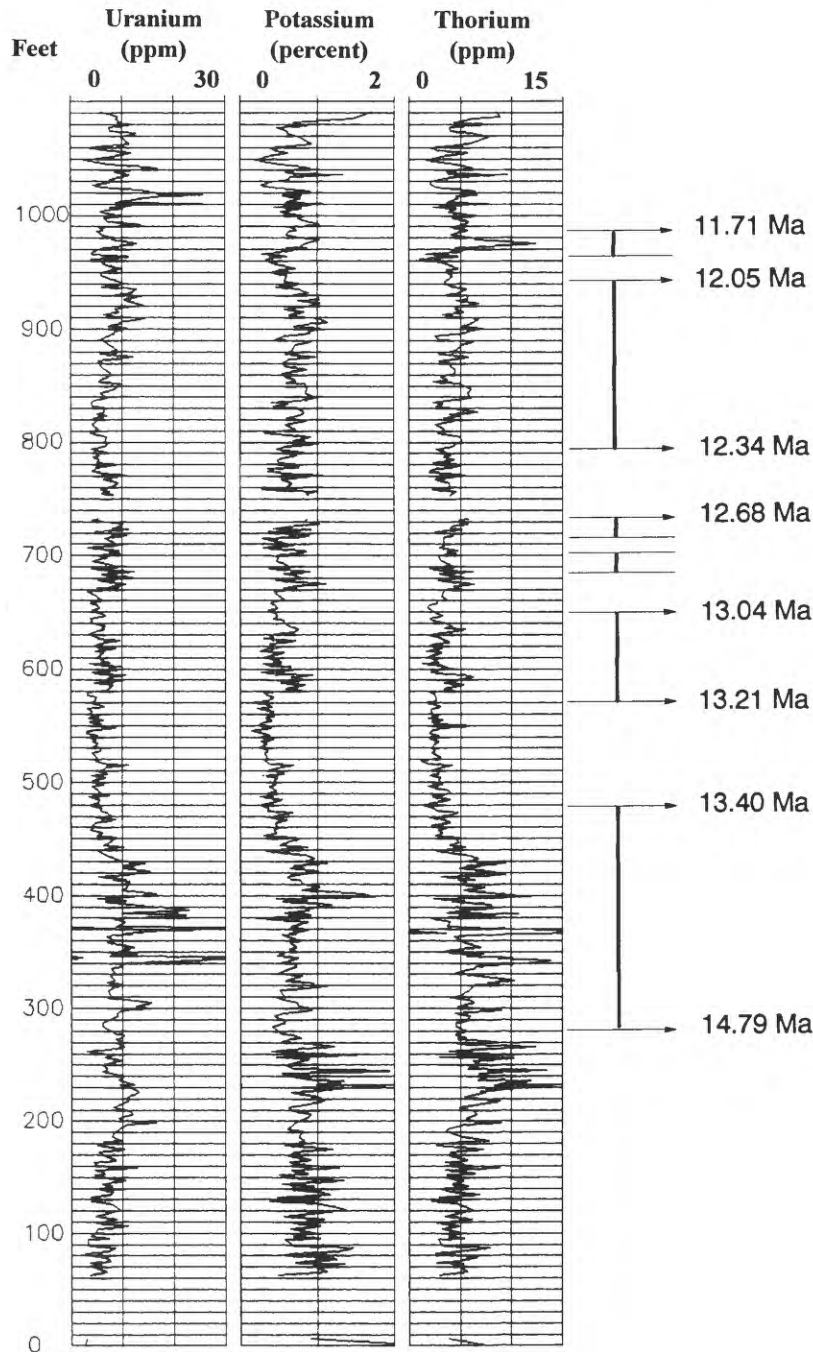


Figure 19. Magnetostratigraphy of Khan and others (1989) correlated to the spectral gamma-ray profile of Shell Beach (from Schwalbach, 1992).

cumulation rate (Schwalbach, 1992). The thicker tuff beds (>10 cm) cause a distinct spike in the thorium concentration ranging from two to five times above the background levels. Thinner tuff beds, particularly those occurring close together, cause broader shoulders on the thorium logs that are more than twice the background levels. Peaks in uranium concentration ranging from two to four times above background levels occur associated with, but slightly offset from, the major thorium peaks. The increase in uranium is tied to the higher concentration of organic matter and the presence of phosphatic nodules.

- Khan and others (1989) suggest that the phosphatic lags represent minimal deposition between 14.3 and 13.25 Ma. A volcanic ash bed adjacent to the phosphatic hardground at 370 ft of the stratigraphic section yielded a maximum age of 15.2 Ma based on Ar-Ar isotope study (analyses performed by M. Heizler, 1991, University of California, Los Angeles). This is not necessarily inconsistent with the magnetostratigraphy for the interval above the hardground, but it does suggest a potentially longer hiatus and perhaps an older age than previously assigned for the basal part of the Monterey Formation at Shell Beach.

- A relatively subtle lithofacies change occurs above 417 ft. The rocks contain more biogenic silica, and the proportion of siliceous shale increases. This lithofacies change results in a decrease in all three components of the gamma-ray spectra and is interpreted to reflect higher total sediment accumulation rates driven by increased biogenic silica production and deposition (Schwalbach, 1992). This increased sediment accumulation dilutes the organic matter (reflected by lower uranium concentration) and detritus (reflected by lower potassium and thorium concentrations).

453 to 1,082 ft

This interval of the stratigraphic section contains much more biogenic silica than the strata below and hence is dominated by porcelanites, with interbeds of dolomite, phosphatic and clay shale, and chert. Cyclic stratal stacking occurs through much of the interval, at a variety of scales (see White, 1989).

- The rapid shift to very siliceous lithotypes at 453 ft is interpreted to mark a fundamental change in paleoceanography. The enhanced productivity of biogenic silica is related to lower sea level, increased thermal gradients with more vigorous ocean circulation, and enhanced up-

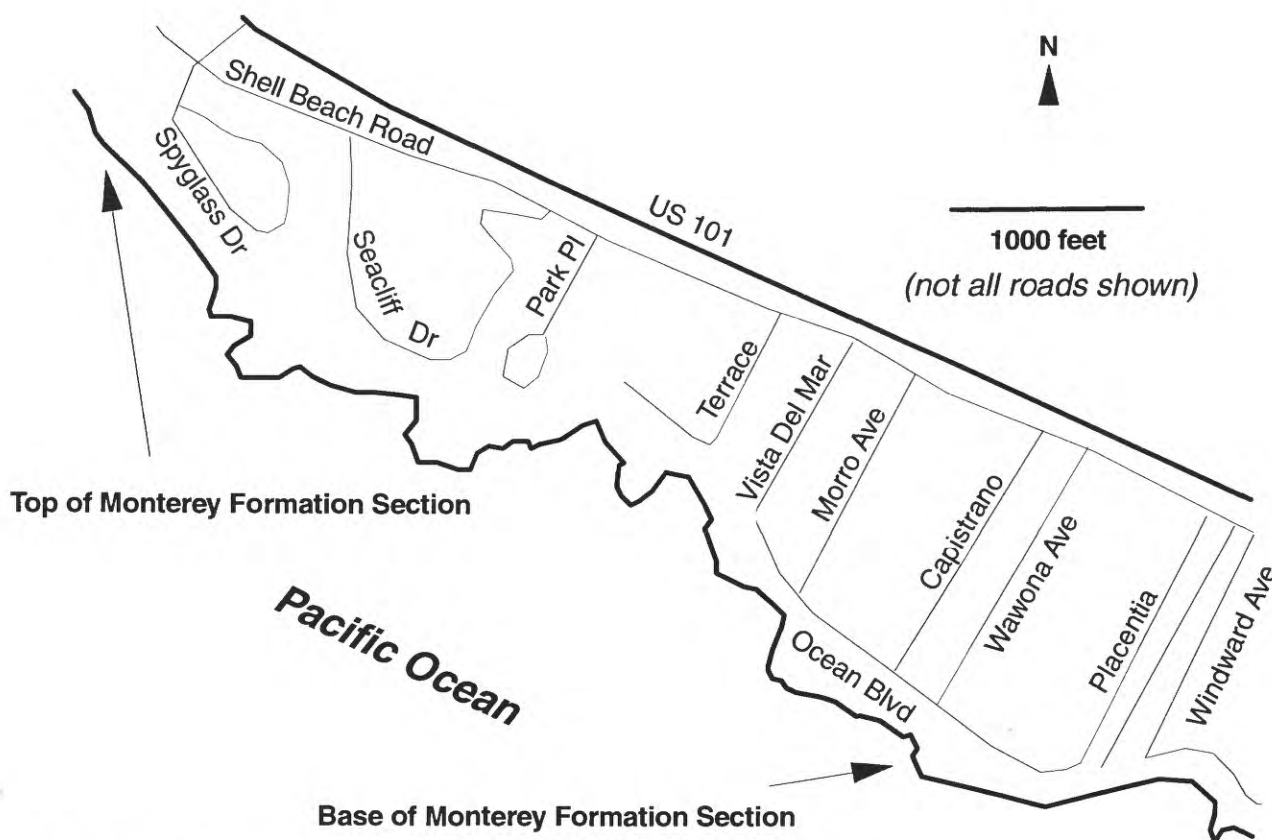


Figure 20. Shell Beach outcrop location map (from Schwalbach and Bohacs, 1992b).

welling related to the development of the Antarctic ice cap (see Barron, 1986a; Khan and others, 1989). Bed and lamina geometry are mostly planar parallel above

453 ft. Rocks are much more brittle and very highly fractured because of their high biogenic silica content. Most of the beds are thin, ranging from 1 to 10 cm, and most

Shell Beach Outcrop Section

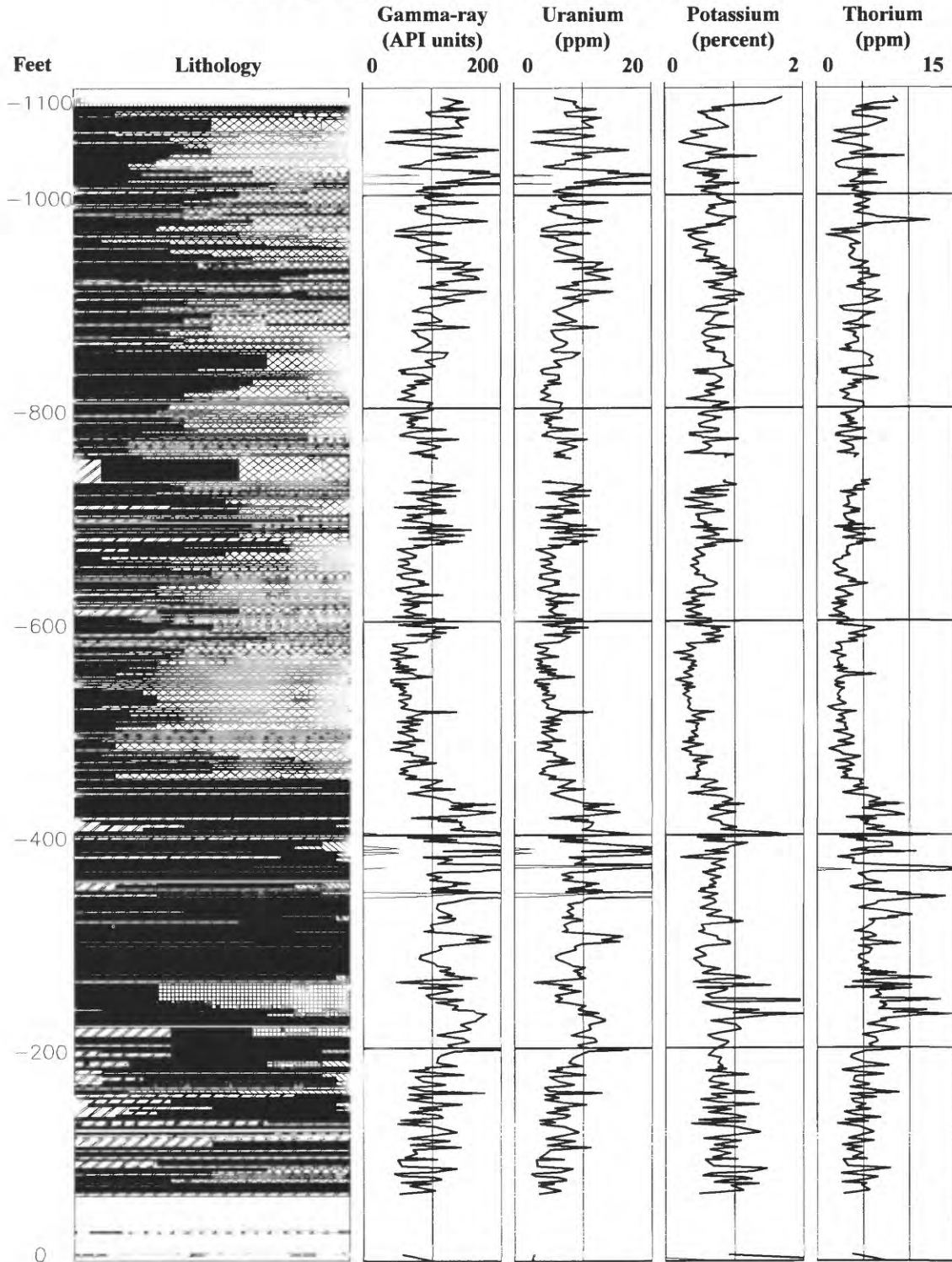


Figure 21. Stratigraphic section from Shell Beach outcrop with accompanying gamma-ray survey (modified from Schwalbach and Bohacs, 1992b).

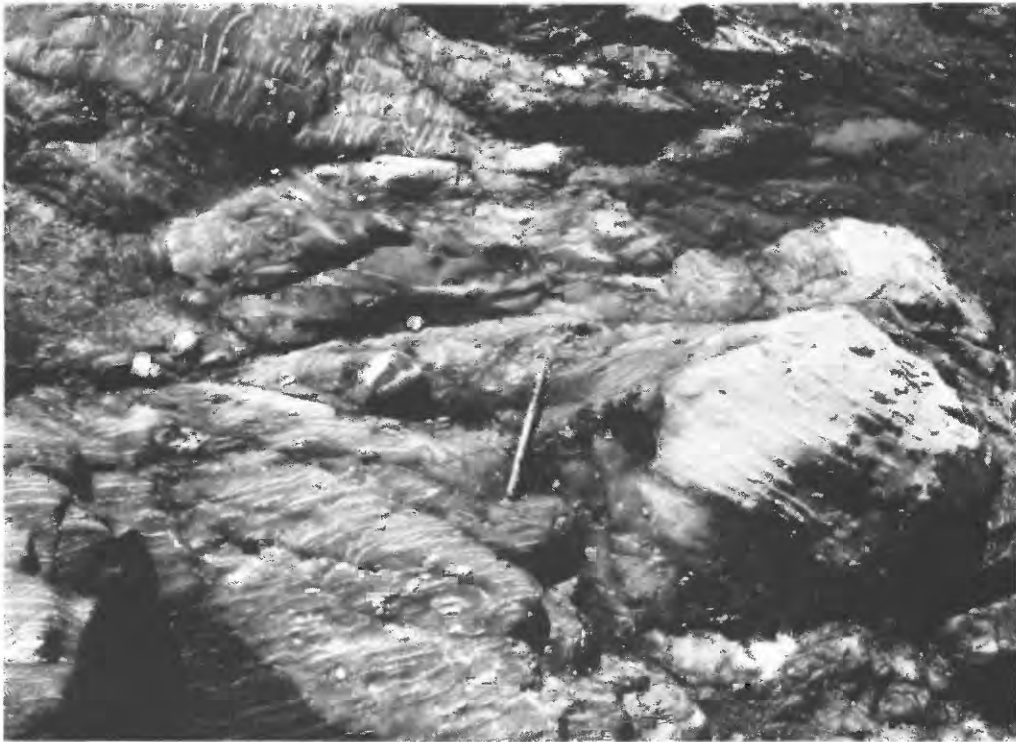


Figure 22. Shell Beach outcrop illustrating disrupted, slump-folded beds between 170 and 180 ft (from Schwalbach and Bohacs, 1992b). Steel probe is 16 cm in length.

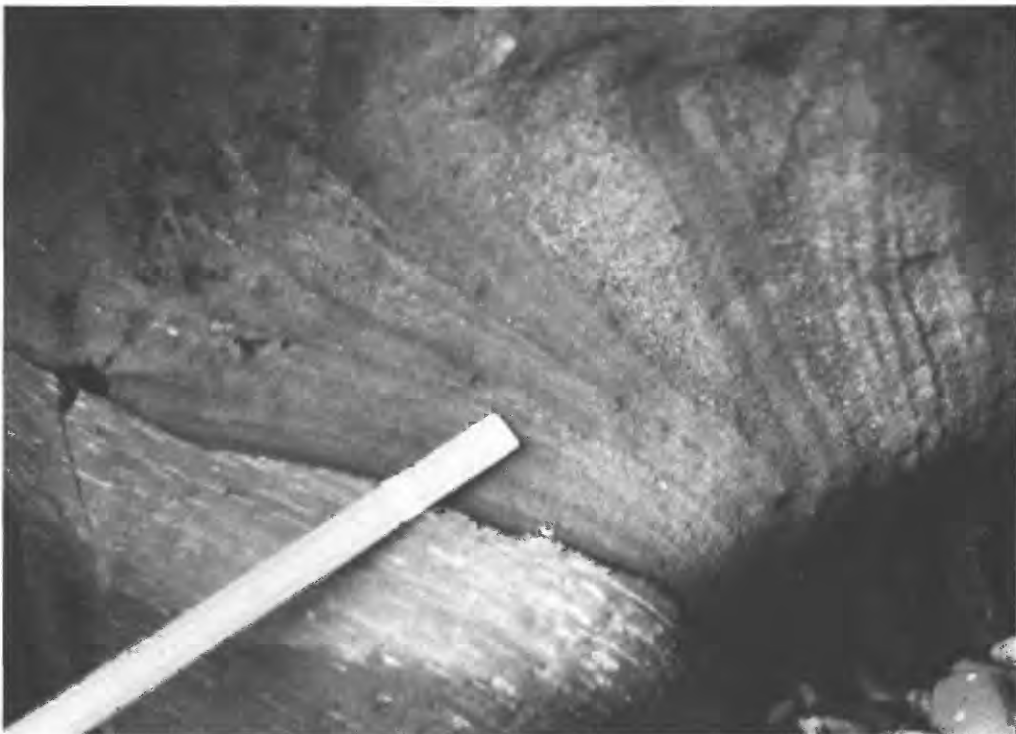


Figure 23. Shell Beach outcrop at 233 ft. Sandstone beds truncate phosphatic shale lamina (from Bohacs and Schwalbach, 1992). Length of ruler in photograph is ≈ 0.4 m. This portion of the outcrop is now covered by a concrete retaining wall.



Figure 24. Shell Beach outcrop at 286 ft. Phosphatic lamina are continuous to discontinuous, with evidence of scouring. Small-offset faults are indicative of slope-failure processes (from Bohacs and Schwalbach, 1992). Steel probe is 16 cm in length.

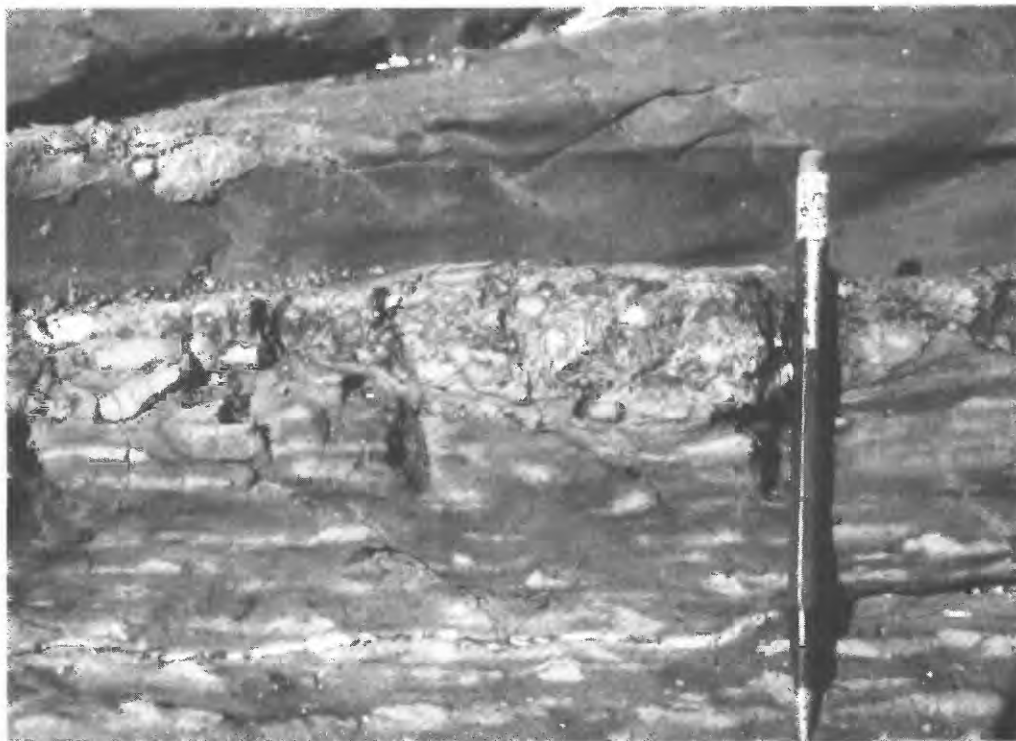


Figure 25. Shell Beach outcrop at 370 ft. Phosphatic hardground is interpreted to represent a downlap surface and records deposition during a time of very low sediment accumulation rate (from Bohacs and Schwalbach, 1992). Pencil is 14 cm in length.

are less than 5 cm thick, except for dolomites that range from 20 to 50 cm in thickness.

- Throughout this interval, there are cyclic stratigraphic packages ranging from 4 to 8 ft thick (on average) that generally are very siliceous at their bases and become more detritus rich at their tops, often capped by dolomites. White (1989) associated these packages with Milankovitch cycles and attempted to estimate their frequency by counting dolomite beds in the intervals. Including both the gamma-ray spectra and the complete lithostratigraphic column provides a better representation of these cyclic strata, particularly when looking at the entire stratigraphic interval. Over the entire siliceous interval, it appears that between 5 and 15 of these smaller “cycles” are grouped together to form larger stratal packages.

1,082 ft and higher

Fine-grained, bituminous, and burrowed sandstones assigned to the Pismo Formation rest unconformably on top of the Monterey Formation at 1,082 ft (fig. 26). Khan and others (1989) date the unconformity at 10.6 to 11.2 Ma based on correlation with the eustatic curve of Haq and others (1987). However, Surdam and Stanley (1984) report diatoms from 120

ft above the unconformity that are latest Miocene to early Pliocene in age (species include *Thalassiospira antiqua*, base of range 7.6 Ma, and *Rouxia californica*, last common occurrence around 6.1 Ma) based on diatom zonations listed in Barron (1986b). Thus, this unconformity could represent a hiatus of 4- to 5-m.y. duration. The abrupt change in sediment character from bathyal Monterey rocks to shelfal Pismo rocks may record such a scenario in basin-edge positions of tectonically active margin environments.

- A 1- to 2-ft-thick layer of pebble to boulder conglomerate with a bituminous sand matrix sits on the unconformity surface. Many of the clasts are lithified and transported rocks derived from the Monterey Formation. The same surface can be identified in the sea cliffs south of the beach access area of The Cliffs Beach Resort. Truncation below the erosional surface is even more dramatic at this locale. More of the stratigraphic section above the unconformity is exposed, and sandstone of the Pismo Formation has abundant trace fossils (assemblage suggests shelfal environments), a significant departure from the Monterey Formation strata below (fig. 27).
- The composite total gamma-ray measurement does not vary dramatically across the unconformity surface, but the contributions of the individual radioactive elements



Figure 26. Shell Beach outcrop at 1,082 ft. The major unconformity at 1,082 ft is represented by a 0.5-m-thick bed of pebble to boulder conglomerate (containing clasts derived from the Monterey Formation) truncating planar-parallel bedded porcelanites. The conglomerate is overlain by bituminous sandstone of the Pismo Formation (from Schwalbach and Bohacs, 1992b).

do. K increases two to three times over values typical of siliceous rocks of the Monterey Formation. Bedsets are also much thicker in the Pismo Formation.

Point Buchon Outcrop

The Point Buchon outcrop section is located in the Pismo basin on land presently owned by Pacific Gas and Electric Company (PG&E) as part of a buffer zone around its Diablo Canyon Nuclear Power Generating Facility. The land is immediately south of Coon Creek and the Montana de Oro State Park boundary, and in recent history it has been referred to as the Pecho or Field Ranch (fig. 28). Access requires permission from PG&E. Our measured section begins adjacent to a fault/shear zone at the south end of the second cove south of Coon Creek. Nearly 1,500 ft of strata of the Monterey Formation are continuously exposed to the north. The rocks dip consistently to the north, and the measured section ends near the State Park boundary at Coon Creek (Figure 28). Below the base of the measured section, there are at least a few hundred ft of Monterey strata. An anticline south of the measured section repeats a significant amount of the strata measured to the north. Steep cliffs, wave action, and significant tidal ranges

limit access to the southernmost section and preclude continuous measurements to the area where the Monterey Formation rests on volcanic rocks of the Obispo Formation. The Monterey is very siliceous in all places where this lowermost interval has been examined. Lithotypes include porcelanites, dolomites, siliceous shales, and cherts. The brittle strata are folded and sheared, particularly in the lowest part of the stratigraphic interval. However, because of limited access to this area we were unable to determine whether this is a faulted or stratigraphically continuous contact.

The Monterey Formation in our measured section consists of two large-scale lithostratigraphic packages (fig. 29). The lower 800 ft of the measured section is very siliceous, composed dominantly of porcelanite and chert, with thin interbeds of siliceous shale and, more rarely, thicker beds of dolomite. The strata above 800 ft contain more terrigenous detritus. Clay shale and siliceous shales are the dominant lithotypes, with a few intervals containing significant proportions of porcelanite and chert. Dolomites occur more frequently in this interval than in the siliceous section below.

Chronostratigraphic control for the Point Buchon outcrop section is sparse. Previous mapping by Hall (1973) suggested that the contact between the Monterey and Pismo Formations is conformable and located within the uppermost

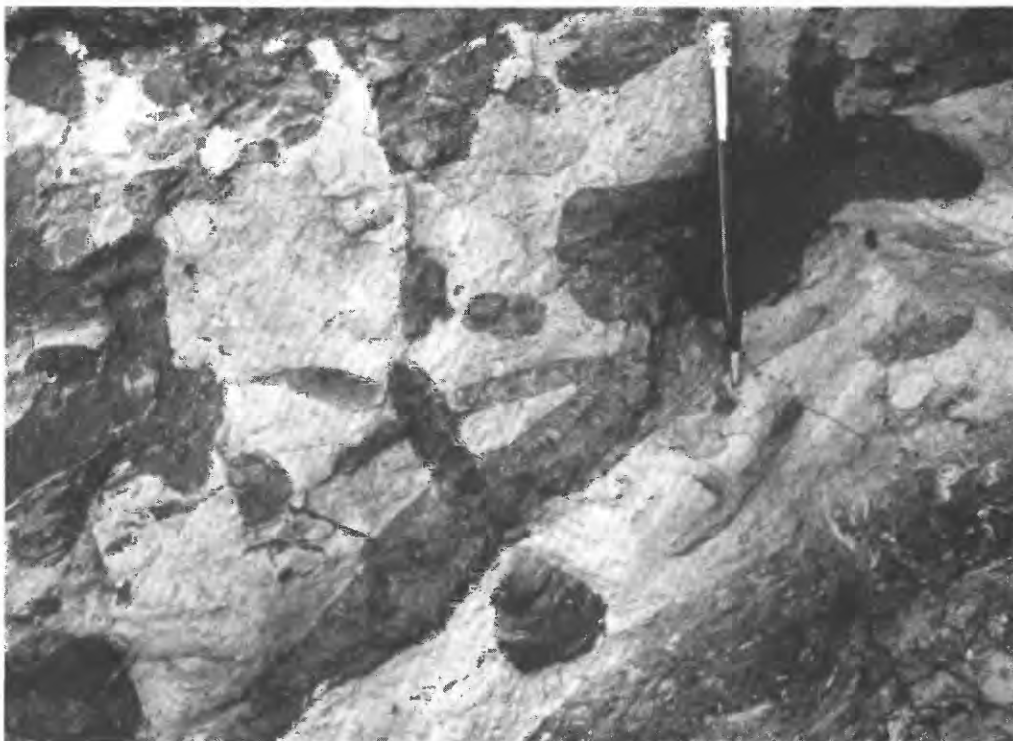


Figure 27. Burrowed sandstone of the Pismo Formation. The outcrop is below The Cliffs Beach Resort, approximately 75 ft above the unconformity surface (from Schwallbach and Bohacs, 1992b). Pencil is 14 cm in length.

part of the section measured for this study. Stanley and Surdam (1984) extended this idea using a sequence stratigraphic approach and correlated a conformable surface equivalent to the 6.6-Ma sequence boundary through this interval (6.3-Ma age on the Haq and others (1987) chart). Recent work, however, suggests that this chronostratigraphy is not correct. Diatoms recovered from dolomites at 1,130 and 1,270 ft of the measured section indicate ages of 11.4–10.5 Ma and 10.4 Ma (maximum), respectively. These samples were examined by John Barron of the U.S. Geological Survey. Barron (Keller and Barron, 1993) has also examined samples from the overlying outcrop section assigned to the Pismo Formation by Hall (1973) and Stanley and Surdam (1984) and derived ages of 6.7–6.0 Ma for the youngest exposed strata and 10.4–9.0 Ma for strata near Coon Creek (see also Keller, 1992). Thus, these data indicate that the entire Point Buchon and adjacent Montana de Oro outcrops are of Monterey age.

We interpret a lower slope to basinal environment of deposition for the strata of our study based on lithofacies association and bedset geometries. Although preservation of calcareous forms is poor throughout this highly siliceous section, a few benthic foraminifers were recovered from 1,156.5, 1,363.5, and 1,375 ft. Although not age diagnostic, these samples indicated bathyl to upper bathyl water depths.

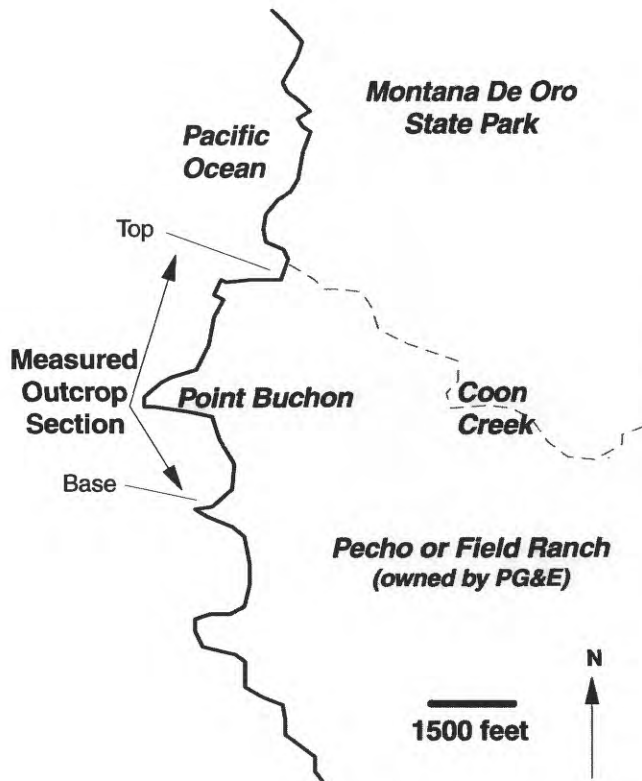


Figure 28. Location map of Point Buchon measured section (modified from Schwalbach and Bohacs, 1992b).

Lithostratigraphy and Gamma-Ray Spectra

0 to 800 ft

This siliceous interval contains porcelanite and chert beds, with thinner interbeds of clay and siliceous shale. Dolomite beds are rare in comparison with other outcrops of the Monterey Formation of similar age (for example, Shell Beach). Many of the cherts are nodular along bedding horizons; laterally equivalent porcelanite strata are often characterized by curved lamina geometries due to differential compaction (fig. 30).

- Some of the most siliceous bedsets are folded but adjacent to other bedsets with planar, parallel geometry. We interpret many of these folded strata as representing slumps, sometimes associated with other indicators of relatively high bottom-energy levels, such as turbidites. One such association occurs in the interval from 610 to 640 ft. At 611 ft and 616 ft, there are fine-grained sand and silt turbidites approximately 3 to 5 cm thick (fig. 31). These have current-ripple lamination and fine upward. Above the turbidites at 620 ft is a 4-m-thick interval of slump-folded tiger-striped chert, with curved parallel and nonparallel, continuous to discontinuous lamina. The slump-folded cherts and turbidite beds indicate higher levels of bottom energy, at least on an intermittent basis.
- Thorium and potassium contents as measured by the gamma-ray spectrometer are generally lowest from 400 through 700 ft, coinciding with the most siliceous strata. Slightly higher values correlate with the intervals of higher detritus content. Because this outcrop contains little carbonate material, the gamma-ray spectra are particularly useful for lithofacies definition.

800 to 1,461 ft

The strata above 800 ft have a larger detritus component and higher concentrations of potassium and thorium as measured by the gamma-ray spectrometer (and verified by laboratory elemental analysis). In a fashion similar to the Shell Beach outcrop, the strata are cyclic on a number of different scales. Individual bedsets exhibit variation in the proportion of biogenic silica and detritus on a 1- to 3-m-thick scale, and these individual bedsets are grouped in 20- to 40-m-thick cyclic packages.

- A thick volcanic ash bed occurring from 960 to 963 ft serves as an excellent stratigraphic marker. The ash bed is marked by an extraordinarily high thorium value recorded by the gamma-ray spectrometer.
- Bedding and lamina geometries in the detritus-rich strata are generally planar parallel. However, scour and low-angle stratal truncation occur along some bedding surfaces, and the overlying strata tend to onlap the scour surfaces (fig. 32).

Point Buchon Outcrop Section

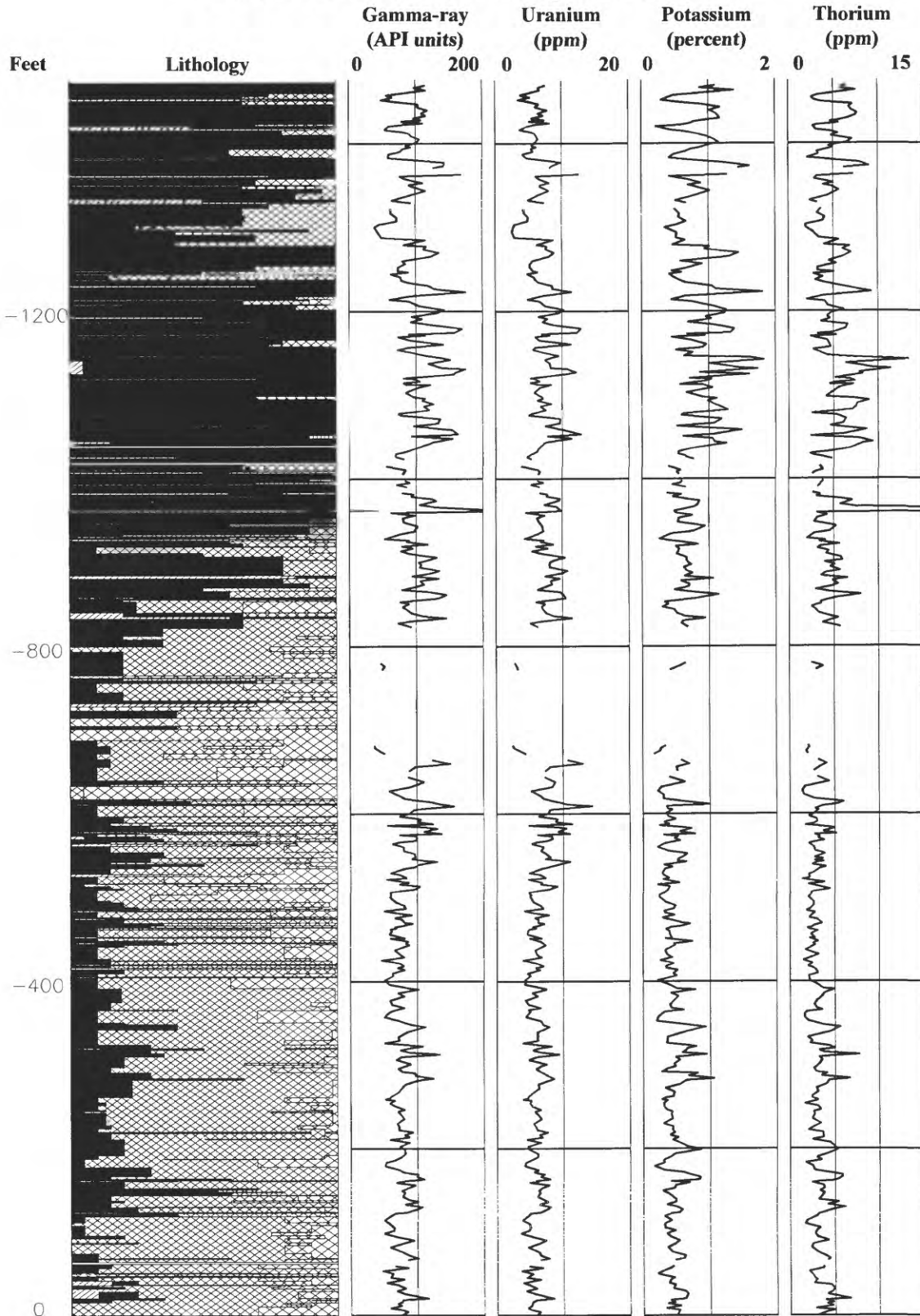


Figure 29. Stratigraphic section from Point Buchon outcrop with accompanying gamma-ray survey (modified from Schwalbach and Bohacs, 1992b).



Figure 30. Point Buchon outcrop from 184 ft. Silica diagenesis is responsible for the lateral juxtaposition of porcelanite and chert. Subsequent differential compaction is responsible for the curved lamina geometry around the chert nodules (from Schwalbach and Bohacs, 1992b).



Figure 31. Point Buchon outcrop from 600 to 640 ft. Planar turbidite beds (recessive weathering) at 611 and 616 ft intersect left side of arch. These rocks are overlain by slump-folded chert beds (from Schwalbach and Bohacs, 1992b).

- Local maxima of uranium, potassium, and thorium occur around clay shale beds from 1,042 to 1,048 ft. A fine-grained sand to silt turbidite occurs at 1,051 ft. This marks the beginning of an interval with a maximum proportion of fine-grained detritus and organic material and a minimum of biogenic silica. High values are recorded in the gamma-ray spectra for U, K, and Th.
- A relatively abrupt increase in biogenic silica occurs around 1,280 ft and is reflected in local minima of uranium, thorium, and potassium measured by the gamma-ray spectrometer. Stratal packages of alternating detritus-rich and detritus-poor beds alternate above 1,280 ft. The packages range from about 3 to 15 m thick. The potassium and thorium data from the gamma-ray spectrometer clearly delineate these packages.

DISCUSSION AND CONCLUSIONS

The primary purpose of this paper is to present these five measured sections and spectral gamma-ray data together in one publication. However, the data also provide a unique basis for stratigraphic interpretation and facies analysis. We have shown that the gamma-ray spectra profiles reflect the lithostratigraphy of each outcrop. In a previous publication, we addressed the issues of identifying key stratigraphic sur-

faces and interpreting these rocks within a sequence stratigraphic framework (Bohacs and Schwabach, 1992). The sequence stratigraphic framework facilitates the comparison of genetically related strata.

An interpreted sequence stratigraphic cross section of the gamma-ray profiles for each of the outcrops is provided in figure 33. The chronostratigraphic data compiled for each measured section is incorporated with observations about the physical characteristics of the rocks, especially the diagnostic features of significant stratigraphic surfaces. The five stratigraphic sections we have presented were deposited in at least three separate basins or subbasins over a broad geographic area. Therefore, this cross section does not necessarily imply specific facies relations, although Shell Beach and Point Buchon (Pismo basin) and Lion's Head and Point Pedernales (Santa Maria basin) probably shared common depositional basins. These data illustrate the wide lithofacies variation that exists even between equivalent-age strata. Lithofacies are clearly time transgressive.

Bohacs (1993) illustrated this relation for the strata deposited above the 10.5-Ma sequence boundary at Point Pedernales and Naples Beach (fig. 34). Both sections contain disrupted, slump-folded strata above the sequence boundary and exhibit similar trends in physical aspects. However, the rocks at Point Pedernales have a large component of biogenic silica reflected by high chert content. The rocks at Naples



Figure 32. Point Buchon outcrop from 1,356 ft. Low-angle scouring and sedimentary onlap is common in this mudstone interval (from Schwabach and Bohacs, 1992b). Pen is 17 cm in length.

Beach, in comparison, have higher levels of detritus and phosphatic shale. The contrast in composition reflects the more distal depositional environment of Point Pedernales. Similar observations can be made for time-equivalent strata among the other outcrops, and these relations can be “remotely sensed” by using the gamma-ray data.

The logical progression of this analysis is then to project these outcrop observations into the subsurface using the gamma-ray data. Schwabach (1992) correlated gamma-ray data from a grid of 13 wells in the offshore Santa Maria Basin. This correlation between the gamma-ray spectra from the Shell Beach outcrop and the 427-1 well log is illustrated in figure 35. Recall from the previous section that detailed magnetostratigraphy provides excellent age control at Shell

Beach. Thus, this is a particularly important outcrop to project into the subsurface.

Gamma-ray data are also valuable for facies analysis (Hornafius, 1991). Since potassium serves as a reliable proxy for detritus, and uranium for organic matter, the potassium/uranium ratio is valuable for predicting source-rock quality (Bohacs, 1993; Bohacs and Schwabach, 1994). Uranium alone is generally a reliable indicator of TOC content, and the gamma-ray spectra can be used in conjunction with the sequence stratigraphic framework to calculate accumulation rates for sediment components (Schwabach, 1992).

These are just a few examples of how gamma-ray spectra, obtained in conjunction with detailed outcrop descriptions, enhance our ability to interpret fine-grained strata. In the clean,

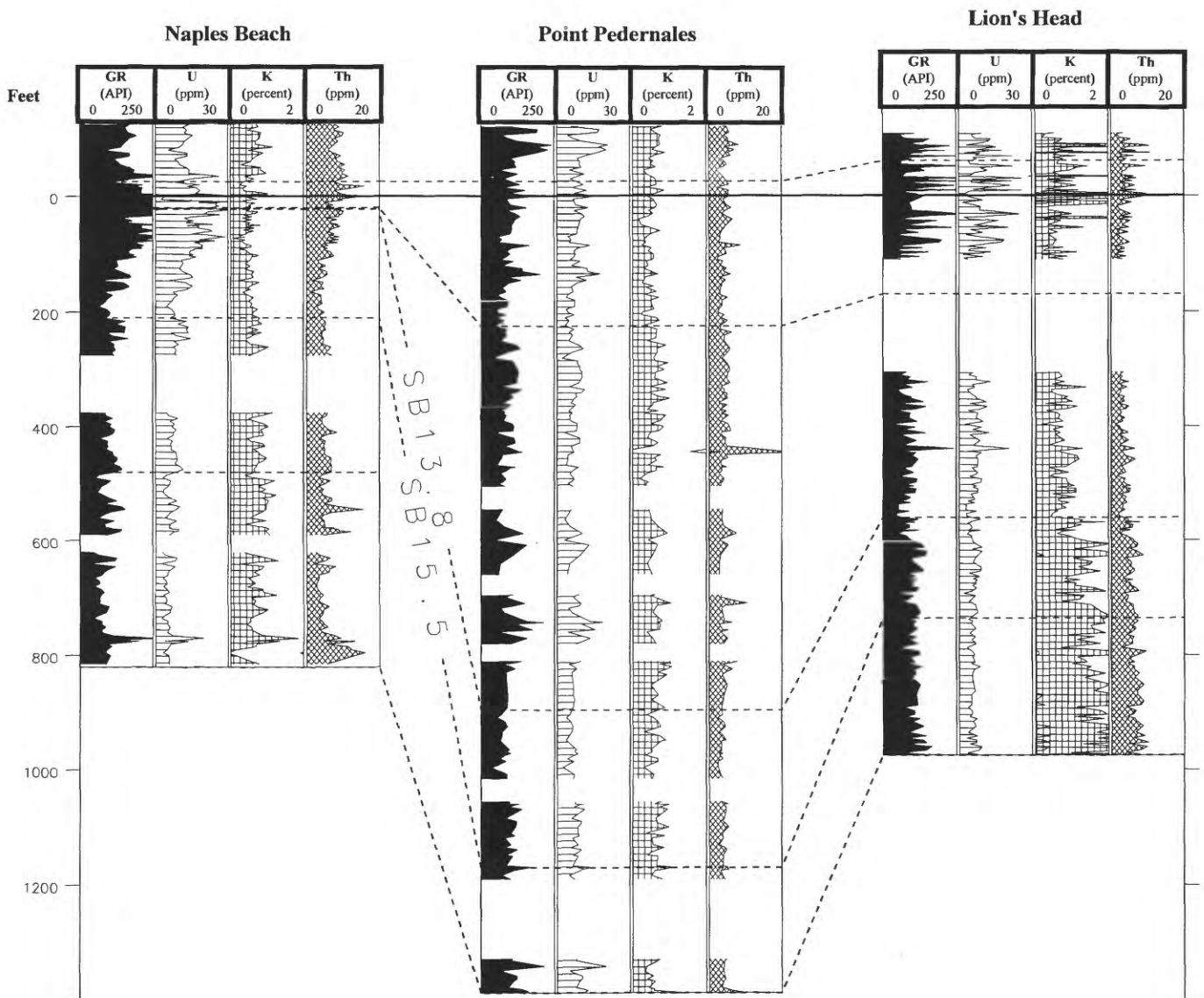


Figure 33. Stratigraphic cross section: (A), Naples Beach to Point Pedernales to Lion's Head; (B), Lion's Head to Shell Beach to Point Buchon. Correlation horizons are interpreted sequence boundaries (dashed lines). The cross section is datumed on an interpreted downlap surface (approx. 11 Ma.). Total gamma-ray and element components are from outcrop gamma-ray spectrometry.

coastal cliff exposures of these outcrops, gamma-ray surveying requires only about five additional minutes per meter of stratigraphic section. This is a relatively small expenditure of time considering the wealth of compositional data gained by employing the technique.

REFERENCES CITED

Arends, R.G., and Blake, G.H., 1986, Biostratigraphy and paleoecology of the Naples Bluff coastal section based on diatoms and benthic foraminifera, *in* Casey, R. E., and Barron, J.A., eds., Siliceous microfossils and microplankton of the Monterey Formation and modern analogs: Pacific Section, Society of Economic

Paleontologists and Mineralogists, p. 121-136.

Barron, J.A., 1986a, Paleoclimatologic and tectonic controls on deposition of the Monterey Formation and related siliceous rocks in California: *Palaeogeography, Palaeoclimatology, Palaeoecology*, v. 53, p. 27-45.

——— 1986b, Updated diatom biostratigraphy of the Monterey Formation of California, *in* Casey, R. E., and Barron, J.A., eds., Siliceous microfossils and microplankton of the Monterey Formation and modern analogs: Pacific Section, Society of Economic Paleontologists and Mineralogists, p. 105-119.

Bohacs, K.M., 1990, Sequence stratigraphy of the Monterey Formation, Santa Barbara County: Integration of physical, chemical, and biofacies data from outcrop and subsurface, *in* Keller, M.A., and McGowen, M.K., eds., Miocene and Oligocene petroleum reservoirs of the Santa Maria and Santa Barbara—Ventura ba-

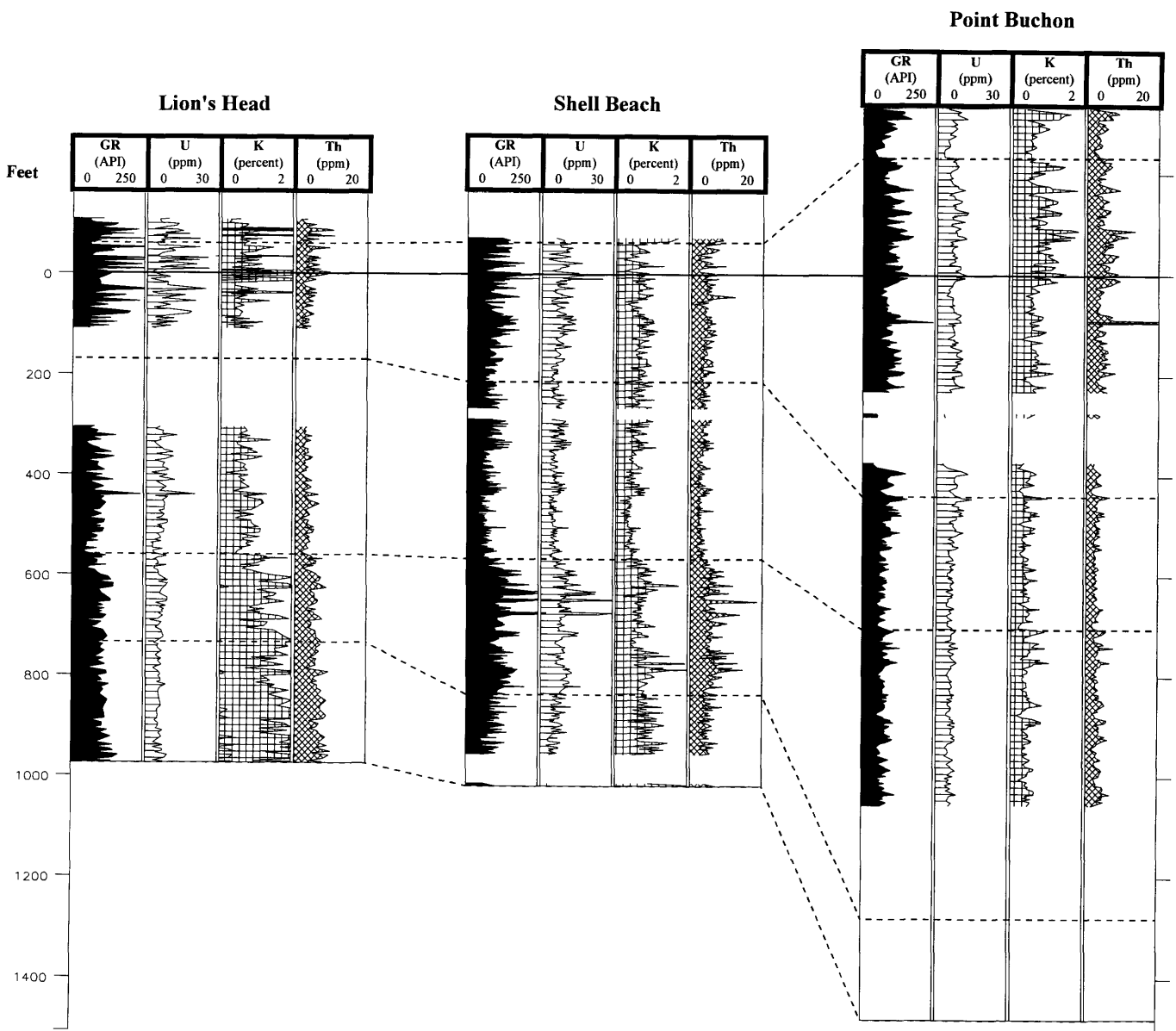


Figure 33. Continued.

sins, California: Society of Economic Paleontologists and Mineralogists, Core Workshop No. 14, p. 139-201.

—1993, Source quality variations tied to sequence development in the Monterey and associated formations, southwestern California, in Katz, B.J., and Pratt, L.M., eds, *Petroleum source rocks in a sequence stratigraphic framework*: American Association of Petroleum Geologists, Studies in Geology no. 37, p. 177-204.

Bohacs, K.M., and Schwalbach, J.R., 1991, Physical expression and stratigraphic distribution of hiatuses in mudrocks [abs.]: Abstracts, 1991 Society of Economic Paleontologists and Mineralogists Annual Theme Meeting, Continental Margins, Portland, Oregon, p. 4.

—1992, Sequence stratigraphy of fine-grained rocks with special reference to the Monterey Formation, in Schwalbach, J.R.,

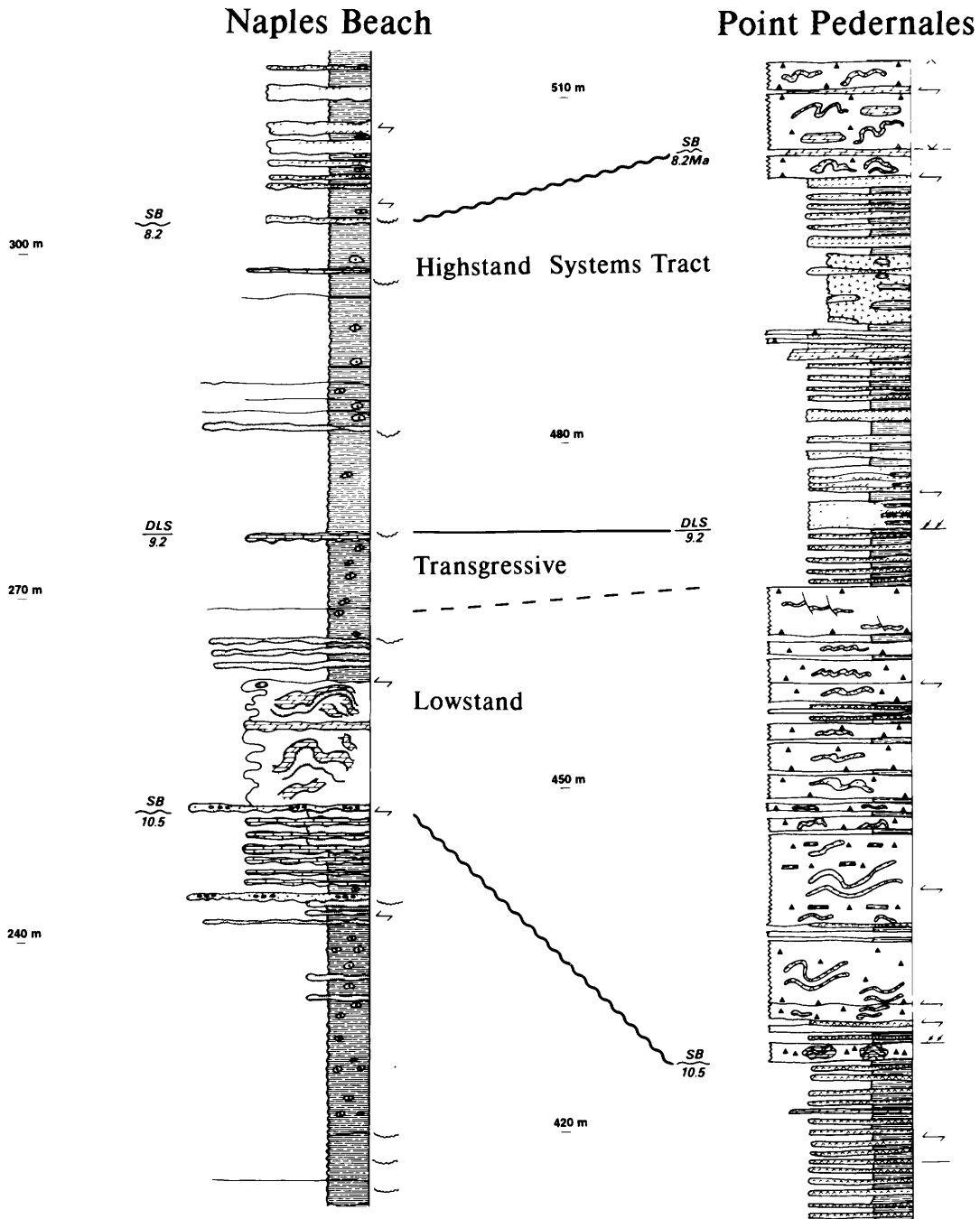


Figure 34. Correlation of single sequence between Point Pedernales and Naples Beach. These outcrops are from different basins, but nonetheless they illustrate the time-transgressive nature of the lithofacies of the Monterey Formation (Bohacs, 1993; reprinted by permission).

and Bohacs, K.M., eds., Sequence stratigraphy in fine-grained rocks: examples from the Monterey Formation: Society of Economic Paleontologists and Mineralogists, Pacific Section, v. 70, p. 7-20.

—1994, Natural gamma-ray spectrometry of the Monterey Formation at Naples Beach, California: insights into lithology, stratigraphy, and source-rock quality, in Hornafius, J.S., ed., Field guide to the Monterey Formation between Santa Barbara and Gaviota: Pacific Section, American Association of Petroleum Geologists, v. GB72, p. 85-94.

Bramlette, M.N., 1946, The Monterey Formation of California and

the origin of siliceous rocks: U.S. Geological Survey Professional Paper 212, 57 p.

Clark, L., 1989, Strontium isotope variation and dating of dolomites in the Monterey Formation, California: Los Angeles, Calif., California State University, M.S. thesis.

Clayton, J.L., and Swetland, P.J., 1978, Subaerial weathering of sedimentary organic matter: Geochimica et Cosmochimica Acta, v. 42, p. 305-312.

DePaolo, D.J., and Finger, K.L., 1991, High-resolution strontium-isotope stratigraphy and biostratigraphy of the Miocene Monterey Formation, central California: Geological Society of America

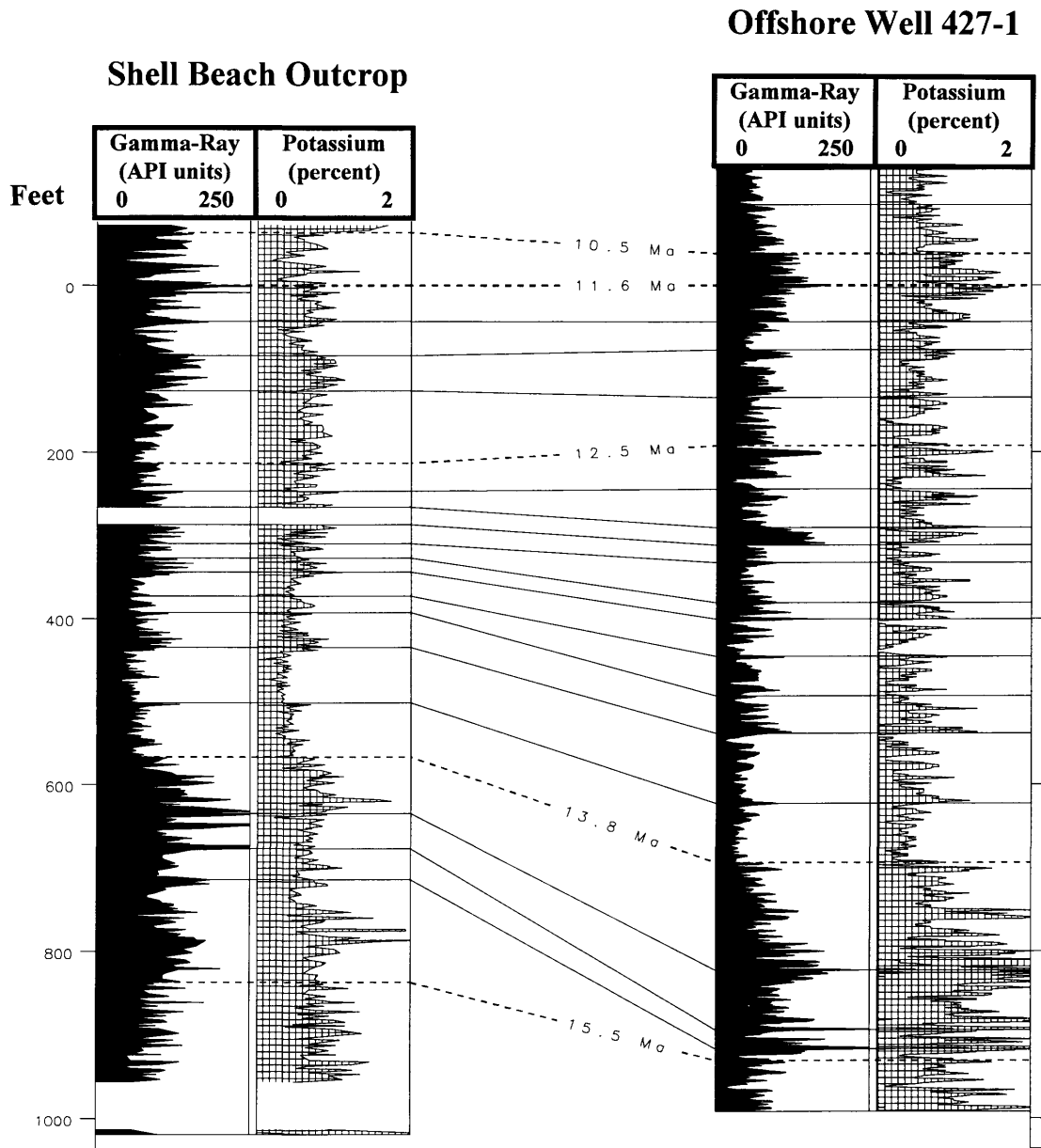


Figure 35. Stratigraphic cross section: lower part of the Monterey Formation between the Shell Beach outcrop and the 427-1 well from the offshore Santa Maria Basin (from Schwalbach and Bohacs, 1992b). Shell Beach values are from outcrop gamma-ray spectrometry; well 427-1 values are from a borehole well log.

- Bulletin, v. 103, p. 112–124.
- Dunham, J.B., and Blake, G.H., 1987, Guide to coastal outcrops of the Monterey Formation, western Santa Barbara County, California: Society of Economic Paleontologists and Mineralogists, Pacific Section Guidebook, 36 p.
- Dunham, J.B., and Cotton-Thornton, M.L., 1990, Lithology of the Monterey Formation in the western Santa Maria Valley field, Santa Maria basin, California, *in* Keller, M.A., and McGowen, M.K., eds., Miocene and Oligocene petroleum reservoirs of the Santa Maria and Santa Barbara—Ventura basins, California: Society of Economic Paleontologists and Mineralogists, Core Workshop No. 14, p. 202–244.
- Grivetti, M.C., 1982, Aspects of stratigraphy, diagenesis, and deformation in the Monterey Formation near Santa Maria–Lompoc, California: Santa Barbara, Calif., University of California, M.A. thesis, 155 p.
- Hall, C.A., Jr., 1973, Geology of the Arroyo Grande 15 minute quadrangle, San Luis Obispo County, California: California Division of Mines and Geology, Map Sheet 24, scale 1:48,000.
- Haq, B.U., Hardenbol, J., and Vail, P.R., 1987, Chronology of fluctuating sea levels since the Triassic: *Science*, v. 235, p. 1156–1166.
- Hornafius, J.S., 1985, Neogene tectonic rotation of the Santa Ynez Range, western Transverse Ranges, California, suggested by paleomagnetic investigation of the Monterey Formation: *Journal of Geophysical Research*, v. 90, p. 12,503–12,522.
- 1991, Facies analysis of the Monterey Formation in the northern Santa Barbara Channel: *American Association of Petroleum Geologists Bulletin*, v. 75, p. 894–909.
- Isaacs, C.M., 1980, Diagenesis in the Monterey Formation examined laterally along the coast near Santa Barbara, California: Stanford, Calif., Stanford University, Ph.D. dissertation, 329 p.
- 1981a, Field characterization of rocks in the Monterey Formation examined laterally along the Santa Barbara Coast, California, *in* Isaacs, C.M., ed., Guide to the Monterey Formation in the California coastal area, Ventura to San Luis Obispo: Pacific Section, American Association of Petroleum Geologists, v. 52, p. 39–52.
- 1981b, Lithostratigraphy of the Monterey Formation, Goleta to Pt. Conception, Santa Barbara coast, California, *in* Isaacs, C.M., ed., Guide to the Monterey Formation in the California coastal area, Ventura to San Luis Obispo: Pacific Section, American Association of Petroleum Geologists, v. 52, p. 25–38.
- 1983, Compositional variation and sequence in the Miocene Monterey Formation, Santa Barbara coastal area, California, *in* Larue, D.K., and Steel, R.J., eds., Cenozoic marine sedimentation, Pacific margin, U.S.A.: Pacific Section, Society of Economic Paleontologists and Mineralogists Special Publication, p. 117–132.
- 1992, Data report—uranium, thorium, and other trace elements in strip samples from cores 128–798B–13H through 15H, *in* Tamaki, K., Suyehiro, K., Allan, J., McWilliams, M., and others, eds., Proceedings of the Ocean Drilling Program: Scientific Results, v. 127/128, pt. 2, p. 1367–1372.
- Isaksen, G.H., and Bohacs, K.M., 1995, Geological controls of source-rock geochemistry through relative sea level: Triassic; Barents Sea, *in* Katz, B.J., ed., Petroleum source rocks: Berlin, Springer-Verlag, p. 25–50.
- Keene, J.B., 1975, Cherts and porcelanites from the North Pacific, D.S.D.P. leg 32, *in* Larson, R.L., and others, eds., Initial reports of the deep sea drilling project, v. 32: Washington, D.C., U.S. Government Printing Office, p. 429–507.
- Keller, M.A., 1992, Field guide to the upper Miocene siliceous coastal sequence of Montana de Oro State Park, California, *in* Schwalbach, J.R., and Bohacs, K.M., eds., Sequence stratigraphy in fine-grained rocks: examples from the Monterey Formation: Society of Economic Paleontologists and Mineralogists, Pacific Section, v. 70, p. 21–30.
- Keller, M.A., and Barron, J.A., 1993, Re-evaluation of the Miguelito Member of the Pismo Formation of Montana de Oro State Park, California, including new diatom age data [abs.]: *American Association of Petroleum Geologists Bulletin*, v. 77, p. 703–704.
- Khan, S.M., Coe, R.S., and Barron, J.A., 1989, High-resolution magnetic polarity stratigraphy of Shell Beach section of the Monterey Formation in Pismo Basin, California, *in* Garrison, R.E., ed., Japan-U.S. seminar guidebook on Neogene siliceous sediments of the Pacific region, p. 106–120.
- Langmuir, D., 1978, Uranium solution-mineral equilibria at low temperatures with applications to sedimentary ore deposits: *Geochimica et Cosmochimica Acta*, v. 44, p. 1753–1766.
- Leythaeuser, D., 1973, Effects of weathering on organic matter in shales: *Geochimica et Cosmochimica Acta*, v. 37, p. 113–120.
- Murata, K. J., and Larson, R.R., 1975, Diagenesis of Miocene siliceous shales, Temblor Range, California: U.S. Geological Survey, *Journal of Research*, v. 3, p. 553–556.
- Myers, K.J., and Wignall, P.B., 1987, Understanding Jurassic organic-rich mudrocks - new concepts using gamma-ray spectrometry and paleoecology: examples from the Kimmeridge Clay of Dorset and the Jet Rock of Yorkshire, *in* Leggett, J.K., and Zuffa, G.G., eds., Marine clastic sedimentology: London, Graham and Trotman, p. 172–189.
- Piper, D.Z., and Isaacs, C.M., 1995, Minor elements in Quaternary sediment from the Sea of Japan: a record of surface-water productivity and intermediate-water redox conditions: *Geological Society of America Bulletin*, v. 107, p. 54–67.
- Raiswell, R., and Berner, R.A., 1986, Pyrite and organic matter in normal marine shales: *Geochimica et Cosmochimica Acta*, v. 50, p. 1967–1976.
- Schwalbach, J.R., 1991, Fractured reservoir description: an example for the Monterey at Hondo [abs.]: Program and Abstracts, 1991 Pacific Section, AAPG–SEPM–SEG–SPWLA Meeting, Bakersfield, California, p. 46.
- 1992, Stratigraphic and sedimentologic analysis of the Monterey Formation: Santa Maria and Pismo Basins, California: Los Angeles, Calif., University of Southern California, Ph.D. dissertation, 360 p.
- Schwalbach, J.R., and Bohacs, K.M., 1991, Depositional sequences in continental margin settings: hemipelagic and pelagic facies of the Monterey Formation, California [abs.]: Abstracts, 1991 Society of Economic Paleontologists and Mineralogists Annual Theme Meeting, Continental Margins, p. 30.
- 1992a, Field investigation techniques for analysis of the Monterey Formation, *in* Schwalbach, J.R., and Bohacs, K.M., eds., Sequence stratigraphy in fine-grained rocks: examples from the Monterey Formation: Society of Economic Paleontologists and Mineralogists Pacific Section, v. 70, p. 21–30.
- 1992b, Field guide to the Monterey Formation outcrops at Shell Beach and Point Buchon, Pismo Basin, California, *in* Schwalbach, J.R., and Bohacs, K.M., eds., Sequence stratigraphy in fine-grained rocks: examples from the Monterey Forma-

- tion: Society of Economic Paleontologists and Mineralogists, Pacific Section, v. 70, p. 31–46.
- Schwalbach, J.R., and Lockman, D.F., 1988, Sedimentologic controls on brittle deformation of siliceous and dolomitic mudstones: Pismo Formation, California [abs.]: Program and Abstracts, 1988 Pacific Section, AAPG–SEPM–SEG–SPWLA Meeting, Santa Barbara, California.
- Scintrex, 1979, GAD–6 four channel stabilized gamma-ray spectrometer instruction manual: Toronto, Canada, Scintrex, Ltd., 64 p.
- Stanley, K.O., and Surdam, R.C., 1984, The role of wrench fault tectonics and relative changes of sea level on deposition of upper Miocene-Pliocene Pismo Formation, Pismo syncline, California, *in* Surdam, R.C., ed., A guidebook to the stratigraphic, tectonic, thermal, and diagenetic histories of the Monterey Formation, Pismo and Huasna basin, California: Society of Economic Paleontologists and Mineralogists, Guidebook No. 2, p. 21–37.
- Surdam, R.C., and Stanley, K.O., 1984, Stratigraphic and sedimentologic framework of the Monterey Formation, Pismo syncline, California, *in* Surdam, R.C., ed., A guidebook to the stratigraphic, tectonic, thermal, and diagenetic histories of the Monterey Formation, Pismo and Huasna basin, California: Society of Economic Paleontologists and Mineralogists, Guidebook No. 2, p. 75–83.
- Turner, D.L., 1970, Potassium-argon dating of Pacific coast Miocene foraminiferal stages, *in* Bandy, O.L., ed. Radiometric dating and paleontologic zoning: Geological Society of America Special Paper 124, p. 91–129.
- White, L.D., 1989, Chronostratigraphic and paleoceanographic aspects of selected chert intervals in the Miocene Monterey Formation, California: Santa Cruz, Calif., University of California, Ph.D. thesis, 236 p.
- Zelt, F.B., 1985, Natural gamma-ray spectrometry, lithofacies, and depositional environments of selected Upper Cretaceous marine mudrocks, Western United States, including Tropic Shale and Tununk member of Mancos Shale: Princeton, N.J., Princeton University, Ph.D. thesis.

SELECTED SERIES OF U.S. GEOLOGICAL SURVEY PUBLICATIONS

Periodicals

Earthquakes & Volcanoes (issued bimonthly).

Preliminary Determination of Epicenters (issued monthly).

Technical Books and Reports

Professional Papers are mainly comprehensive scientific reports of wide and lasting interest and importance to professional scientists and engineers. Included are reports on the results of resource studies and of topographic, hydrologic, and geologic investigations. They also include collections of related papers addressing different aspects of a single scientific topic.

Bulletins contain significant data and interpretations that are of lasting scientific interest but are generally more limited in scope or geographic coverage than Professional Papers. They include the results of resource studies and of geologic and topographic investigations, as well as collections of short papers related to a specific topic.

Water-Supply Papers are comprehensive reports that present significant interpretive results of hydrologic investigations of wide interest to professional geologists, hydrologists, and engineers. The series covers investigations in all phases of hydrology, including hydrogeology, availability of water, quality of water, and use of water.

Circulars present administrative information or important scientific information of wide popular interest in a format designed for distribution at no cost to the public. Information is usually of short-term interest.

Water-Resource Investigations Reports are papers of an interpretive nature made available to the public outside the formal USGS publications series. Copies are reproduced on request unlike formal USGS publications, and they are also available for public inspection at depositories indicated in USGS catalogs.

Open-File Reports include unpublished manuscript reports, maps, and other material that are made available for public consultation at depositories. They are a nonpermanent form of publication that may be cited in other publications as sources of information.

Maps

Geologic Quadrangle Maps are multicolor geologic maps on topographic bases in 7 ½- or 15-minute quadrangle formats (scales mainly 1:24,000 or 1:62,500) showing bedrock, surficial, or engineering geology. Maps generally include brief texts; some maps include structure and columnar sections only.

Geophysical Investigations Maps are on topographic or planimetric bases at various scales; they show results of surveys using geophysical techniques, such as gravity, magnetic, seismic, or radioactivity, which reflect subsurface structures that are of economic or geologic significance. Many maps include correlations with the geology.

Miscellaneous Investigations Series Maps are on planimetric or topographic bases of regular and irregular areas at various scales; they present a wide variety of format and subject matter. The series also includes 7 ½-minute quadrangle photogeologic maps on planimetric bases that show geology as interpreted from aerial photographs. Series also includes maps of Mars and the Moon.

Coal Investigations Maps are geologic maps on topographic or planimetric bases at various scales showing bedrock or surficial geology, stratigraphy, and structural relations in certain coal-resource areas.

Oil and Gas Investigations Charts show stratigraphic information for certain oil and gas fields and other areas having petroleum potential.

Miscellaneous Field Studies Maps are multicolor or black-and-white maps on topographic or planimetric bases on quadrangle or irregular areas at various scales. Pre-1971 maps show bedrock geology in relation to specific mining or mineral-deposit problems; post-1971 maps are primarily black-and-white maps on various subjects, such as environmental studies or wilderness mineral investigations.

Hydrologic Investigations Atlases are multicolor or black-and-white maps on topographic or planimetric bases presenting a wide range of geohydrologic data of both regular and irregular areas; principal scale is 1:24,000, and regional studies are at 1:250,000 scale or smaller.

Catalogs

Permanent catalogs, as well as some others, giving comprehensive listings of U.S. Geological Survey publications are available under the conditions indicated below from the U.S. Geological Survey, Books and Open-File Reports Sales, Federal Center, Box 25286, Denver, CO 80225. (See latest Price and Availability List.)

"Publications of the Geological Survey, 1879-1961" may be purchased by mail and over the counter in paperback book form and as a set of microfiche.

"Publications of the Geological Survey, 1962-1970" may be purchased by mail and over the counter in paperback book form and as a set of microfiche.

"Publications of the Geological Survey, 1971-1981" may be purchased by mail and over the counter in paperback book form (two volumes, publications listing and index) and as a set of microfiche.

Supplements for 1982, 1983, 1984, 1985, 1986, and for subsequent years since the last permanent catalog may be purchased by mail and over the counter in paperback book form.

State catalogs, "List of U.S. Geological Survey Geologic and Water-Supply Reports and Maps For (State)," may be purchased by mail and over the counter in paperback booklet form only.

"Price and Availability List of U.S. Geological Survey Publications," issued annually, is available free of charge in paperback booklet form only.

Selected copies of a monthly catalog "New Publications of the U.S. Geological Survey" are available free of charge by mail or may be obtained over the counter in paperback booklet form only. Those wishing a free subscription to the monthly catalog "New Publications of the U.S. Geological Survey" should write to the U.S. Geological Survey, 582 National Center, Reston, VA 22092.

Note.—Prices of Government publications listed in older catalogs, announcements, and publications may be incorrect. Therefore, the prices charged may differ from the prices in catalogs, announcements, and publications.

